https://theses.gla.ac.uk/

Theses Digitisation:

https://www.gla.ac.uk/myglasgow/research/enlighten/theses/digitisation/

This is a digitised version of the original print thesis.

Copyright and moral rights for this work are retained by the author

A copy can be downloaded for personal non-commercial research or study, without prior permission or charge

This work cannot be reproduced or quoted extensively from without first obtaining permission in writing from the author

The content must not be changed in any way or sold commercially in any format or medium without the formal permission of the author

When referring to this work, full bibliographic details including the author, title, awarding institution and date of the thesis must be given

Enlighten: Theses
https://theses.gla.ac.uk/
research-enlighten@glasgow.ac.uk

Tn3 resolvase-catalysed recombination: Assembly and activation of the site I synapse

A thesis submitted for the degree of
Doctor of Philosophy
at the
University of Glasgow

by

Femi John Olorunniji

Division of Molecular Genetics
Institute of Biomedical and Life Sciences
Anderson College

56 Dumbarton Road
Glasgow

November 2006

© F.J. Olorunniji, 2006

ProQuest Number: 10905118

All rights reserved

INFORMATION TO ALL USERS
The quality of this reproduction is dependent upon the quality of the copy submitted.

In the unlikely event that the author did not send a complete manuscript
and there are missing pages, these will be noted. Also, if material had to be removed,
a note will indicate the deletion.

ProQuest 10905118

Published by ProQuest LLC (2018). Copyright of the Dissertation is held by the Author.

All rights reserved.
This work is protected against unauthorized copying under Title 17, United States Code
Microform Edition © ProQuest LLC.

ProQuest LLC.
789 East Eisenhower Parkway
P.O. Box 1346
Ann Arbor, MI 48106 – 1346

GLASGOW
UNIVERSITY
LIBRARY:

Contents

Abbreviations

Units

k	10^3	h	hours
m	10^{-3}	M	molar
μ	10^{-6}	cps	counts per second
n	10^{-9}	kb/kbp	kilo base pairs
p	10^{-12}	V	volts
bp	base pairs	MBq	megabecquerels
A	Ampères	g	grams
W	Watts	m	metres
°C	degrees Celsius	mol	moles
l	litres	rpm	revolutions per minute
		OD	optical density

Chemicals/Reagents

AcOH	acetic acid
APS	ammonium persulphate
ATP	adenosine triphosphate
DNA	deoxyribonucleic acid
DTT	dithiothreitol
EDTA	ethylenediaminetetra-acetic acid (disodium salt)
EtBr	ethidium bromide
KOAc	potassium acetate
PAGE	polyacrylamide gel electrophoresis
SDS	sodium dodecyl sulphate
TAE	tris-acetate-EDTA (electrophoresis buffer)
TBE	tris-borate-EDTA (electrophoresis buffer)
TGE	tris-glycine-EDTA (electrophoresis buffer)
TMED	*N,N,N',N'*-tetramethylethylenediamine
Tris	tris(hydroxymethyl)aminomethane
UV	ultraviolet

Acknowledgements

A lot of thanks to my dear wife, Kemi for her selfless love and support for me since we met, and especially over the period of this project. Anna Olawumi and Ayobami Stephanie (our wee girls) played their expected parts in making it nearly impossible to write this thesis! Really, they have added to the fun and excitements of the past three years. Many thanks to the friends here at Kelvin for their support and encouragement throughout our stay.

Special thanks to Marshall Stark for his effective and helpful supervision during the course of this project, and for his careful attention in reading the drafts of the thesis. I also appreciate the contributions of Sean Colloms and Richard McCulloch for the timely and insightful assessments they conducted. Many thanks to Mary Burke for patiently taking me through the basics of laboratory techniques at the start of the programme, and Amy Bednarz for helpful comments on the drafts of the thesis. I equally appreciate the helpful discussions with Martin Boocock. A lot of thanks to Sally, Elizabeth, Arlene, Lily, Paula, Chris, Al, Marko, Gero, Marcelo, Feng, Aram, and others for their helpful support and encouragement during the course of this project.

I appreciate the contributions of the Commonwealth Scholarship Commission in the UK for awarding me a Commonwealth Academic Staff Scholarship, and the University of Ilorin, Nigeria, for granting me a study leave. A lot of thanks to Sylvia Malomo for her encouragement all through, and to my other colleagues at the Biochemistry Department in Ilorin.

Summary

The assembly and catalytic activation of the site I synapse in resolvase-catalysed recombination was investigated by a combination of mutagenesis and chemical modification of DNA substrates. The binding and catalytic properties of activated Tn3 resolvase mutants were compared with those of wild-type resolvase with the aim of understanding how activating mutations deregulate site I synapsis and catalysis. The findings indicate that structural changes in the resolvase-site I dimer complex are important for the formation of a stable site I synapse. Efficient catalysis of site I x site I recombination by activated resolvase mutants is highly correlated with formation of stable site I synapse in polyacrylamide bandshift assays. Conserved residues that are presumed to form the active site of resolvase were mutated in activated mutants of Tn3 resolvase, and the binding, synapsis and catalytic properties of the mutant resolvases were characterised. Certain mutations in putative active site residues of resolvase resulted in decrease in the yield and/or stability of the site I synapse, while mutations in another set of residues in the putative active site destabilised the dimer complex and stabilised the site I synapse. These results suggest a role for the active site in site I synapsis. Methylphosphonate replacements of phosphodiester groups close to the scissile position in site I show that direct contact of resolvase with the centre of site I is important for synapsis, but not necessarily for binding. Such contacts are not seen in the published structures of the site I synapse. The apparent lack of contact between catalytic residues and the DNA in cocrystal resolvase structures suggests that the engagement of catalytic residues with the substrate is at the point of catalytic activation. The results of site I cleavage experiments with resolvase mutants show that while several conserved residues are important for the recombination activity of resolvase, only a few of these are essential for the activation of the catalytic process. The effects of methylphosphonate substitution at the phosphate immediately 3' to the scissile position on site I cleavage suggests a catalytic role for this phosphate, such as recruitment of positively charged catalytic residues into the active site prior to catalysis.

Chapter One

Introduction

1.1 Site-specific recombination

Site-specific recombination is a process whereby a DNA molecule is cut at two specific sites and the ends are rejoined to new partners. It involves a pair of sequence-specific DNA sites that serve as a recognition signal for the recombinase that mediates the DNA exchange. Each site-specific recombination system encodes a recombinase enzyme that catalyses the DNA exchange. The reactions involve the rearrangement of DNA sequences in a specific way and are different from homologous recombination reactions in that extensive homology within the region of strand exchange is not required. The systems do not involve synthesis or degradation of DNA, and no high-energy co-factors are required (Stark *et al.*, 1992).

Site-specific recombination of DNA is important in many biological processes in prokaryotic and eukaryotic organisms. Some of these include the resolution of co-integrate intermediates in DNA transposition (e.g. Tn3 resolvase), the regulation and switching of alternate gene expression (e.g. Hin and Gin recombinases), the monomerisation of multimeric plasmids and chromosomes (e.g. XerC and XerD), and the integration and excision of bacteriophage DNA into and out of host chromosomes (e.g. phage integrases). The generation of antibody diversity in metazoans by the VDJ gene shuffling system is an example of a site-specific recombination system in eukaryotes (Stark *et al.,* 1992; Grindley *et al.*, 2006).

Site-specific recombination reactions can be broken down into four stages. First, the recombinase binds to its cognate site by specifically interacting with DNA recognition sequences. Secondly, the two sites are brought together to form a synaptic protein-DNA complex. Thirdly, in the chemical steps, the DNA strands are broken and rejoined in a recombinant configuration (strand exchange). Finally, the complex containing the paired recombination sites dissociates to release the products (Stark *et al.,* 1992).

In prokaryotic systems, the substrates for site-specific recombination reactions are usually circular plasmid DNAs, and the outcome of the reaction depends on the position and orientation of the recombining sites (Figure 1.1). Intermolecular recombination between

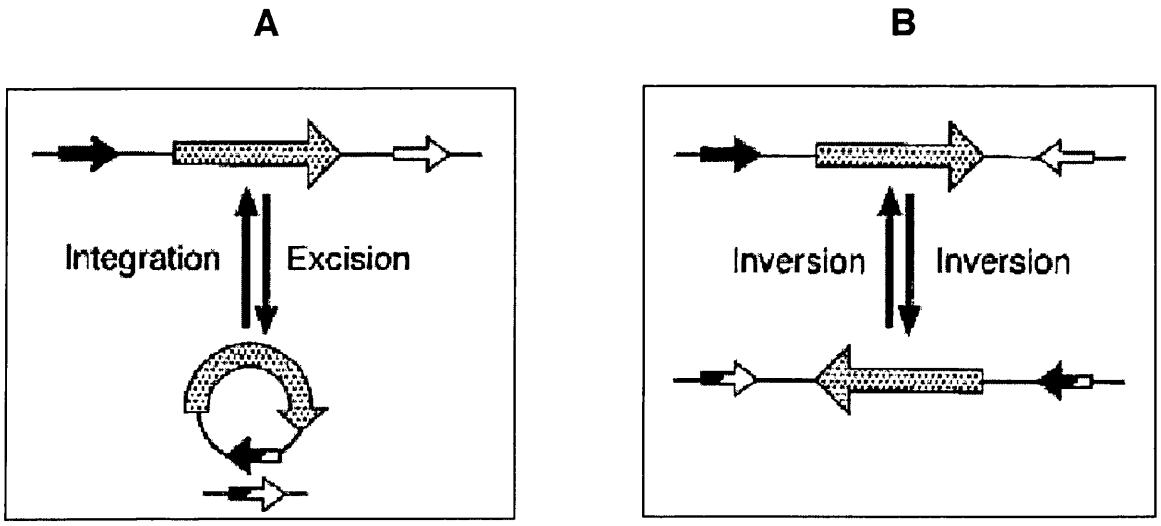

Figure 1.1 Substrates and products of site-specific recombination reactions
The relative positions and orientations of the two recombining sites (small black and white arrows) determine the outcome of recombination. The big arrow represents the DNA segment between the recombining sites. **Panel A**: The excision of the DNA segment between directly repeated sites results in an excision, and the reverse reaction generates an integration product. **Panel B** shows the inversion of the DNA segment between sites in inverted repeat. The figure is adapted from Akopian & Stark (2005).

sites on two circular molecules results in their fusion to form a single DNA molecule. Intramolecular recombination between sites on the same circular molecule has two possible outcomes, which are determined by the relative orientation of the sites (Figure 1.1). Recombination between sites in direct repeat generates two circular products in a reaction known as resolution, deletion or excision, while recombination between inverted repeat sites results in the inversion of the DNA segment between the sites (for a review see Stark *et al.*, 1992).

1.2 The tyrosine and serine recombinases

Two families of conservative site-specific recombination systems can be identified, based upon sequence similarities in the recombination enzymes and the recombination sites, as well as the similarity in the reaction mechanisms (Stark *et al.*, 1992; Argos *et al.*, 1986). The tyrosine recombinases use an invariant active site tyrosine residue to catalyse the cleavage step of the recombination reaction, while the serine recombinases use a conserved serine residue. The recombination sites of the tyrosine and serine recombinases often contain in addition to the crossover site, additional sites that the recombinase or other accessory proteins bind. Proteins bound to these additional or accessory sites often perform structural roles in the assembly of the functional catalytic system required for recombination, or regulatory roles that determine the outcome of recombination. In both systems, DNA cleavage is accomplished by nucleophilic displacement of a DNA hydroxyl by the hydroxyl group of a serine or tyrosine side chain of the recombinase (Figure 1.2). The phosphoryl transfer reactions are believed to occur through the in-line nucleophilic displacement of the DNA hydroxyl group by the hydroxyl group of the protein side chain, via a pentacoordinate transition state (Mizuuchi & Baker, 2002; Grindley *et al.*, 2006). Catalysis is carried out in a synaptic complex involving a protein tetramer, and recombination proceeds via a protein-DNA covalent intermediate (Figure 1.2).

Members of the tyrosine recombinase family include phage λ integrase, Cre recombinase of phage P1, FLP recombinase of the yeast 2-micron plasmid, and the XerC and XerD recombinases of *E.coli*. The tyrosine recombinases are flexible with respect to substrate

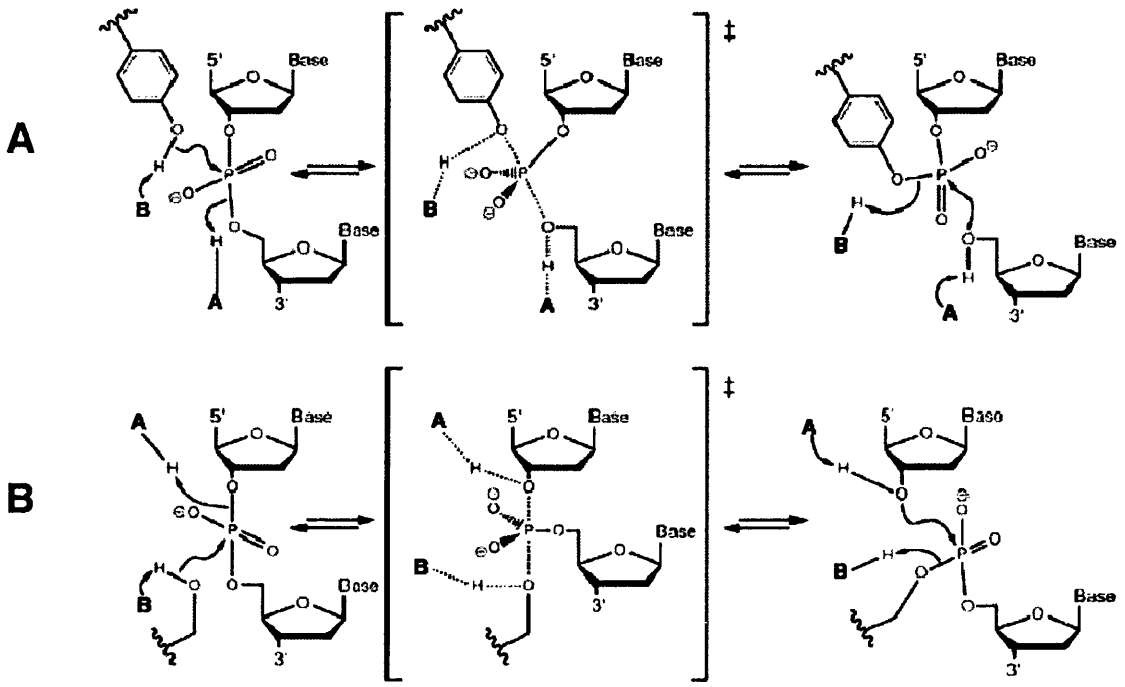

Figure 1.2 Phosphoryl transfer reactions catalysed by tyrosine (A) and serine (B) recombinases.

Cleavage likely proceeds through the in-line nucleophilic displacement of a DNA hydroxyl by the nucleophilic protein side chain and ligation by the reverse reaction involving the 5' OH (tyrosine recombinases) or 3' OH (serine recombinases) of the DNA. Catalysis may involve the participation of a general base (B) to accept a proton from the appropriate protein side chain and a general acid (AH) to protonate the leaving DNA oxygen (and vice versa for the ligation reaction). Conserved residues in the active site may position the scissile phosphate and stabilise the transition state during catalysis. The nonbridging oxygens in the transition state are each given a formal negative charge for illustrative purpose since the nature of charge distribution is not clear. (Figure from Grindley *et al.*, 2006)

requirements. For instance, Cre and FLP can use sites in either direct or indirect repeat, or in different DNA molecules, and do not require DNA supercoiling (Craig and Nash, 1983; Hoess & Abremski, 1985; Cox, 1989). Certain members of the tyrosine recombinase family can perform all three types of site-specific recombination reaction (i.e. integration, resolution and inversion), if the sites are in the correct relationship. The tyrosine recombinases are rather divergent, with only four residues (Arg, His, Arg, and Tyr) being highly conserved. They possess a two-domain structure consisting of a carboxyl terminal domain, which contains the catalytic residues for recombination, and a variable N-terminal domain that provides specific DNA binding to the cognate core sites (Hallet and Sherratt, 1997). The overlap region of the recombination core sites (i.e. the sequence between the cleavage positions in the top and bottom strands) consists of a 6-8 bp asymmetric sequence. Strand exchange takes place at the boundary of this region, giving staggered 3' recessed ends. A highly conserved tyrosine residue provides the nucleophile that attacks the scissile bond, giving a 3' phosphotyrosyl linkage (Hallet and Sherratt, 1997; Figure 1.2). Detailed insights into the mechanism of the tyrosine recombinases have come from X-ray structures of synaptic complexes and catalytic intermediates of Cre, Flp, and λ Int (reviewed in Grindley *et al.*, 2006). These structures and other biochemical studies form the basis for the mechanism of recombination by the tyrosine recombinases illustrated in Figure 1.3. Strand exchange within the tyrosine recombinase family involves strands of the same polarity from each recombining partner being exchanged in a sequential fashion to form a four-way junction (Holliday junction) intermediate (Figure 1.3). Resolution of the junction then takes place by the exchange of the second pair of bottom strands (Nunes-Düby *et al.*, 1995) to form the recombinant products.

The serine recombinases include the DNA invertases Gin, Hin and Cin, and many transposon resolvases such as Tn3, γδ, Tn*21*, Tn*552*, Tn*501*, Tn*1721* and Tn*2501*. The phage integrases, φc31 Int and BxB1 Int are also members of the serine recombinases (Smith & Thorpe, 2002). These enzymes are related at the amino acid level (Hatfull and Grindley, 1988). Members of the serine recombinase family are more selective than the tyrosine recombinases with respect to the reactions they catalyse. The constraint in site

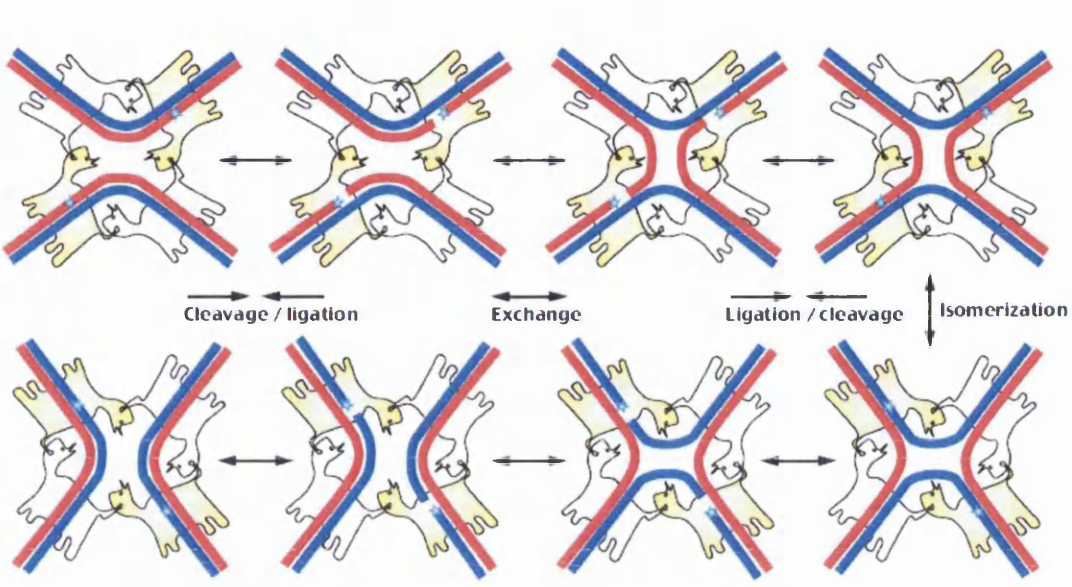

Figure 1.3 Mechanism of recombination by tyrosine recombinases.
The scheme illustrates the catalysis of strand exchange by the tyrosine recombinases. The synaptic complex comprises two DNA duplexes bound by four recombinase subunits arranged in a head-to-tail fashion. The DNA strands are shown as blue and red lines. Recombinase subunits that are active at the different steps are in pale yellow, while the inactive ones are in white. The blue stars represent active catalytic centers in the active recombinase subunits. One strand from each duplex is cleaved, exchanged, and ligated to form a Holliday junction (rightmost two panels). Isomerization of this junction switches catalytic activity in the synapse between the two pairs of recombinase subunits. (Figure from Grindley *et al.*, 2006).

configuration for resolvases/invertases (inverted repeated sites for invertase; directly repeated sites for resolvases) strongly suggests that the reactions they can catalyse are strictly controlled. This is evident by the characteristic changes in DNA topology and the limited number of topological products formed by each reaction (Section 1.4.4). Cleavage occurs at the 2 bp overlap sequence in the centre of the core sites, producing 2 bp staggered double-strand breaks with recessed 5' ends and a 5' DNA-phosphoseryl intermediate. Attack by the 3' OH of the partner duplex strand, followed by religation of ends, produces the recombinant configuration (Stark *et al.*, 1992; Figure 1.4). The topology of resolution and inversion can be accounted for by a model in which strand exchange proceeds by a concerted cleavage of all four DNA strands, to yield double strand breaks with a recombinase subunit covalently attached to each 5' phosphate. A right handed 180^{o} rotation of a pair of half sites (one half-site from each substrate site) then reorganises the DNA into the recombinant configuration (Stark *et al.,* 1992; Figure 1.4). The details of the chemical mechanisms of the serine recombinases are less understood compared to the tyrosine recombinases. However, recent structures of the catalytic synaptic complex of γδ resolvase have provided more insights into the mechanism of the serine recombinases (Section 1.10; Grindley *et al.*, 2006).

1.3 Tn3 transposition

Tn3 (4957 bp) is a transposable element (transposon) found in some gram-negative bacteria (including *E. coli*) where it confers resistance to penicillins such as ampicillin. The transposon encodes the proteins transposase and resolvase and contains a recombination site (*res*). It is flanked by inverted repeats of 38 bp (Figure 1.5). The biology and regulation of Tn3 transposition are reviewed in Grindley (2002). The initial product of the replicative transposition reaction catalysed by Tn3 transposase is a cointegrate, in which there are two copies of Tn3, in direct repeat. They are resolved into two functional plasmids which both contain a copy of Tn3 by resolvase (Figure 1.5), encoded by the *tnpR* gene.

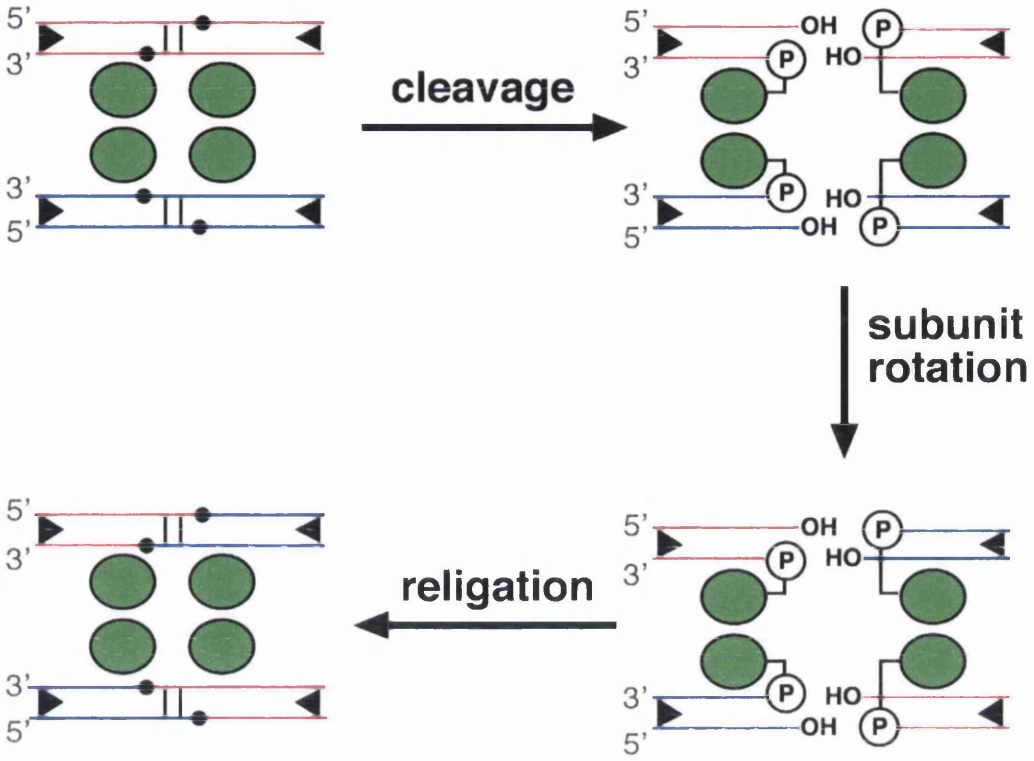

Figure 1.4 Mechanism of recombination by serine recombinases.
The scheme illustrates the cleavage, subunit rotation, and religation steps of recombination. The cartoon shows a synaptic complex, formed from a pair of resolvase-bound site Is. Only the catalytic domains of the resolvase subunits (green ovals) are shown. The small black ovals represent the phosphate groups attacked by the recombinase. The inverted black arrowheads represent the ends of site I. The DNA strands are shown as red and blue lines. Strand exchange is assumed to involve rotation of the resolvase subunits in covalent attachment to the DNA, followed by the religation step. (Adapted from Stark *et al.*, 1992).

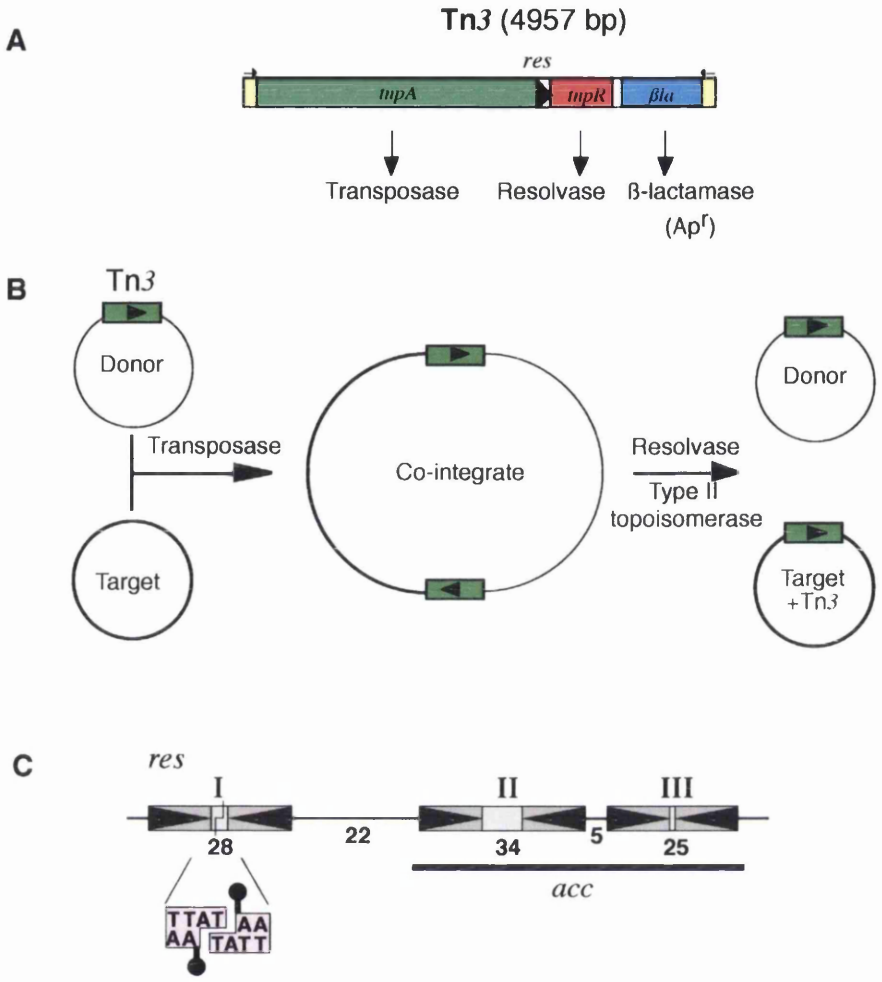

Figure 1.5 Schematic illustration of Tn3 transposition and cointegrate resolution **Panel A**: Structural organization of Tn3 transposon. The yellow boxes represent the transposon ends, and the black arrowhead represents the *res* site. The green, red and blue segments represent the genes coding for transposase, resolvase, and β-lactamase. **Panel B**: Schematic illustration of the transposition pathway. The transposase catalyses the duplication and insertion of Tn3 into a target plasmid, to form a cointegrate. Resolvase separates the cointegrate into two plasmids, each having a copy of Tn3. **Panel C**: Structural organization of the functional units of *res* (114 bp). The resolvase binding sites I, II, and III are shown as rectangular boxes. The Arabic numbers indicate the length of the various segments in base pairs. The imperfect conserved motifs at each end of the sites (black arrowheads) are 12 bp in length, and are separated by 4 bp, 10 bp, and 1 bp in sites I, II, and III respectively. The pink box shows the central six base sequence of site I and the staggered breaks made by resolvase in the DNA during cleavage and recombination. The lollipops represent resolvase subunits covalently joined to the 5' end of the cleaved DNA. (Panels A and B are from Blake, 1993; Panel C is from Burke *et al.*, 2004)

1.4 Mechanism of resolvase-catalysed recombination

DNA recombination catalysed by resolvase is mechanistically complex. The process involves binding of resolvase to the recombining *res* sites, synapsis of the two *res* sites, cleavage of the DNA, strand exchange, and religation of the DNA in the recombinant configuration (Figure 1.6). Wild-type Tn3 resolvase only catalyses recombination on substrates in which the *res* sites are in direct repeat on the same DNA molecule, and the DNA substrate has to be negatively supercoiled (Stark *et al.*, 1992).

1.4.1 Tn3 *res* site

Tn3 resolvase-catalysed recombination occurs at sites called *res* (114 bp) that contain three distinct binding sites, site I (the crossover site), and sites II and III (the accessory sites or *acc*) (Figure 1.5). The recombination reaction requires the interaction of 12 subunits of resolvase with the two recombining *res* sites that have to be in the same molecule in direct repeat (Grindley, 2002). In addition, negative supercoiling is required for resolvase to act upon its substrate (Reed, 1981). Sites I, II, and III are irregularly spaced within *res* and have different sequences (Benjamin & Cozzarelli, 1990). Each consists of an imperfect inverted repeat of a recognition motif separated by a short spacer (Figure 1.5). Each binding site (I, II, and III) binds a resolvase dimer in conformations that could reflect their different functional roles in catalysis (Grindley, 2002). The recombination reaction occurs in a synaptic complex (called in this thesis the "*res* synapse"), which comprises two basic functional units (Figure 1.6). The catalytic unit where the chemical and conformational steps of recombination are mediated is described here as the "site I synapse". A structure involving sites II and III (here called the "*acc* synapse") is believed to be the regulatory unit that controls the assembly and activation of the site I synapse (Figure 1.6).

1.4.2 Binding to *res*

There are three binding sites in each *res* site (Section 1.4.1; Figure 1.5), and each of the binding sites binds two subunits of resolvase. How is the resolvase dimer-DNA complex formed at the dimer-binding sites? Tn3 resolvase forms the site II dimer complex by a two-step cooperative binding of monomer subunits to the site, while γδ resolvase dimer

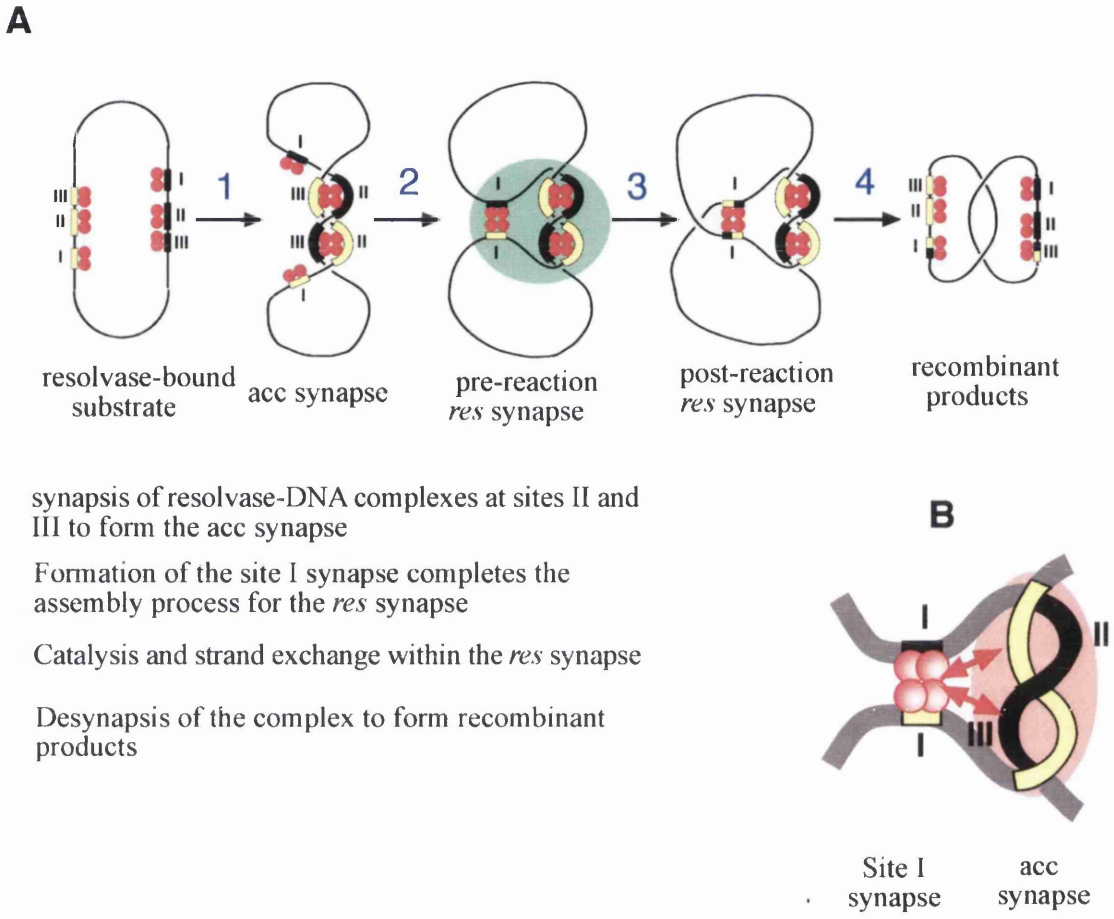

Figure 1.6 Schematic illustration of synapsis and recombination by Tn3 resolvase. **Panel A:** The cartoon shows the hypothetical pathway for the assembly of the *res* synapse and subsequent strand exchange. The red spheres represent resolvase subunits bound to the recombining *res* sites (yellow and black boxes) on the supercoiled substrate. The green shading in the pre-reaction *res* synapse indicates that the exact nature of the complex is unknown. **Panel B:** This picture illustrates the hypothetical role of the *acc* synapse in activation and regulation of catalysis at the site I synapse. The red arrows indicate a proposed interaction between the site I synapse and the *acc* synapse. (The Figure is adapted from W.M. Stark, personal communication).

binds to site II in a single step (Blake *et al.*, 1995). Tn3 and γδ resolvases are dimeric in solution at high concentrations (Symington, 1982; Liu *et al.*, 1993). Sedimentation equilibrium and sedimentation velocity analytical ultracentrifugation experiments showed that at concentrations less than 1 μM, Tn3 resolvase is > 95% monomeric in solution (Nollmann *et al.*, 2005). While γδ resolvase likely binds as a dimer to the subsites of *res* (Hughes *et al.*, 1993), the more monomeric character of Tn3 resolvase suggests a stepwise binding mechanism in forming the dimer complex at the subsites. Fluorescence anisotropy measurements showed that site II and site III of *res* have the highest affinity for Tn3 resolvase followed by site I (Nollmann *et al.*, 2005). The estimated dissociation binding constants reported were 40 nM (site I), 20 nM (site II), and 30 nM (site III). It is believed that resolvase, like other DNA-binding proteins, interacts with DNA non-specifically and then slides along the molecule by a three-dimensional diffusion process until it finds and binds specifically to the *res* site (Gowers & Halford, 2003). Negative supercoiling may facilitate the collision of two *res* sites by reducing the volume of the DNA (Benjamin *et al.*, 1996).

Binding of resolvase to *res* leads to the bending of the binding sites in ways that reflect the different geometries of the individual binding sites (Salvo & Grindley, 1988). The bend at site I is toward the major groove with the catalytic domains of resolvase on the outside of the bend (Yang & Steitz, 1995). Bandshift and DNase I cleavage experiments suggest that sites II and III are each bent into the minor groove placing the catalytic domains of resolvase on the inside (Salvo & Grindley, 1988; Grindley, 2002). The binding of resolvase to the binding sites is a cooperative process and the formation of the resolvase-*res* complex involves protein-protein interactions between the subunits bound at the different binding sites (Grindley, 2002).

1.4.3 The *res* synapse

Synapsis is the process in which two resolvase-bound *res* sites come together to assemble the active protein-DNA complex (the "*res* synapse") capable of carrying out recombination (Figure 1.6). Since all three dimer-binding sites of *res* are required for recombination (Grindley *et al.*, 1982), the *res* synapse presumably consists of twelve

subunits of resolvase in association with a pair of *res* sites. The assembly of this highly organised catalytic structure is one of the least understood events in resolvase-catalysed recombination, and may involve the coordination of several protein-DNA and protein-protein interactions. The coordinated catalytic and conformational events of recombination by resolvase happen within the *res* synapse (Grindley, 2002). The biochemical properties of activated resolvase mutants (Section 1.9) show that resolvase has an inherent catalytic prowess that is not dependent on the presence of a complete *res* site. This suggests that one of the requirements for the *res* synapse in recombination by wild-type resolvase is to ensure that catalysis by resolvase is activated only in the context of *res*.

Details of the structure of the *acc* synapse (the resolvase-DNA complex formed with the accessory sites II and III) and its specific role in the activation of catalysis at the site I synapse are unknown. This role could be structural and/or regulatory (Stark *et al.*, 1992). The *acc* synapse may be involved in bringing the two copies of site I together prior to the assembly of the complete *res* synapse. The intertwining of the *acc* sequences, a requirement for the formation of the *res* synapse, is implicated in topological selectivity (Benjamin and Cozzarelli, 1988; Grindley, 2002; Stark *et al.*, 1994; Watson *et al.*, 1996). Recent evidence suggests that the *acc* synapse may be important for activation of the catalytic functions of the site I synapse in wild-type resolvase (Murley & Grindley, 1998; Nollmann *et al.*, 2005; Figure 1.6). This activation could involve holding the two site Is together in a configuration suitable for catalysis and/or direct activation of catalysis.

1.4.4 Synaptic models and topological selectivity of Tn3 resolvase

Significant insights into the nature of the *res* synapse came from a series of topological and biochemical experiments (reviewed in Stark *et al.*, 1992 and Grindley, 2002). In the *res* synapse, the two *res* sites are interwrapped and the synapsed site Is trap three negative superhelical interdomainal nodes by intertwining of the sites II and III DNA (Figure 1.7; Wasserman *et al.*, 1985; Benjamin & Cozzarelli, 1988; 1990; Stark *et al.*, 1989). Stark *et al.* (1989) showed that the interwrapping of the *res* sites was due to plectonemic and not solenoidal supercoiling.

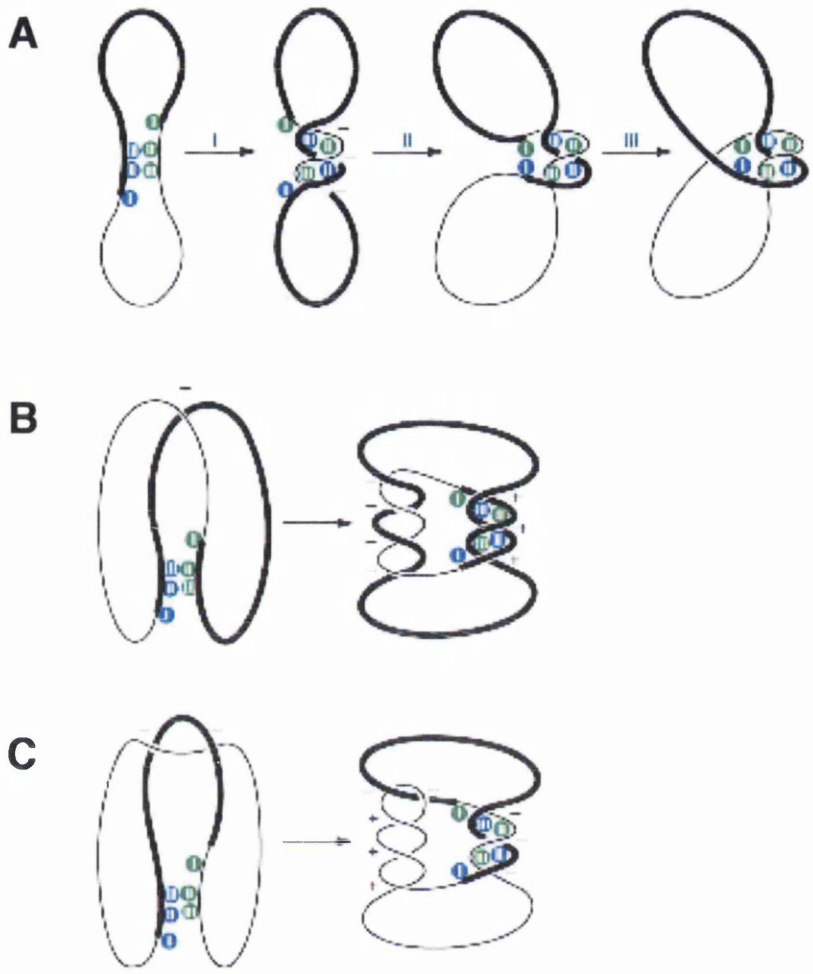

Figure 1.7 Two-step topological filter model for *res* site synapsis
Sites I, II, and III of each *res* site on the supercoiled DNA substrate are shown as blue and green ovals. **Panel A** shows the two-step synapsis model in which synapsis is initiated by resolvase-mediated antiparallel pairing of subsites II and III, trapping three negative nodes. This first step facilitates the productive pairing of both site Is. **Panel B** illustrates the consequence of pairing inverted *res* sites. To obtain antiparallel pairing of subsites II and III, at least one interdomain node must be formed. The subsequent interwrapping of the two *res* sites causes a further four interdomain nodes to form. The consequence of trapping two negative interdomain nodes at the initiation stage is illustrated in **Panel C**. To compensate for the wrapping of subsites II and III around resolvase, three positive intradomain nodes must be introduced into one of the two substrate domains. (Figure is from Grindley *et al.*, 2006).

Several models have been proposed to explain the assembly of the *res* synapse (reviewed in Grindley, 2002). The main features of these models are highlighted below. The tracking model proposes that a resolvase-*res* complex forms a loop and then scans along the DNA until the second resolvase-*res* complex is located by one dimensional diffusion (Krasnow and Cozzarelli, 1983). This model explains the selection against intermolecular recombination and reactions between inverted *res* sites. However, this model has been refuted based on the results of an experiment in which reporter rings catenated to the two-*res* DNA substrate were used (Benjamin *et al.*, 1985). The slithering model involves the movement of DNA round a fixed superhelical axis. The interwound segments of DNA are proposed to move past each other, eventually leading to the juxtaposition of the two *res* sites across the superhelical axis (Benjamin and Cozzarelli, 1990; Sessions *et al.*, 1997). However, there is no direct evidence to show that slithering drives diffusion in supercoiled DNA.

The topological filter model (Boocock *et al.*, 1987; Stark *et al.*, 1989; Figure 1.7) proposes that the formation of the *res* synapse is controlled by DNA topology. In this model, the *res* sites initially interact by random collision to give synaptic complexes with varying topologies. The synaptic conformations where the *res* sites initially form a structure where no interdomainal nodes are trapped (Figure 1.7, Panel A) will give rise to the productive synapse (in which three negative supercoils are trapped between the *res* sites), which is required for recombination. Any unproductive synapses formed would need to dissociate and re-attempt to build a correct initial synaptic complex (Watson *et al.,* 1996). The model assumes that synapsis occurs in two steps, both of which are topological in concept; The first step is the interwrapping to generate three negative interdomainal nodes, and the second step is the parallel alignment of the site Is. The topological filter model explains the selectivity of the resolvase reaction. For instance, experiments using protein crosslinking reagents have given direct experimental evidence for synapsis of inverted repeat sites (Watson *et al.*, 1996). The topological filter model would propose that the inverted repeat sites may interact to form a stable synaptic complex, but one that is completely unproductive (Figure 1.7).

1.4.5 Crossover site cleavage

The assembly of a productive *res* synapse is followed by a series of catalytic events starting with the nucleophilic attack of the four resolvase subunits in the site I synapse to form two double-strand breaks (Grindley *et al.*, 2006). In this reaction, the resolvase subunits are covalently joined via phosphoseryl linkages to the 5' end of the cleaved DNA strands and free hydroxyl groups are left at the 3' ends (Reed & Grindley, 1981; Reed & Moser, 1984; Figure 1.4). Crossover site cleavage involves staggered cuts around the central AT dinucleotide of site I and results in two-base single strand extensions at the 3' end (Reed & Grindley, 1981; Figure 1.4). Falvey *et al.* (1988) showed that single-strand nicking was observed in experiments on DNA containing mutations at the central dinucleotide, providing support for a sequential single-strand cleavage mechanism. Furthermore, studies on heterodimers of wild-type and mutant resolvases showed that single-strand cleavage products are formed, and that the top strand is cleaved more frequently (Boocock *et al.*, 1995). In addition, the asymmetric arrangement of the DNA-resolvase dimer complex in the crystal structure suggests that cleavage may occur first on one strand and then on the other (Yang and Steitz, 1995). Hence, while all four DNA strands must be broken before strand exchange occurs, the cleavage events likely happen in a sequential rather than concerted fashion. Targeting experiments with resolvase mutants which bind specifically to altered DNA half-sites were used to show that the S10 nucleophile required for strand cleavage and other putative active site residues are provided by the resolvase subunit bound at the adjacent half-site (Boocock *et al.*, 1995).

1.4.6 Strand Exchange

Subunit rotation is a simple model that explains resolvase-catalysed strand exchange and accounts for most of the experimental biochemical and topological data (Sherratt, 1989; Stark *et al.*, 1989a; Stark *et al.*, 1992). In this model, the resolvase subunits that form the site I synapse catalyse double-strand cleavage of both crossover sites with each resolvase monomer covalently attached to the half-site at which it is bound. This is followed by a 180° right-handed rotation of one half of the complex along with the attached half-sites to bring the cleaved DNA molecules into a recombinant configuration. The strands are then

re-ligated, and the synapse dissociates to release the recombinant catenated products (Figure 1.4).

No direct biochemical evidence exists for subunit rotation, but the model is consistent with all of the topological data obtained (Cozzarelli *et al.*, 1984; Wasserman *et al.*, 1985; Kanaar *et al.*, 1988; Kanaar *et al.*, 1990; Stark *et al.*, 1991; Heichman *et al.*, 1991; Klippel *et al.*, 1993; Stark & Boocock, 1994). The main topological evidence in support of subunit rotation came from experiments in which the changes in superhelicity (ΔLk) accompanying recombination were measured (Stark *et al.*, 1989; Stark and Boocock, 1994). A value of +4 was obtained for Tn3 resolution and -4 for fusion of the two catenanes, which implied that catenane fusion was a reversal of the forward reaction (Stark *et al.*, 1994). The subunit rotation model also explains the minor products formed in resolvase-catalysed reactions (the four-noded knot, five-noded catenane and six-noded knot) by simple repetition of the rotation step without re-ligation of the recombinant intermediate.

1.5 Structure of resolvase

Research on the structures and mechanisms involved in resolvase-mediated recombination has benefited greatly from a series of crystal structures from the Steitz laboratory, revealing γδ resolvase and complexes of γδ resolvase with DNA. The first structures to be solved were of the N-terminal domain of γδ resolvase (Sanderson *et al.*, 1990; Rice & Steitz, 1994 a, b; PDB codes 2RSL and 1GDR; see Section 1.6, Figure 1.10). These were followed by a structure of an entire γδ resolvase dimer bound to site I (Yang & Steitz, 1995; PDB code 1GDT; see Section 1.6, Figure 1.11). Recently, structures of activated γδ resolvase mutant tetramers in synaptic complexes with cleaved site I DNA have been solved, as well as a related structure of a γδ resolvase tetramer without DNA (Li *et al.*, 2005; Kamtekar *et al.*, 2006; PDB codes 1ZR2, 1ZR4, 2GM4, 2GM5; see Section 1.10, Figure 1.15). Further structural information on resolvase has come from NMR (Pan *et al.*, 2001) and small-angle scattering studies (Nollmann *et al.*, 2004).

Tn3 resolvase is a 20 kDa (185 amino acids) protein. Information on its structure is based on the solved crystal structures of the closely related serine recombinase, γδ resolvase. Tn3 and γδ resolvase share approximately 80% sequence identity (Figure 1.8, Panel A), have very similar *res* sites, and bind and catalyse recombination at each other's *res* sites (Grindley, 2002). Other serine recombinases related to Tn3 resolvase and which have been studied *in vitro* include Tn21 resolvase, and the DNA invertases Gin and Hin (Grindley, 2002). The three dimensional structure of γδ resolvase consists of seven α-helices (αA, αB, αE, αF, αG, and αH) and five β-helices (β1, β2, β3, β4, β5) (Figure 1.9). The protein consists of two functional domains, as was first observed in chymotryptic cleavage analyses (Abdel-Meguid *et al.*, 1984). The N-terminal domain (residues 1-140) is the catalytic part of resolvase, which mediates interactions that sustain its dimer structure (Yang & Steitz, 1995). The N-terminal domain is also required for the interdimer contacts needed for the assembly of the site I synapse (Li *et al.*, 2005). The C-terminal domain (residues 141-185) is involved in DNA binding (Abdel-Meguid *et al.*, 1984; Rimphanitchayakit & Grindley, 1990). When in contact with DNA, the C-terminal domain adopts a helix-turn-helix conformation characteristic of major groove-binding proteins (Yang & Steitz, 1995), but it appears to be disordered in the absence of DNA (Rice & Steitz, 1994b).

There are five recognizable clusters of well-conserved residues in Tn3 resolvase and related resolvases/invertases (Grindley, 2002; Figure 1.8, Panel B). Motif A consists of residues 5 to 19. This region includes some residues (Y6, R8, V9, Q14, and Q19) that form parts of the active site, and S10, which is the nucleophile in the first transesterification reaction (cleavage step) of recombination (Section 1.8). Motif B (residues 35 to 48) is perhaps the least understood region of the resolvase molecule. Putative active site residues D36, S39, and R45 are located in this region. Crystallographic evidence shows that motif B adopts variable folding patterns (Rice & Steitz, 1994b; Yang & Steitz, 1995) and hence is often referred to as the 'mobile loop'. The region might be involved in the regulation of recombination or might have a direct role in the catalytic process. Residues 58 to 71 make up motif C, which along with the highly conserved motif A forms a major part of the enzyme's active site. The conserved

A

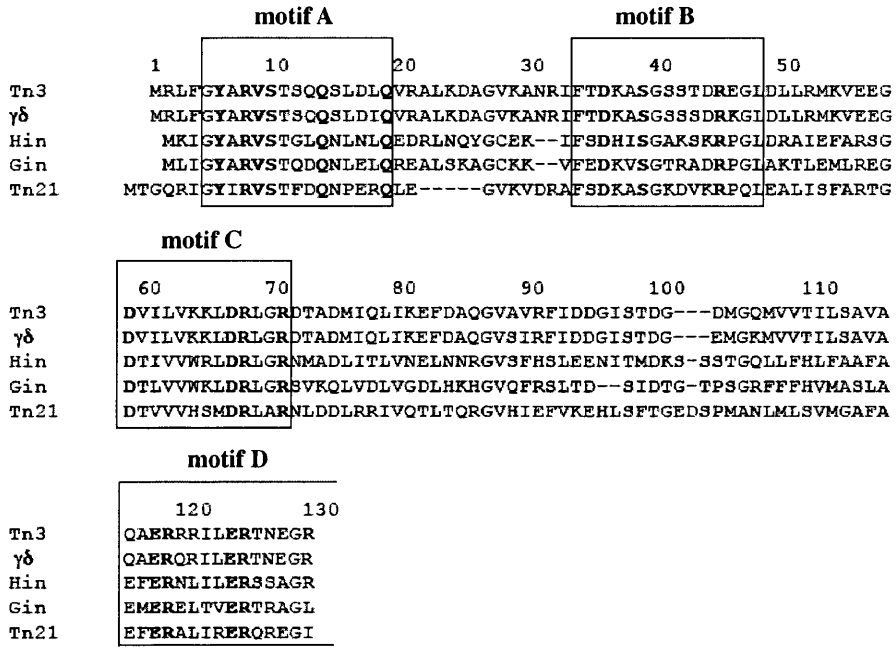

B

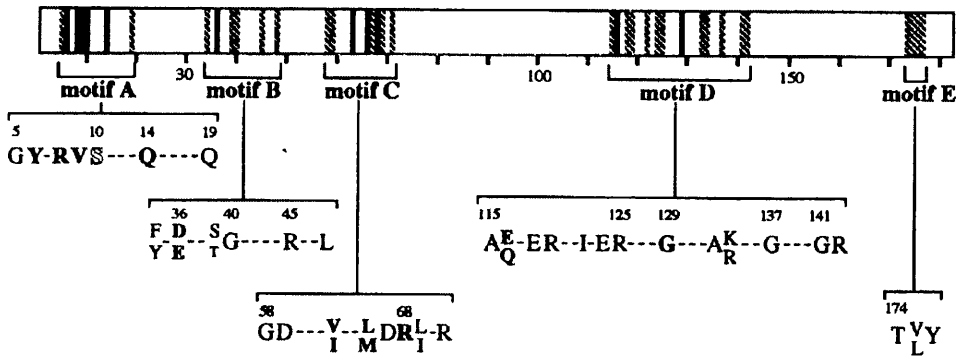

Figure 1.8 Conserved sequence motifs and sequence alignment of part of the N-terminal domain of selected resolvases and invertases closely related to Tn3 resolvase

Panel A: Sequence alignment of part of the N-terminal domain of serine recombinases. The sequence alignment was generated with CLUSTAL W (1.83). The highlighted residues are the ones chosen for mutagenesis in this study (Section 4.1). The sequences of the resolvases and invertases most studied *in vitro* are shown. Residues that form the motifs shown in Panel B are enclosed in boxes. **Panel B** shows conserved motifs in the structure of resolvase. The bar represents the amino acid sequence of γδ resolvase. Residues that are totally conserved are shown as black bars; those that are highly conserved are crosshatched (Grindley, 2002).

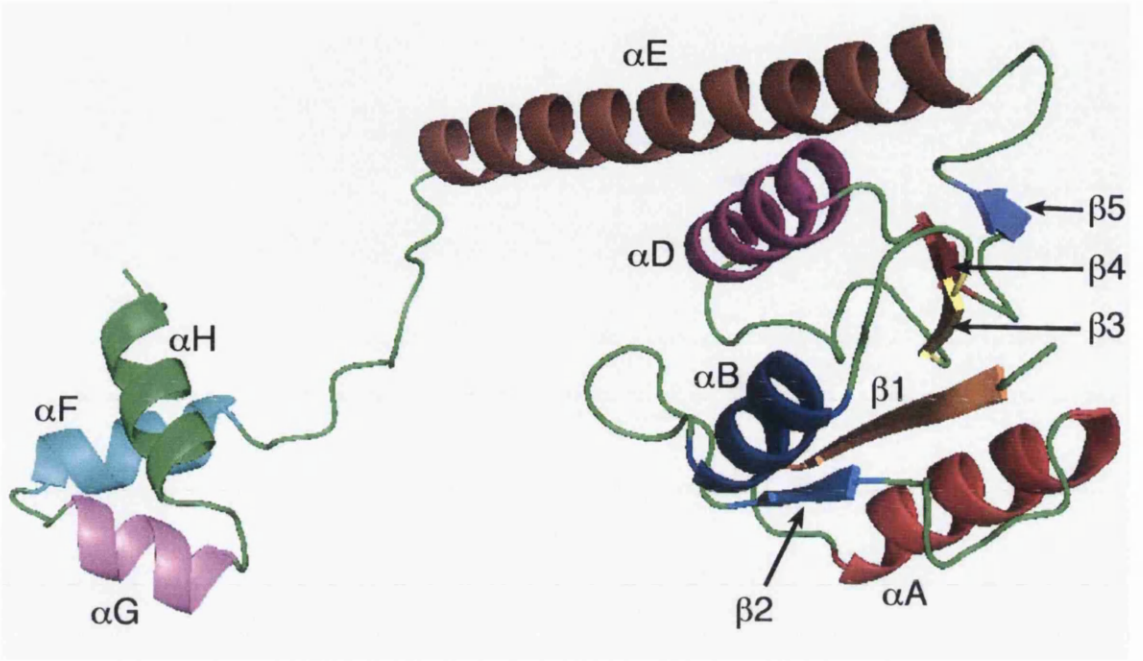

Figure 1.9 Three-dimensional structure of γδ resolvase, highlighting the secondary structures.

The N-terminal domain consists of the α-helices A, B, D, and E, and the β-sheets 1, 2, 3, 4, and 5. The α-helices F, G, and H are in the C-terminal domain. The picture was generated from PDB coordinates of 1GDT (Section 2.35). Subunit B of the resolvase dimer-DNA complex is shown (Yang & Steitz, 1995).

residues with likely catalytic function in this motif are D67, R68, and R71. In addition, L66 and G70, residues of which activating mutations were identified (Section 1.9), could have regulatory roles in controlling the accessibility of the nearby catalytic residues during synapsis and catalysis (Burke *et al.*, 2004). Motif D (residues 115 to 142) forms part of the E-helix that makes close contacts with DNA and is involved in some intersubunit contacts stabilising the resolvase dimer. The role of the E-helix in the structural transitions accompanying synapsis has been revealed by recent crystal structures of the site I synapse (Li *et al.*, 2005; Kamtekar *et al.*, 2006; Section 1.10). Several activating mutations were found on or close to the E-helix (Section 1.9) suggesting the important regulatory function of motif D in recombination. Furthermore, the well-conserved residues E118, R119, E124, and R125 likely have important structural, catalytic and regulatory roles in recombination. The only cluster recognisable in the C-terminal domain, motif E (residues 174 to 176) is linked with the site recognition and DNA binding function of the domain (Grindley, 2002).

1.6 The 1-2 dimer interface and resolvase dimer-DNA complex

The crystal structure of the catalytic domain (residues 1-120) of γδ resolvase (Sanderson *et al*, 1990; Figure 1.10) provided the first line of evidence for the relevance of the 1-2 dimer interface in resolvase function. Mutagenesis of residues along the crystallographic dimer interfaces and crosslinking experiments were subsequently used to demonstrate that the 1-2 dimer is the solution form of resolvase that binds DNA (Hughes *et al*, 1993).

The structure of γδ resolvase complexed with a 34 bp site I DNA (Figure 1.11; Yang & Steitz, 1995) provides direct evidence for the role of the 1-2 dimer interface. The resolvase subunits dimerise along the 1-2 interface and the dimer interacts with site I near the scissile position. The N-terminal domain assumes the same structure as seen in the earlier crystal structures of the protein without DNA. The distance between the two S10 residues in the dimer is over 30 Å, as it is in the monomer structure (Sanderson *et al.*, 1990; Rice & Steitz, 1994), and the hydroxyl groups of the S10 residues are situated 17 Å and 11 Å away from the phosphorus atoms of the closest scissile phosphates. Hence, while the dimer complex likely represents a relevant form of resolvase-DNA complex in

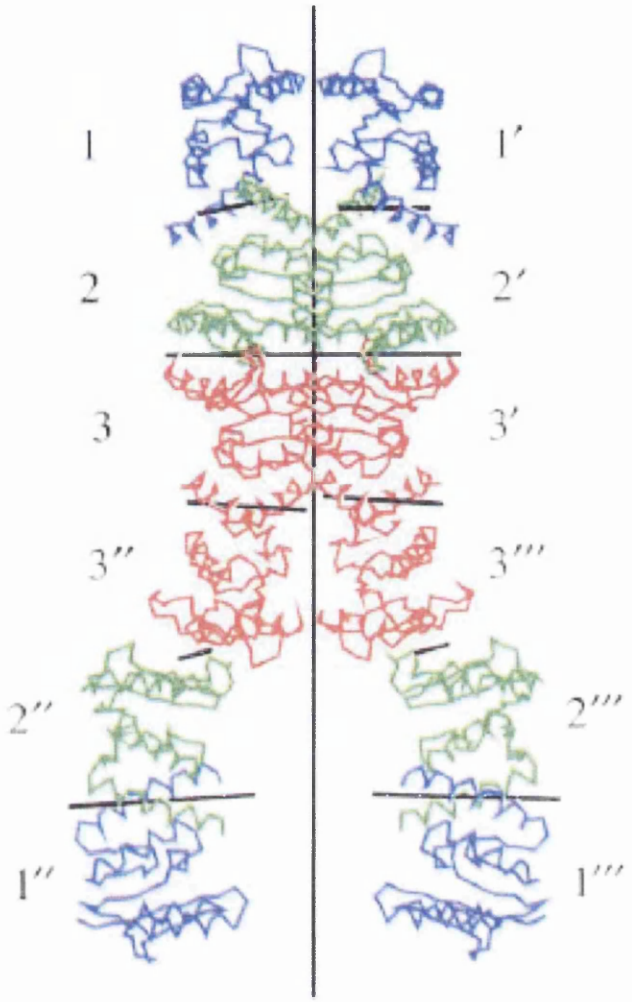

Figure 1.10 Diagram of the packing of resolvase monomers in the γδ resolvase crystal structure

The diagram shows the α-carbon backbones of 12 monomers comprising four asymmetric units, along with the dyad axes that relate them to one another. Each asymmetric unit contains three independent monomers (numbered 1, 2, and 3) related to one another by imperfect non-crystallographic dyad axes. Monomer 1 and all symmetry related molecules are shown in blue; monomer 2, green; and monomer 3, red. (Figure is from Rice & Steitz, 1994b).

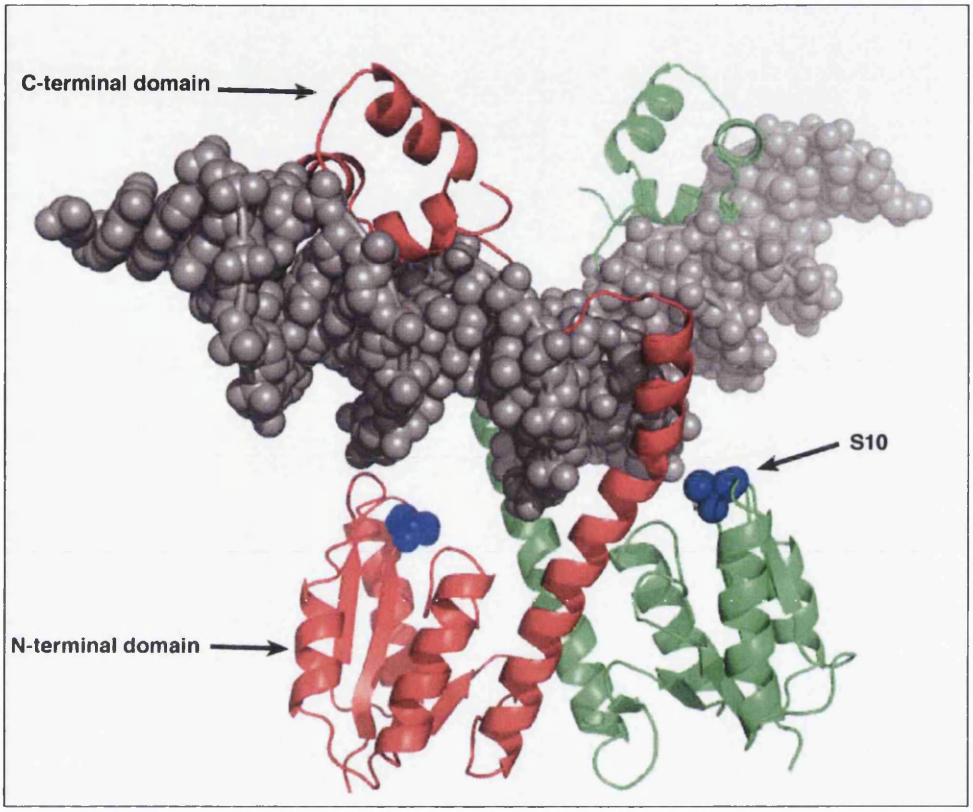

Figure 1.11 Structure of the γδ resolvase site I-DNA complex
Resolvase monomers A and B are shown as red and green cartoons respectively, while the DNA is coloured grey. In both resolvase subunits, the nucleophilic S10 residues are shown as blue spheres. The picture was generated from PDB coordinates of 1GDT (Section 2.35).

the recombination pathway, the catalytic S10 residues are not functionally positioned for catalytic interactions. One of the key features of the dimer-DNA complex is that the C-terminal domain, which was disordered in the absence of DNA (Sanderson *et al.*, 1990; Rice & Steitz, 1994a) forms a 3-helix (αF, αG, and αH) major groove-recognising DNA-binding domain on the opposite side of the DNA from the catalytic domain.

The "arm region" of resolvase that connects the globular part of the N-terminal domain to the DNA-binding domain in both monomers binds the minor groove of the central 16 bp of site I in the dimer complex (Figure 1.11). In contrast, the DNA-binding domains interact via the major groove with the outer 6 bp of site I. Thus, the resolvase dimer completely encircles the entire 28 bp of site I in the cocrystal structure. The dimer complex reveals an asymmetric arrangement. The arm region of monomer B contains a straight E-helix sitting above the minor groove. The corresponding E-helix in monomer A is kinked toward the minor groove. In addition, the centre of the DNA is closer to monomer B than monomer A. It has been suggested that this asymmetry raises the possibility of a sequential single-strand cleavage mechanism during catalysis (Yang & Steitz, 1995; Grindley, 2002). The DNA in the complex is bent by 60^{o} toward the major groove and away from the N-terminal catalytic domains of resolvase at the central TATA base pairs of site I. The structural distortion may be important for the chemical and/or conformational steps of recombination.

1.7 The 2-3' interface

The 2-3' interface is a crystallographic surface (Figure 1.12) between monomer subunits of γδ resolvase (Sanderson *et al.*, 1990; Rice & Steitz, 1994a, 1994b). The 2-3' interface is formed by the four residues R2, R32, K54, and E56. However, these residues do not interact in any of the DNA-resolvase co-crystal structures solved so far (Yang & Steitz, 1995; Li *et al.*, 2005; Kamtekar *et al.*, 2005). These residues are remote from the active site of resolvase and the 1-2 interface that mediates dimerisation of resolvase monomers. Though important for recombination by wild-type resolvase, the 2-3' interactions are not required for the catalytic steps of recombination (Hughes *et al.*, 1990; Grindley, 1993; Murley and Grindley, 1998; Sarkis *et al.*, 2001; Wenwieser, 2001; Burke *et al.*, 2004).

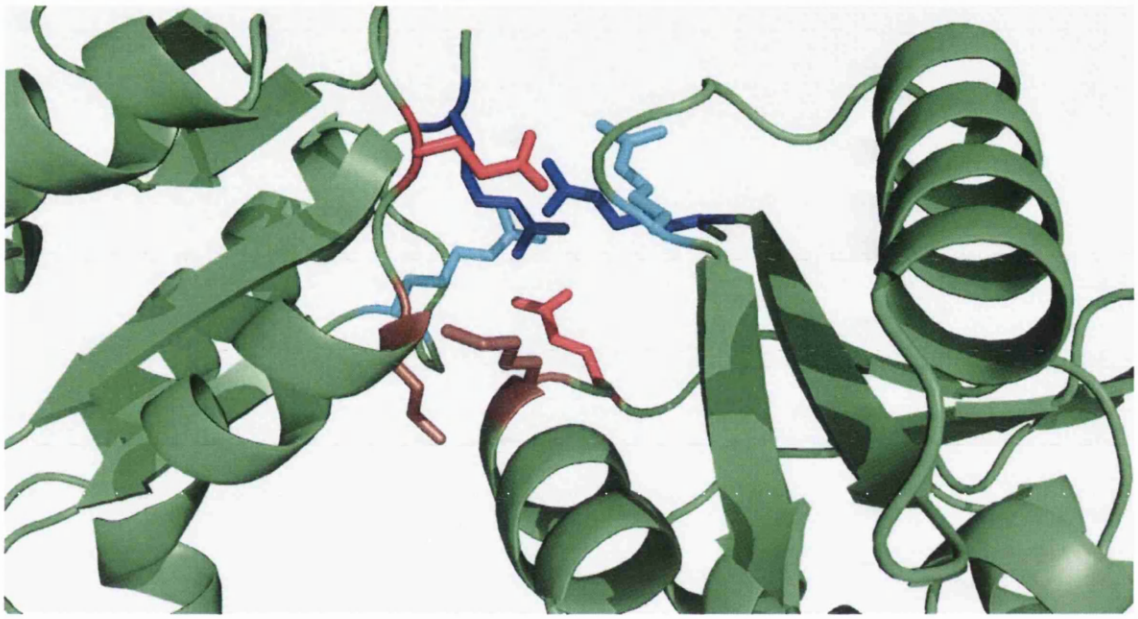

Figure 1.12 Residues of the 2-3' interface in the N-terminal domain of γδ resolvase
The polypeptide backbone of the resolvase molecules is represented as green cartoon, while the side chains of the residues are shown as sticks with the following colouring representations: R2 (blue), R32 (cyan), K54 (brown), and E56 (red). The picture was generated from PDB coordinates of 2RSL (Section 2.35).

Mutations at the 2-3' interface also result in defects in cooperative binding to *res* and synapsis in γδ resolvase (Hughes *et al.*, 1990; Murley & Grindley, 1998).

How is the 2-3' interface involved in synapsis and recombination? Experiments in which 2-3'-deficient resolvase mutants are targeted to sites I, II, and III of *res* show that 2-3'-proficient resolvase subunits are required at the left half-sites of sites II and III for *res* synapsis, and additionally at the right half-sites of sites I and III for recombination (Murley & Grindley, 1998). This suggests that a possible communication between the site I synapse and the *acc* synapse (Section 1.4.3) in the assembly and activation of the *res* synapse is via 2-3' interactions. Significantly, mutations at the 2-3' interface enhance the site I x site I recombination activities of certain activated resolvase mutants (Section 1.9).

1.8 The putative active site of resolvase

The residues that might make up the active site of resolvase were identified from conserved residues in sequence alignment among the serine recombinases (Figure 1.8), biochemical characterisation of site-specific mutants (Hatfull & Grindley, 1986; Hatfull *et al.*, 1989; Hughes *et al.*, 1990; Leschziner *et al.*, 1995), and recognizable motifs in resolvase crystal structures (Sanderson *et al.*, 1990; Yang & Steitz, 1995; Section 1.5). These include: Y6, R8, V9, S10, Q14, Q19, D36, S39, R45, D59, D67, R68, R71, E118, R119, E124, and R125. Initial evidence for the role of S10 as the nucleophile in the cleavage step of recombination came from the finding that the 5'-phosphates of the cleaved DNA were covalently joined to a serine residue in the protein (Reed & Moser, 1984). Subsequent mutational experiments showed that S10 rather than the other well-conserved S39 is essential for catalytic activities (Hatfull & Grindley, 1986). The recently solved crystal structures of the site I synapse show that the cleaved DNA strands are covalently attached to the S10 residues of the resolvase subunits (Li *et al.*, 2005).

It is not entirely clear which of the other conserved residues in the active site have direct roles in catalysis. Some of the catalytic functions that the residues could perform include contribution of functional groups needed to build the geometric and electronic environment of the active site, guide the substrate into the active site, activate the scissile

phosphodiester group, deprotonate the nucleophilic S10, and protonate the leaving group (Mizuuchi & Baker, 2002; Figure 1.2). Based on their high degree of conservation (Figure 1.8), and closeness to S10 in the dimer-site I crystal structure (Figure 1.13; Yang & Steitz, 1995) Y6, R8, Q14, Q19, D36, R68, and R71 are the most likely to be critical residues involved in catalysis. Experiments in which mutant resolvases are targeted to modified half-sites (Boocock *et al.*, 1995) suggest that the complete catalytic site of resolvase requires residues from only one subunit. This is in contrast to the tyrosine recombinase Flp, in which a complete active site is assembled by the contribution of residues from two recombinase subunits (Chen *et al.*, 1992; Lee *et al.*, 1994).

In addition to direct participation in catalysis, conserved residues in the N-terminal domain could be involved in maintaining the structure of the active site such that the catalytic residues are well positioned relative to one another. It is also likely that some residues are required to interact with and position catalytic residues in an inactive configuration in order to prevent activation of catalysis in the wrong context. Apart from functions having to do with catalysis at site I, some conserved residues could be involved in interactions at sites II and III. The importance of some of the putative active site residues in binding and recombination has been studied in Tn3/γδ resolvase and related serine recombinases. The findings of these studies are summarised in Chapter 4 (Table 4.1).

1.9 Deregulation of resolvase by activating mutations

Recent studies on the mechanism of the serine recombinases have been facilitated by the isolation from mutagenesis screens of mutants that bypass some requirements for wild-type recombination (Haffter & Bickle, 1988; Klippel *et al.*, 1988; Klippel *et al.*, 1993; Crisona *et al.*, 1994; Arnold *et al.*, 1999; Burke *et al.*, 2004). These recombinase mutants have been described as having 'hyperactive', 'activated', or 'deregulated' properties. Activated resolvase mutants catalyse recombination on substrates containing only site I without the accessory sites II and III (*acc*), and no longer require supercoiled substrates or directly repeated sites. Some activated Tn3 resolvase mutants catalyse site I x site I

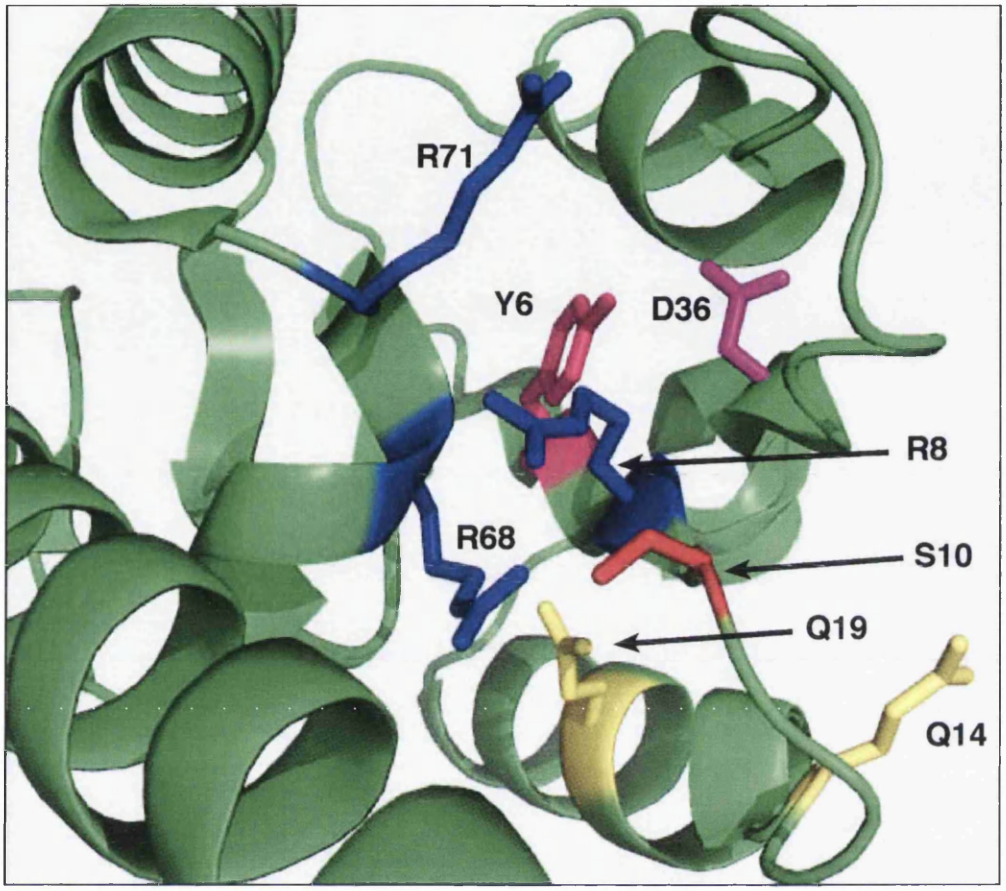

Figure 1.13 Close-up view of putative active site residues in monomer A of the γδ resolvase site I-DNA complex

The polypeptide backbone of the molecule is represented as green cartoon, while the side chains of the residues are shown as sticks with the following colouring representations: Arg (blue), Ser (red), Asp (purple), Gln (yellow), and Tyr (pink). The picture was generated from PDB coordinates of 1GDT (Section 2.35).

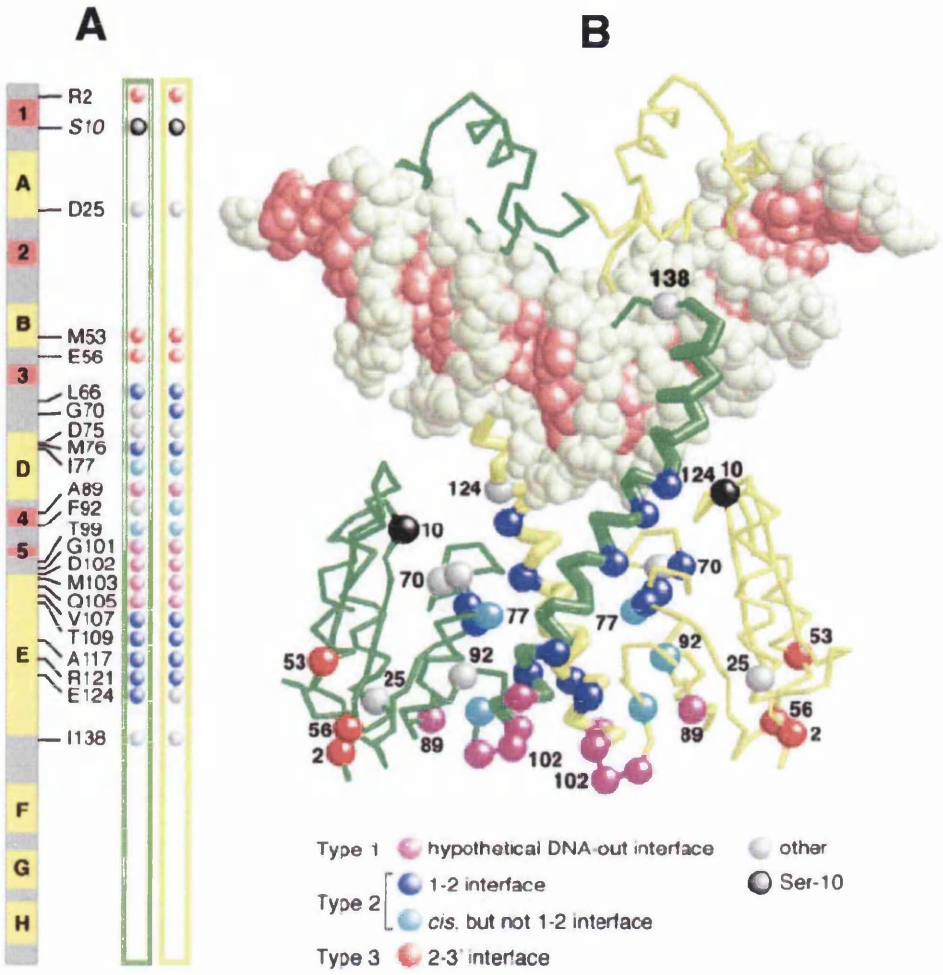

Figure 1.14 Positions of the activating mutations found in Tn3 resolvase
Panel A: The Tn3 resolvase primary sequence is shown as a bar, with predicted α-helix in yellow and β-sheet in red. The secondary structure elements are designated as in Yang and Steitz (1995). The positions of residues where activating mutations are found are indicated. The residue type is indicated by coloured spheres, as in the crystal structure image (green box, subunit A; yellow box, subunit B). **Panel B**: The γδ resolvase-DNA structure (Yang and Steitz, 1995) is shown with the DNA in pink and cream spacefill representation, and the backbones of subunits A and B in green and yellow respectively. The α-carbons of the residues where activating mutations are found are shown as spheres, coloured according to type as indicated, and as described in Burke *et al.* (2004). The hypothetical DNA-out interface comprises of residues predicted to mediate dimer-dimer interactions in the site I synapse (see Sarkis *et al.*, 2001). The *cis* interface comprises contacts made by the globular part of the N-terminal domain with the E-helix of its own subunit. The figure is adapted from Burke *et al.* (2004).

recombination efficiently, while certain ones still require at least one complete *res* site for activity, being able to catalyse only *res* x site I recombination (Arnold *et al.*, 1999).

The mutations that confer these deregulated properties on resolvase are referred to as 'activating mutations' (Arnold *et al.*, 1999; Burke *et al.*, 2004; Figure 1.14). The residues that produce activating effects when mutated have been described as "REG" residues (Burke *et al.*, 2004), based on the suggestion that they are involved in the regulation of recombination. The mutations having the strongest activating effects in Tn3 resolvase (G101S, D102Y, M103I, Q105L, and E124Q) are of residues on the E-helix and the loop connecting the E-helix with the catalytic domain (Burke *et al.*, 2004). This region of resolvase structure was described as the 'DNA-out' interface in Sarkis *et al.* (2001) and Burke *et al.* (2004). Several other residues in the N-terminal domain have been found to be activating when mutated (Burke *et al.*, 2004). Some of these residues (e,g, L66, G70, and A85) lie on the crystallographic 1-2-dimer interface (Sanderson *et al.*, 1990; Yang & Steitz, 1995). These "secondary" mutations are thought to enhance the effects of the "primary" activating changes found on the DNA-out interface (Burke *et al.*, 2004; Figure 1.10). One current explanation for the effect of activating mutations is that they relieve regulatory mechanisms in the wild-type system by affecting subunit and dimer interfaces that control recombination in the *res* synapse, thereby facilitating the formation of the site I synapse (Burke *et al.*, 2004). It is interesting to note that the REG residues around D102 are solvent-exposed in the dimer complex (Figure 1.14), and the residues are not involved in subunit or protein-DNA interactions in the structures of the dimer complex or the synaptic complex (Yang & Steitz, 1995; Li *et al.*, 2005; Kamtekar *et al.*, 2005).

Introduction of 2-3' interface mutations (R2A E56K) into some activated mutants enhances their site I x site I recombination activities (Wenwieser, 2001; Burke *et al.*, 2004). The reasons for the opposite effects of 2-3' mutations in the context of wild-type resolvase (Section 1.7) and activated mutants were explored by Burke *et al.* (2004). It was suggested that the mutations could be inhibiting some dimer-dimer interactions that are not required by the activated mutants and have become counterproductive. The other suggestion given is that the mutations could be stimulating catalysis by mimicking an

effect of the *acc* synapse. It is likely that the signal from the *acc* synapse to the site I dimer complex for the assembly of the site I synapse by wild-type resolvase is passed via 2-3' interactions (Murley & Grindley, 1998). The *in vitro* recombination reaction catalysed by activated resolvase mutants generates products that are not normally formed by the wild-type enzyme (Arnold *et al.*, 1999). Equal amounts of resolution and inversion products are formed in site I x site I reactions and the topologies of the products were variable with no preference for 2-noded catenanes (Sections 1.4.4 and 1.4.6). This suggests that the mutants have disposed of the regulatory mechanisms used in the wild-type reaction to specify the outcome of recombination. In addition, certain activated mutants have a tendency to accumulate unligated cleaved intermediates (Arnold *et al.*, 1999; Wenwieser, 2001).

One of the interesting properties of some activated resolvase mutants is the formation of a stable site I synapse that can be visualised directly in bandshift assays (Sarkis *et al.*, 2001; Nollmann *et al.*, 2004). This is significant since it has not been possible to observe a site I synapse with wild-type resolvase in such experiments. It appears that there are structural constraints in the wild-type resolvase dimer complex that forbid *acc*-independent formation of the site I synapse (Bednarz *et al*, 1990). The property of activated resolvase mutants to assemble stable site I synapse that can be studied in bandshift experiments should facilitate the study of the pre-catalytic steps of recombination (see Results chapters in this thesis).

1.10 Crystal structure of the site I synapse

Two types of interactions between resolvase subunits and the DNA duplexes were proposed for the architecture of the site I synapse (Figure 1.15, Panel A). The 'DNA-out' model proposes that the DNA is bound on the outside of a tetramer of the N-terminal catalytic domains of resolvase, while the 'DNA-in' model puts the two DNA duplexes close together at the centre of the synapse, with the catalytic domains on the outside (Rice & Steitz, 1994a; Yang & Steitz, 1995; Murley & Grindley, 1998; Sarkis *et al.*, 2001).

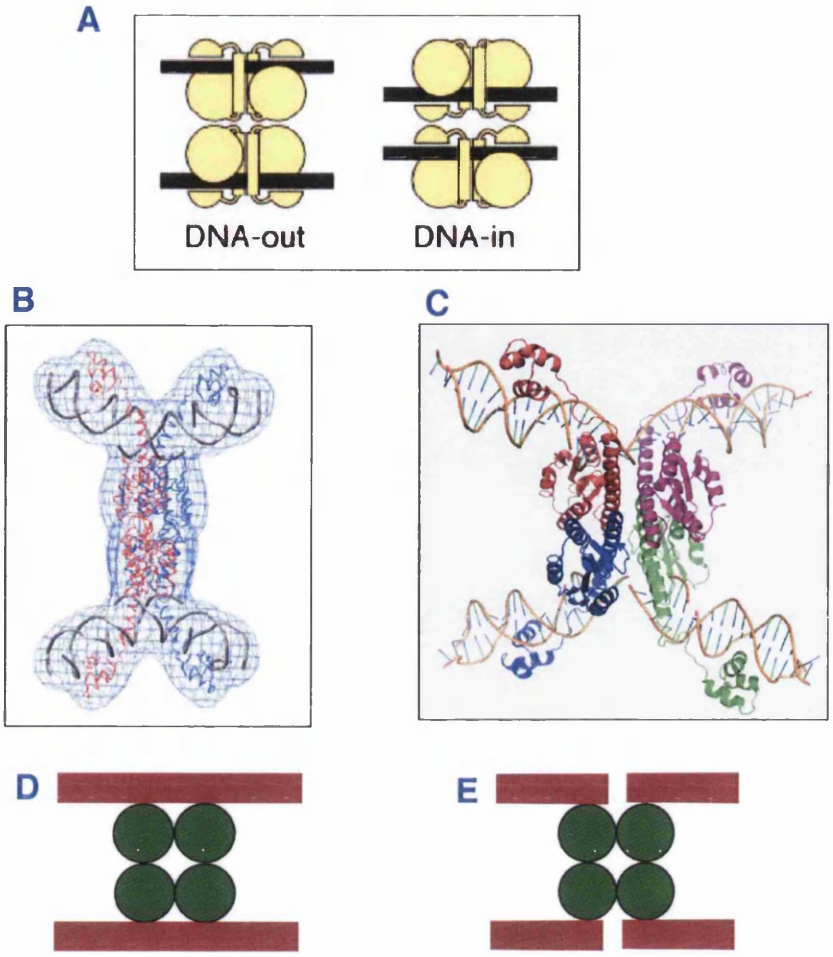

Figure 1.15 Structures of resolvase site I synapse
Panel A: Hypothetical interactions of two resolvase dimer-site I complexes, as may be required for site I synapsis and catalysis (adapted from Burke *et al.*, 2004). The DNA is shown as a thick black line. The subunit structure of resolvase is shown as tripartite: the N-terminal domain (approximately residues 1–98; large oval), the E-helix (residues 103–136; cylinder), and the C-terminal domain (residues148–183; small hemisphere). **Panel B**: Mesh representation of SAXS solution structure of NM-resolvase synapse before DNA cleavage (Nollmann *et al.*, 2004). The pre-catalytic synapse was kept stable by modifying the scissile phosphates with a phosphorothioate group to prevent cleavage of the DNA. **Panel C**: X-ray crystal structure of the post-cleavage site I synapse of activated γδ resolvase (Li *et al.*, 2005). The picture was generated from PDB coordinates of 1ZR4 (Section 2.35). The four resolvase subunits in the synapse are coloured red, purple, blue and green. **Panels D** and **E** are cartoons of the pre-cleavage and post-cleavage structures respectively. The green spheres and the red bars represent resolvase subunits and the DNA respectively. Both structures show that the complex is "DNA-out" (see Section 1.5.2)

Insights into the structure of the site I synapse have come from a series of mutagenesis, biochemical, and structural investigations. The localisation of activating mutations found in Tn3 resolvase to the N-terminal domain (Burke *et al.*, 2004) implies that the region is involved in mediating synaptic interactions. In addition, Dhar *et al.* (2004) used chemical cross-linking of introduced cysteine residues around the N-terminus of the E-helix in an activated Hin mutant to show that the catalytic domain is involved in synaptic interactions; hence, placing the DNA on the outside of the synapse. Leschziner & Grindley (2003) used the recombination efficiency of constrained DNA substrates by an activated γδ resolvase mutant to probe the structural arrangement of the site I synapse. The results show that the catalytic domains form the core of the synapse, and the DNA-binding domains and the DNA are on the outside. Structural evidence for the 'DNA-out' model of the synapse was obtained by Nollmann *et al.* (2004) who used small-angle X-ray and neutron scattering experiments to obtain a low-resolution solution structure of the site I synapse formed by NM-resolvase (an activated Tn3 resolvase mutant) with uncleaved site I (Figure 1.15). The structure shows that the two DNA duplexes are on the outside and the four resolvase subunits form the core of the synapse.

The structure of the post-cleavage synaptic complex of γδ resolvase (Figure 1.15; Li *et al.*, 2005) provides further details on the architecture of the site I synapse and useful insights into synapsis and strand exchange. The structure consists of a tetramer of resolvase, with each subunit in a phosphoseryl covalent linkage to a 5' phosphate of the cleaved DNA via the S10 residues. As predicted from earlier studies (see above), the core of the synapse is formed by the resolvase catalytic domains and the long E-helices, with the DNA-binding domains and the DNA on the outside.

The site I synapse consists of two dimeric units in which the resolvase monomers forming the dimers are arranged in a way that is different from the subunit interactions formed along the 1-2 interface in the dimer complex (Yang & Steitz, 1995; Li *et al.*, 2005). Some residues that are buried in the pre-catalytic dimer interface are exposed in the synapse. The resulting flat interface that separates the synaptic complex into left and right halves is essentially hydrophobic, and it is thought that the hydrophobic interaction along this

interface may be relevant to the mechanism of strand exchange (Li *et al.*, 2006; Grindley *et al.*, 2006; Section 1.4.6). The N-terminal parts of the four E-helices cross and form a central inner core of the synapse (Li *et al.*, 2005), where each resolvase subunit interacts with each of the three partner subunits. The core region could be an important feature that sustains the structure of the synapse.

Comparison of the tertiary structure of resolvase subunits and the DNA in the dimer-site I complex with those in the synaptic complex reveal some differences. The catalytic domain is rotated toward the E-helix using the residues at the N-terminus of the E-helix (100-102) as a hinge, and the E-helix is bent toward the catalytic region of the N-terminal domain in the synapse structure (Figure 1.16). These conformational changes in the resolvase subunits in the synapse bring the catalytic domain into closer proximity to the scissile phosphate to facilitate the nucleophilic attack on the DNA. In addition, the D-helix is rotated toward the E-helix in the synaptic structure (Figure 1.16).

The significant differences in the structural arrangement of the dimer-site I complex (Yang & Steitz, 1995) and the post-cleavage synapse (Li *et al.*, 2005; Kamtekar *et al.*, 2006; Figure 1.16) suggest that there are steps in the assembly and activation of the synapse that are yet to be described. While speculations on the mechanism and dynamics of the transition have been made based on these structures (Li *et al.*, 2005; Kamtekar *et al.*, 2006), there has been no direct application of biochemical methods to probe the differences in resolvase-DNA interactions between wild-type resolvase which fails to form stable site I synapse and the activated resolvase mutants that do.

The structure of the post-cleavage site I synapse (Li *et al.*, 2005; Figure 1.15) provides further evidence in support of the subunit rotation mechanism of strand exchange. The two halves of the synaptic complex are separated by a flat interface that is essentially hydrophobic. Hence, Li *et al.* (2005) proposed that the flat hydrophobic interface allows the two halves of the synapse to rotate relative to each other without any steric hindrances. The R121 and R125 residues of each subunit make specific interactions with D94 and D95 of the partner subunit on the flat interface. Grindley *et al.* (2006) suggest

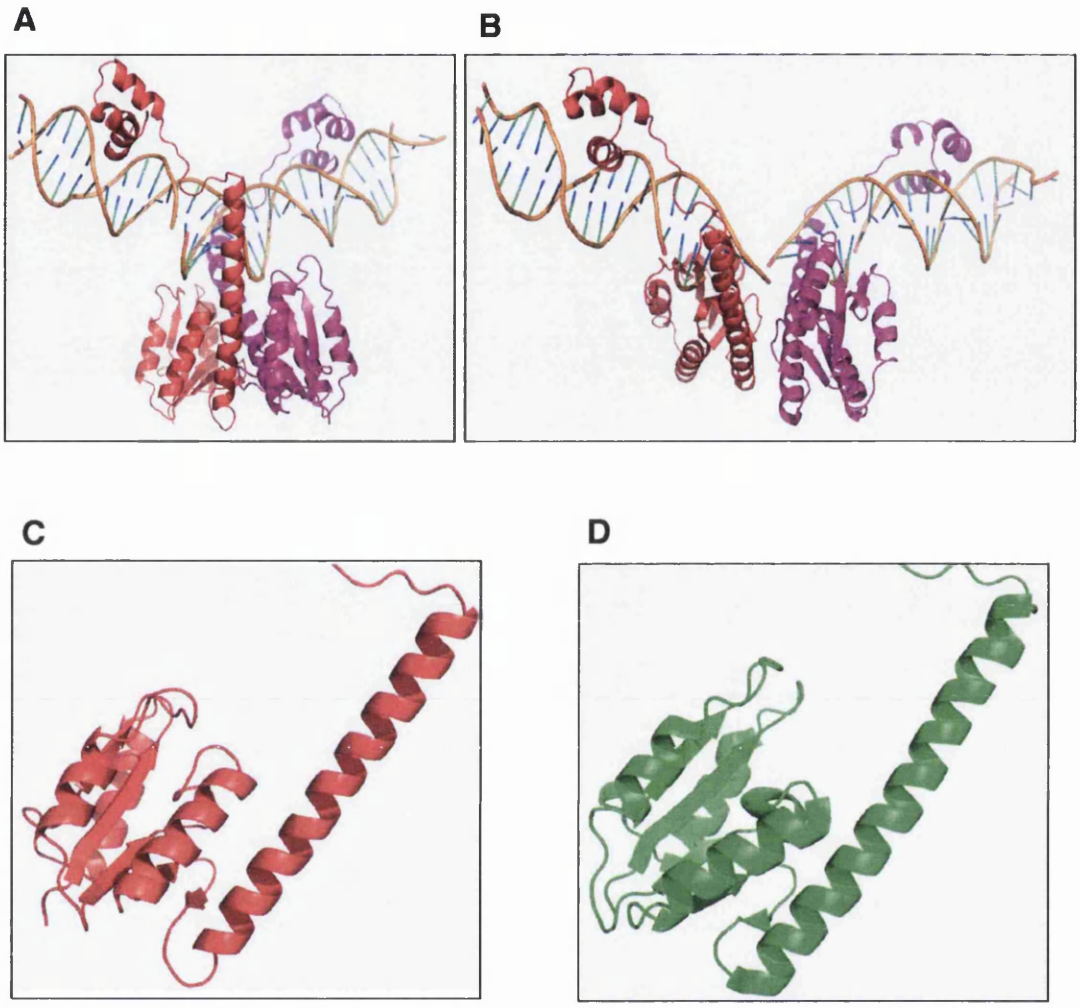

Figure 1.16 Conformational differences in resolvase in the dimer-site I complex and the post-cleavage synaptic complex.

Panels A and **B** are cartoon representations of the dimer complex at the pre-synaptic (Yang & Steitz, 1995) and post-cleavage synaptic (Li *et al.*, 2005) stages respectively. The dimer complex in B is the upper half of the cleaved site I synapse (Figure 1.11, Panel C). Assembly and catalytic activation of the synapse are accompanied by a restructuring of the intradimer contacts present in the pre-synaptic dimer. The orientation of the globular part of the B subunit N-terminal domain relative to the E-helix in the dimer configuration (**panel C**) has changed in the synaptic configuration (**panel D**). The pictures in panels A and C were generated from PDB coordinates of 1GDT and those in panels B and D from PDB coordinates of 1ZR4 (Section 2.35).

that these ionic interactions may serve as a gating mechanism that enforces rotation in steps of 180°, and position the rotating halves in a state that allows the religation step. Once the rotating half-sites are brought into the recombinant configuration, the free 3'OH groups engage in a nucleophilic attack of the 5'-phosphoseryl linkages to complete the strand exchange process (Figure 1.4).

1.11 Phosphoryl transfer reactions and resolvase catalysis

Significant insights into the mechanism of resolvase-catalysed recombination and the role of the accessory sites in determining the nature of the products formed have come from detailed topological analyses and mutagenesis experiments (Stark *et al.*, 1992; Grindley, 2002; Section 1.10). However, efforts at understanding how the catalytic residues of the active site promote the chemical steps of recombination (Figures 1.2 and 1.4) have not been very successful, principally due to the difficulty in dissecting the highly regulated process in the wild-type system. The only active site residue in resolvase whose function is clearly established is the nucleophilic S10 (Section 1.10).

While it is clear that S10 is the nucleophile in resolvase catalysis, there is the unanswered question of how the hydroxyl group of the serine residue is activated for nucleophilic attack on the scissile phosphate. The side chain hydroxyl group of the serine residue is a poor nucleophile and a general base is required to abstract the proton from the hydroxyl group (Mizuuchi & Baker, 2002; Figure 1.2). It was speculated that D67 in the active site of resolvase is the general base (Pan *et al.*, 2001). However, no biochemical evidence exists for this. Another catalytic requirement in phosphoryl transfer reactions is the need for a general acid to protonate the leaving group (Mizuuchi & Baker, 2002). The leaving group formed at the strand cleavage step (3'-O^-) when the S10 hydroxyl attacks the DNA phosphodiester bond is a nucleophile that could initiate a reversal of the phosphoryl transfer step (Figure 1.2). Enzyme-catalysed phosphoryl transfer reactions are driven in the forward direction by the donation of a proton to the leaving group, usually from an amino acid side chain in the enzyme's active site (Mizuuchi *et al.*, 1999; Yang *et al.*, 2006). The residue that provides the general acid has not been identified in resolvase.

The transition states of enzyme-catalysed phosphoryl transfer reactions usually require stabilisation by divalent metal ions or positively charged residues in the active site (Yang *et al.*, 2006). The cleavage step of resolvase-catalysed recombination does not require the participation of metal ions (Reed & Grindley, 1981). The stabilisation of the anionic transition state could be mediated by positively charged and conserved arginine residues in the active site (Mizuuchi & Baker, 2002; Grindley *et al.*, 2006; Figure 1.2). Arginine residues are important functional components of proteins that bind and modify DNA (Stivers & Nagarajan, 2006; Grindley, 2002; Grindley *et al.*, 2006). Crystallographic and mutational data on wild-type γδ resolvase have been used to suggest roles for R8, R68, and R71 in the chemistry of catalysis (Boocock *et al.*, 1995; Yang & Steitz, 1995; Grindley *et al.*, 2002). These functions include interactions that activate the phosphodiester bond for attack by the nucleophilic S10 hydroxyl group and/or stabilisation of the transition state.

1.12 Side chain-DNA interactions in the active site of resolvase

The structures of γδ resolvase (Sanderson *et al.*, 1990, Rice & Steitz, 1994b; Li *et al.*, 2005) reveal that the putative active site of resolvase is located in the N-terminal domain (Sections 1.6 and 1.10). In these structures, the nucleophilic S10 is not buried in an active site pocket (Rice & Steitz, 1994b; Figure 1.13), but lies on a surface loop with variable conformations among the three monomers in 2RSL (Sanderson *et al.*, 1990; Rice & Steitz, 1994b). Catalytic residues are usually located in well-defined active site pockets where they are arranged in configurations optimal for catalysis (Fersht, 1999; Mizuuchi & Baker, 2002).

The resolvase dimer-DNA structure of γδ resolvase (Yang & Steitz, 1995) provides further insight into the key catalytic residues of the active site. In the structure, R8 and R68 are within 5 Å of S10, while R71 makes direct hydrogen bonds with the DNA backbone 5' to the scissile phosphodiester. These interactions suggest that the arginine residues may be important in positioning the scissile phosphodiester for catalytic activation and stabilising the transition state (Mizuuchi & Baker, 2002). However, the nucleophilic S10 is far removed (11 Å and 17 Å in the two subunits) from the phosphorus

atom of the scissile phosphodiester bond (Yang & Steitz, 1995). The highly conserved Y6 contributes its phenolic ring to the hydrophobic core of the N-terminal domain and forms a hydrogen bond with the carboxylate group of D36. The carboxylate group of D36 makes further hydrogen bond interactions with the N-terminus of helix αB. However, these two essential residues do not make any contact with the DNA. While Y6 and D36 could be essential for maintaining the structure of the active site as suggested by Yang & Steitz (1995), it is likely that they have direct roles in catalysis. The side chains of the highly conserved active site residues Q14 and Q19 do not make contacts with the DNA or with other residues in all the crystal structures (Sanderson *et al.*, 1990; Rice & Steitz, 1994b; Yang & Steitz, 1995; Li *et al.*, 2005; Kamtekar *et al.*, 2006). Hence, more structural rearrangements within the protein-DNA complex than are seen in the structures might be necessary to achieve a functionally active configuration.

The absence of a well-organised active site in the structures of the N-terminal domain and the resolvase dimer-site I complex may be rationalised as being due to the pre-catalytic nature of those structures. However, the structures of the post-cleavage synaptic complex (Li *et al.*, 2005; Kamtekar *et al.*, 2006) did not show the expected interactions between some of the active site residues and the DNA. For instance, while the nucleophilic S10 residues are covalently linked to the DNA in the post-cleavage synaptic complex (Li *et al.*, 2005; Figure 1.9), no direct information can be obtained from the crystal structure on the roles of Y6, D36, Q14, and Q19 either in maintaining the structure of the synapse or in catalysing the cleavage reaction. The synaptic structures show that residues R8 and R68 interact with the nonbridging oxygens of the 5' phosphoserine linkage, yet there is no direct evidence for the actual roles played by the residues in the catalytic process. However, the proximity of R8 and R68 to the scissile phosphate suggests that they might have roles in stabilising the transition state, as has been proposed for positively charged residues in the active site of the tyrosine recombinases (Grindley *et al.*, 2006). The conserved R71, unlike in the dimer structure, makes no contact with the DNA in the synapse, but interacts with the mobile loop formed by residues 39 to 45. This suggests that the presumed catalytic interactions made by R71 in the transition from the pre-

catalytic dimer complex to the post-cleavage synaptic complex are not reflected in the crystal structures.

Hence, it appears that more contacts may be made between resolvase active site residues and site I than are revealed in the available crystal structures. These 'unseen contacts' which could be important for both synapsis and catalysis are likely made prior to and during catalytic interactions involved in breaking and making bonds. These synaptic conformations seem to be elusive to trap in crystallographic studies. In contrast, snapshots of synaptic conformations close to catalysis have been characterised for the tyrosine recombinases (Grindley *et al.*, 2006). The difficulty in seeing the expected side chain-DNA contacts in resolvase suggests that the functional active site might be assembled just before catalysis. It also suggests that the active site has disassembled from the substrate following cleavage in the structures of Li *et al.* (2005) and Kamtekar *et al.* (2006).

1.13 Research goals and strategy

The overall aim of this project was to understand aspects of the molecular mechanism of strand exchange in Tn3 resolvase. One of the primary foci was on the roles of the conserved residues of the active site in resolvase-DNA interactions at binding, synapsis, catalysis, and strand exchange steps. Mutational studies on the catalytic mechanism of wild-type resolvase are complicated due to the multi-component nature of the reaction system (see Section 1.4). In contrast to wild-type resolvase, activated mutants catalyse site I x site I recombination in a site I synapse (Section 1.9). Studies with activated mutants could be open to a more straightforward interpretation, and may provide detailed insights into the catalytic mechanism of resolvase as has been carried out for the tyrosine recombinases such as Type IB DNA topoisomerase and Cre recombinase (Krogh & Shuman, 2000; Grindley *et al.*, 2006; Stivers & Nagarajan, 2006). Since activated resolvase mutants synapse isolated site Is and catalyse reactions using oligonucleotide substrates, DNA modifications that selectively interfere with specific catalytic steps may be used to analyse the reaction mechanism. The combination of mutagenesis and DNA modification is an emerging trend in the analysis of phosphoryl transfer reactions catalysed by DNA-modifying enzymes (Stivers & Nagarajan, 2006).

The mechanisms by which activating mutations deregulate resolvase were explored in Chapter 3 by comparing the binding, synapsis and catalytic properties of some activated Tn3 resolvase mutants with those of the wild-type enzyme. In Chapter 4, the effects of mutations of conserved residues that might form the active site were investigated *in vitro*. The mutational studies were carried out primarily in the context of one of the activated mutants of Tn3 resolvase (NM-resolvase) with the mutations R2A E56K G101S D102Y M103I Q105L (Burke *et al.*, 2004; Nollmann *et al.*, 2004). The mutant resolvases were purified and their binding, synapsis, and catalytic properties were characterised. In Chapter 5, the interactions of Tn3 resolvase and activated resolvase mutants with site I DNA in binding, synapsis, and catalysis were investigated by means of methylphosphonate replacements of phosphodiester groups at and around the scissile position.

Chapter Two

Materials & methods

2.1 Bacterial strains

All bacterial strains used for plasmid DNA amplification were derivatives of *Escherichia coli* K-12.

Strain	Genotype	Source
DS941	AB1157, but *rec*F143, *sup*E44, *lac*ZΔM15, *lac*I^q	D.J.Sherratt
BL21 (DE3) pLysS	*hsd*, *gal*, (λ*cI ts* 857, *ind*1, *sam*7, *ini*5, *lac*UV5-T7 gene-1), T7 lysozyme expressing plasmid, pLysS	W. Studier

2.2 Plasmids

The plasmids that were used or constructed in this work are listed in Tables 2.1 and 2.2.

2.3 Chemicals

The sources of most general chemicals are listed below. Specialised chemicals are mentioned in the relevant sections of Chapter 2. Distilled water was used for making all solutions.

Chemicals	Source
General chemicals, biochemicals, organic solvents	Aldrich/Sigma, BDH, May and Baker
Media	Difco, Oxoid
Agarose, acrylamide	FMC, Biorad, Flowgen
Radiochemicals	Amersham Biosciences
Restriction enzyme buffers	Roche, NEB, Promega
Ligase buffer	NEB

2.4 Bacterial growth media

E. coli growth was in L-Broth (10 g bacto-tryptone, 5 g bacto-yeast extract, 5 g NaCl made up to 1 litre with deionised water, and adjusted to pH 7.5 with NaOH), or on L-Agar (L-Broth with 15 g/l agar). Growth media were sterilised at 120 °C for 15 minutes.

2.5 Preparation of competent *E.coli* cells

Chemically competent cells were made as follows. 2 ml of an overnight culture of DS941 (Section 2.1) was inoculated into 100 ml of L-broth, and grown at 37 °C until the OD_{600}

Table 2.1 Plasmids used for cloning resolvase mutants and assays of recombination activities

	Plasmid	Size (bp)	Antibiotic Marker	Description/Derivation	Source/Reference
1	pAL225	4908	Ap Tc	Plasmid with two site Is in direct repeat	Bednarz *et al.*, 1990
2	pMA21	4925	Ap Tc	Plasmid with two *res* sites in direct repeat	Bednarz *et al*, 1990
3	pSA1101	6692	Km	Resolvase overexpression plasmid	Arnold *et al.*, 1999
4	pMS140	5469	Ap	Resolvase expression plasmid	W.M. Stark/J. He
5	pJHL-4	6711	Km	NM-resolvase overexpression plasmid derived from pSA1101	W.M. Stark
6	pSW1511	5465	Ap	Resolvase expression plasmid with unique PacI site and T73C mutation	Wenwieser, 2001
7	pMS74	5465	Ap	Resolvase expression plasmid with G101S and D102Y mutations	W.M. Stark
8	pFO1	5469	Ap	NM-resolvase expression plasmid derived from pMS140 and pJHL-4	Section 2.32
9	pFO2	5469	Ap	NM-resolvase expression plasmid derived from pFO1. Contains unique SpeI, EcoRV, and SstI sites.	Section 2.32
10	pFO3	5469	Ap	NM expression plasmid derived from pFO1. Contains unique PacI site and T73C mutation	Section 2.32
11	pFO4	5469	Ap	AKSY-resolvase expression plasmid derived from pFO1 and pMS74	Section 2.32
12	pFO5	5469	Ap	AKSY-resolvase expression plasmid derived from pFO2 and pMS74. Contains unique SpeI, EcoRV, and SstI sites.	Section 2.32
13	pFO6	5469	Ap	AKSY-resolvase expression plasmid derived from pFO3 and pMS74. Contains unique PacI site and T73C mutation	Section 2.32
14	pFO102	6692	Km	NM-resolvase overexpression plasmid derived from pSA1101 and pFO2	Section 2.33.1
15	pFO105	6692	Km	AKSY-resolvase overexpression plasmid derived from pSA1101 and pFO5	Section 2.33.1

Table 2.2 Mutations in NM and AKSY resolvases; codon changes and expression plasmids

	Mutation	Codon change	pMS140-derived plasmid	pSA1101-derived plasmid
1	Y6F	TAT→TTT	pFO12 (AKSY) pFO29 (NM)	pFO112 (AKSY) pFO129 (NM)
2	R8K	CGC→AAA	pFO13 (AKSY) pFO30 (NM)	pFO113 (AKSY) pFO130 (NM)
3	V9A	GTC→GCG	pFO24 (AKSY) pFO31 (NM)	pFO124 (AKSY) pFO131 (NM)
4	S10A	TCA→GCG	pFO7 (AKSY) pFO32 (NM)	pFO107 (AKSY) pFO132 (NM)
5	Q14E	CAG→GAG	pFO23 (AKSY) pFO33 (NM)	pFO123 (AKSY) pFO133 (NM)
6	Q19E	CAG→GAG	pFO11 (AKSY) pFO34 (NM)	pFO111 (AKSY) pFO134 (NM)
7	D36N	GAC→AAC	pFO22 (AKSY) pFO35 (NM)	pFO122 (AKSY) pFO135 (NM)
8	S39A	TCC→GCG	pFO28 (AKSY) pFO36 (NM)	pFO128 (AKSY) pFO136 (NM)
9	R45K	CGG→AAA	pFO8 (AKSY) pFO37 (NM)	pFO108 (AKSY) pFO137 (NM)
10	D59N	GAC→AAC	pFO25 (AKSY) pFO38 (NM)	pFO125 (AKSY) pFO138 (NM)
11	D67N	GAC→AAC	pFO16 (AKSY) pFO39 (NM)	pFO116 (AKSY) pFO139 (NM)
12	R68K	CGG→AAA	pFO26 (AKSY) pFO40 (NM)	pFO126 (AKSY) pFO140 (NM)
13	R71K	CGC→AAA	pFO27 (AKSY) pFO41 (NM)	pFO127 (AKSY) pFO141 (NM)
14	E118Q	GAA→CAG	pFO19 (AKSY) pFO42 (NM)	pFO119 (AKSY) pFO142 (NM)
15	R119K	CGC→AAA	pFO20 (AKSY) pFO43 (NM)	pFO120 (AKSY) pFO143 (NM)
16	E124Q	GAG→CAG	pFO9 (AKSY) pFO44 (NM)	pFO109 (AKSY) pFO144 (NM)
17	R125K	CGC→AAA	pFO21 (AKSY) pFO45 (NM)	pFO121 (AKSY) pFO145 (NM)
18	R8A	CGC→GCC	pFO67 (NM)	pFO167 (NM)
19	R68A	CGG→GCG	pFO68 (NM)	pFO168 (NM)
20	R71A	CGC→GCC	pFO69 (NM)	pFO169 (NM)

was 0.4-0.5. Cells were cooled and harvested by centrifugation (Beckman Coulter J-20, 5000 rpm, 4 °C, 10 minutes). The pellet was resuspended in 50 ml of cold (4 °C) 50 mM $CaCl_2$ and kept on ice for 30 minutes. Cells were centrifuged as before, resuspended in 1 ml of 50 mM $CaCl_2$ and stored at 4 °C. Cells made by this procedure remained competent for up to 48 hours.

Competent cells made for storage at –70 °C were prepared using a different procedure. 200 ml of pre-warmed L-Broth was inoculated with 4 ml of an overnight culture and grown to an OD_{600} of 0.46-0.6 (1-2 h). Cells were cooled and harvested by centrifugation (Beckman Coulter J-20, 5000 rpm, 4 °C, 10 minutes), resuspended in 40 ml of ice-cold TFBI (30 mM KOAc, 100 mM RbCl, 10 mM $CaCl_2$, 50 mM $MnCl_2$, 15% glycerol, adjusted to pH 5.8 with AcOH) and kept on ice for 30 minutes. The cells were then re-centrifuged (as above), resuspended in 8 ml of ice-cold TFBII (10 mM MOPS, 75 mM $CaCl_2 \cdot 2H_2O$, 10 mM RbCl, 15% glycerol, adjusted to pH 6.8 with HCl or KOH) and kept on ice for 15 minutes. 200 µl aliquots were then dispensed into Nunc tubes, frozen in liquid nitrogen and stored at -70 °C.

'Electrocompetent cells' used for transformation by electroporation were prepared as follows. 5 ml of an overnight culture was inoculated into 500 ml of L-broth, and grown at 37 °C until the OD_{600} was 0.4-0.5. Cells were cooled and harvested by centrifugation (Beckman Coulter J-20, 5000 rpm, 4 °C, 15 minutes). The pellet was resuspended in 500 ml ice-cold 10% glycerol and centrifuged again. The pellet was resuspended in 250 ml ice-cold 10% glycerol and centrifuged for another 15 minutes. The resulting pellet was resuspended in ~20 ml of ice-cold 10% glycerol, transferred to a 30 ml tube and centrifuged as above. The final cell pellet was resuspended in a final volume of 1-2 ml of ice-cold 10% glycerol. 200 µl aliquots were then dispensed into Nunc tubes, frozen in liquid nitrogen and stored at -70 °C.

2.6 Antibiotics

The following concentrations of antibiotics were used in liquid and solid selective growth media:-

Antibiotic	Stock Solution	Selective Conditions
Ampicillin (Ap)	5 mg/ml in H_2O	50 μg /ml
Tetracycline (Tc)	12.5 mg/ml in 70% ethanol	12.5 μg /ml
Chloramphenicol (Cm)	2.5 mg/ml in ethanol	25 μg /ml
Kanamycin (Km)	5 mg/ml in H_2O	50 μg /ml

2.7 Bacterial cultures

Liquid cultures were grown at 37 °C with vigorous shaking. Growth on agar plates was at 37 °C overnight with plates inverted. Antibiotics were used as required (see Section 2.6). For long-term storage, bacterial strains were grown overnight in L-Broth, diluted 2-fold with 40% glycerol, 2% peptone, and then kept at -70 °C.

2.8 Transformation of *E.coli* with plasmid DNA

Aliquots of competent *E.coli* were thawed on ice. 50 μl of cells was added to plasmid DNA on ice and the mixture was maintained at 0 °C for 30 minutes. The samples were heat shocked at 37 °C for 5 minutes and then left on ice for 15 minutes. 5 volumes (approximately 250 μl) of L-broth were added and the samples incubated at 37 °C for 1 h. The cells were then plated out on selective media and incubated at 37 °C overnight.

Transformation of electrocompetent cells by electroporation using the Biorad micropulser was carried out as follows. 50 ml of cells was added to plasmid DNA on ice and transferred to a pre-cooled electroporation cuvette. The liquid was tapped to the bottom of the cuvette before it was inserted into the slide of the shocking chamber. The electrical pulse was delivered, and 1 ml of L-broth was immediately added to the cells. The samples were incubated at 37 °C for 1 h, and the cells were then plated out on selective media and incubated at 37 °C overnight.

2.9 Large-scale preparation of plasmid DNA

This method was adapted from that used by Birnboim and Doly (1979). 200 ml overnight cultures were grown to stationary phase (approximately 12 h vigorous shaking at 37 °C) and the cells were harvested by centrifugation (12 000 g, 4 °C, 5 minutes). The pellet was resuspended in Doly I buffer (50 mM glucose, 25 mM Tris-HCl pH 8.0, 10 mM EDTA), and kept on ice for 5 minutes. 8 ml of fresh ice-cold Doly II buffer (200 mM NaOH, 1% SDS) was added, and the samples were mixed gently and maintained at 0 °C for 4 minutes. 6 ml of ice-cold Doly III buffer (0.6 vol. 5 M KOAc, 0.115 vol. AcOH, 0.285 vol. H_2O) was added and the sample was mixed and kept on ice. The cell debris was then pelleted by centrifugation (39 200 g, 4 °C, 30 minutes) and the supernatant containing the DNA was mixed with 12 ml of isopropanol to allow precipitation at room temperature for 15 minutes. The DNA was pelleted by centrifugation (27 200 g, 20 °C, 30 minutes) and the pellet was washed with 70% ethanol, dried and resuspended in 2 ml of TE buffer (10 mM Tris-HCl pH 8.2, 1 mM EDTA). Caesium gradient purification was then carried out by adding 5 g of CsCl with 3 ml of water to the DNA/TE sample and transferring the mixture into a Beckman ultra-centrifuge tube. 270 µl of 15 mg/ml ethidium bromide was added. The tube was filled with liquid paraffin and heat-sealed. The tube was then centrifuged in a Beckman Ti70 fixed-angle rotor at 200 000 g for 16 h at 15 °C.

DNA bands were visualised using a long-wave UV source (365 nm). Usually two bands were visible, the upper band containing chromosomal and nicked plasmid DNA, and the lower, stronger band containing supercoiled plasmid DNA. The lower band was removed using a 1 ml syringe and the ethidium bromide was removed by repeated extractions with n-butanol. The DNA was recovered by adding 3 volumes of water and 2 volumes of ethanol, mixing the sample and maintaining at 4 °C for 30 minutes. The precipitated DNA was pelleted by centrifugation (27 200 g, 4 °C, 30 minutes). The pellet was washed with 70% ethanol, dried and resuspended in 500 ml TE buffer. The plasmid DNA was then stored at 4 °C.

2.10 Small-scale preparation of plasmid DNA

Plasmid mini-preps were made using a Qiagen mini-prep kit. Plasmid DNA was purified from 3 ml of overnight culture using the Qiagen Spin purification kit according to the manufacturer's instructions (Cat. no. 27106). This kit uses a silica-gel membrane system to bind DNA and allow simple and rapid wash steps to be performed. The purified plasmid DNA was eluted with TE buffer (50 µl).

2.11 Restriction endonuclease digestion of DNA

Restriction digests were usually done in the suppliers' recommended buffer (generally NEB or Roche buffers), with between 2-10 units per microgram of DNA to ensure complete cleavage of the DNA. Digests were incubated at 37 °C for ≥ 1 h and were terminated by the addition of SDS loading buffer (see Section 2.18), or by heating at 70 °C for 5 minutes. Restriction digests of resolvase reaction products were done in a similar way. Resolvase reactions were usually in buffers described in Section 2.31 at 37 °C. After 1 h the reaction was stopped by heating at 70 °C for 5 minutes, the buffer was adjusted appropriately and restriction endonuclease was added for a further 1 h incubation at 37 °C. The reaction was terminated by the addition of SDS loading buffer prior to electrophoresis.

2.12 Ethanol precipitation of DNA

Where necessary, the salt concentration of the DNA solution was adjusted to 0.3 M with ammonium acetate. 2 volumes of ethanol were added, followed by thorough mixing of the sample and incubation at -20 °C or -70 °C for ≥ 15 minutes. The precipitated DNA was pelleted by centrifugation in an Eppendorf microcentrifuge at 14 000 rpm, at 4 °C for 30 minutes. The pellet was then washed in 70% ethanol and re-centrifuged (for 5 minutes). The ethanol was removed, and the pellet was dried and resuspended in TE buffer.

2.13 Purification of DNA by phenol extraction

Extraction of proteins was achieved by addition of one volume of phenol (containing 0.1% 8-hydroxyquinoline and equilibrated with 0.5 M Tris-HCl pH 8.0), vigorous mixing

and centrifugation in an Eppendorf microcentrifuge at 14 000 rpm for 3 minutes. The DNA-containing aqueous layer was recovered and re-extracted if necessary. Any remaining phenol was removed by repeating the above procedure with chloroform instead of phenol.

2.14 Ligation of DNA restriction fragments

Standard ligations for cloning used 1-2 μg DNA (in a volume of 10-20 μl) in 1 x NEB ligase buffer (50 mM Tris-HCl pH 7.5, 10 mM $MgCl_2$, 1 mM ATP, 10 mM DTT, 25 μg/ml BSA) with 1 unit of T4 DNA ligase (NEB). The molar ratio of vector to insert DNA was generally 1 : 3. Samples were incubated at room temperature overnight, and then used to transform competent *E.coli* cells (see Section 2.8).

2.15 Annealing oligonucleotides

Pairs of single-strand oligonucleotides were annealed in 20 μl of TE buffer (10 mM Tris-HCl pH 8.2, 1 mM EDTA) with the addition of 50 mM NaCl. The components were mixed, heated at 70 °C for 5 minutes and then allowed to cool/anneal at room temperature for ≥15 minutes.

2.16 Ligation of oligonucleotides into plasmid vectors

Double-stranded synthetic oligonucleotides (annealed as described above) were ligated into plasmid vectors (1-2 μg) with complementary cohesive ends. The reactions were in 1 x NEB ligase buffer (see Section 2.14) with 1 unit of T4 DNA ligase (NEB) and were incubated at room temperature overnight. The samples were then used to transform the competent *E.coli* cells (Section 2.8).

2.17 Agarose gel electrophoresis

1.0% or 1.2% agarose gels were made by dissolving an appropriate amount of agarose (Biorad, 'Ultrapure') in 300 ml of 1 x TAE running buffer (40 mM Tris-acetate pH 8.2, 20 mM sodium acetate, 1 mM Na_2EDTA) by mixing and heating in a microwave oven. The hot agarose solution was allowed to cool to approximately 60 °C before pouring into a gel former and leaving to set at room temperature. 150 x 200 mm horizontal slab gels

were generally used, giving 22 adjacent sample wells each with a capacity of about 25 µl. The electrophoresis tank required about 3 litres of 1 x TAE buffer, and electrophoresis was through the longest dimension of the gel at an applied voltage of between 2 and 5 V/cm. Agarose gels were generally run at room temperature for approximately 15 h at 40 V or 4 h at 100 V.

2.18 Loading buffers

5 µl of SDS loading buffer (50% glycerol, 1% SDS, 0.01% bromophenol blue) was added to standard 20 µl resolution reactions and restriction digestions prior to loading on an agarose or a polyacrylamide gel. 1 volume of formamide loading buffer (80% deionised formamide, 10 mM EDTA pH 8.0, 1 mg/ml xylene cyanol, 1 mg/ml bromophenol blue) was added to oligonucleotide samples prior to denaturing polyacrylamide gel electrophoresis (Section 2.25). The samples were heated at 80 °C for 5 minutes before being loaded onto the gel.

2.19 DNA molecular weight standards

BRL 1 kb ladder was run unlabelled on both agarose and polyacrylamide gels to help estimate the size of DNA fragments.

2.20 Sequencing plasmid DNA

DNA samples were sequenced by MWG Biotech AG (Ebersberg, Germany).

2.21 UV spectrophotometry

DNA concentrations were estimated by measuring the absorbance of diluted DNA at 260 nm on a Lambda 45 UV/visible spectrophotometer (Perkin Elmer). The concentration was then calculated using the approximation that a solution with an absorbance of 1 at 260 nm contains 50 µg/ml double-stranded DNA. The absorbance of oligonucleotides was also measured at 260 nm and their concentration calculated using the relationship $A=Ecl$, (where 'A' is the absorbance at 260 nm, 'E' is the extinction coefficient (approximately 10 000 l mol^{-1} cm^{-1} per nucleotide), 'c' is the molar concentration and 'l' is the path length of the cell in cm).

2.22 Ethidium bromide staining of DNA, photography and autoradiography

DNA within agarose and polyacrylamide gels was visualised by staining with a 0.6 μg/ml ethidium bromide solution (made by diluting a 15 mg/ml ethidium bromide stock solution in 1 x TAE electrophoresis buffer or water) for 30-60 minutes. The gel was then rinsed several times and soaked in water for another 60 minutes to remove background ethidium bromide fluorescence. Visualisation of ethidium-stained DNA was by short wavelength 254 nm UV illumination unless bands were to be cut from the gel, when a long wavelength 365 nm source was used. Gels were photographed using Polaroid type 667 film.

For autoradiography, the gel (containing labelled DNA) was transferred to 2 layers of 3MM filter paper, then dried under vacuum (on a Biorad slab gel dryer at 80 °C for 45 minutes). Phosphor-imaging was carried out on gels dried as above, by exposing to phosphor screens overnight. The screens were processed in a Fuji BAS-1500 phosphor-imaging system.

2.23 Extraction of DNA from agarose gels

Bands of interest were excised using a scalpel from an ethidium bromide-stained 1.2% agarose gel (using long wavelength transillumination). The gel chip was transferred to a 0.45 μm centrifuge tube filter (Corning Inc.) and centrifuged at 10 000 rpm for 10 minutes. The filtrate was collected and the DNA was recovered by ethanol precipitation followed by resuspension in 1 x TE buffer.

2.24 Polyacrylamide gels

Standard polyacrylamide gels were used for analysis of restriction digests and recombination reactions, and for purifying small double-stranded DNA fragments. Similar gels with the addition of SDS (SDS-PAGE) were used for visualising the products of cleavage assays involving radiolabelled DNA. Varying concentrations of acrylamide and volumes of gel were used, but gels were always constructed in a similar manner.

Glass plates were clamped together with 0.75 mm spacers between them and a length of rubber tubing around the edges of the plates to form a seal. The freshly made acrylamide gel mixture (see below) was poured between the plates. A well-forming comb was inserted in the top and clamped in place. The acrylamide was allowed to polymerise for ≥ 1 h. The clamps, tubing and comb were removed and the gel was clamped into the electrophoresis kit. The buffer reservoirs were filled with 1 x TBE buffer (89 mM Tris-HCl, 89 mM boric acid, 0.2 mM EDTA pH 8.3) and electrophoresis was at a constant voltage of 200 V at room temperature for 3-4 h. The DNA bands were visualised with ethidium bromide or by autoradiography (see Section 2.22).

A standard 30 ml, X% (w/v), polyacrylamide gel was made by mixing X ml 30% acrylamide solution (37.5: 1 ratio of acrylamide to bisacrylamide), 3 ml 10 x TBE buffer, (27-X) ml H_2O, 360 µl 10% APS w/v and 18 µl TMED (N, N, N', N'-tetramethylethylenediamine).

2.25 Purification of oligonucleotides by denaturing PAGE

These gels were used for purification of synthetic oligonucleotides, using a standard polyacrylamide gel kit as described in Section 2.24. Synthetic single-strand oligonucleotides were run on 15% polyacrylamide/7 M urea denaturing gels which were made by mixing 15.75 g of urea, 14.75 ml of a 40% (w/v) acrylamide solution (19: 1 ratio of acrylamide to bisacrylamide), 3.75 ml of 10 x TBE, 7.75 ml of H_2O, 225 µl of 10% APS (w/v) and 18 µl TMED. The running buffer was 1 x TBE and the gel was poured between clamped plates as described in Section 2.24. Samples containing 1 volume of formamide loading buffer (see Section 2.18) were heated to 80 °C for 5 minutes and then loaded onto the gel. Electrophoresis was at 400-500 V (constant voltage) for 2-3 h to keep the gel hot and prevent renaturation of single-stranded oligonucleotides.

The gel was stained with 'Stains-all' (1-ethyl-2-[3-(1-ethylnaphtho[1,2-d]thiazolin-2-ylidene)-2-methylpropenyl)naphtho[1,2-d]thiazolium bromide; from Aldrich). 'Stains-all' is a cationic carbocyanine dye, which can be used for the staining of DNA, RNA or

protein, analysed by PAGE. 70 ml of water and 20 ml of isopropanol were mixed with 10 ml of a 0.1% (w/v) solution of 'Stains-all' in formamide. The oligonucleotide-containing gel was soaked in this solution until sufficient staining was observed (5-10 minutes). The gel was then destained by rinsing several times in water. Single-stranded oligonucleotides gave cyan or purple bands depending on their size (smaller DNAs stained cyan, larger DNAs stained purple).

The full-size oligonucleotide to be purified (usually the slowest migrating, major product on the gel) was cut out with a scalpel and transferred to a Nunc tube. 1 ml of TE buffer was added to the tube and the acrylamide gel chip was crushed with a glass rod. The polyacrylamide gel/TE buffer slurry was incubated on a rotating wheel at 37 °C overnight. The gel fragments were pelleted by centrifugation at 14 000 rpm for 1 minute in an Eppendorf microcentrifuge, and the supernatant was transferred to a fresh tube. A further 0.5 ml of TE buffer was added to the pellet of polyacrylamide; the sample was mixed briefly and re-centrifuged. The clear TE buffer was again removed and the two supernatants were combined. The oligonucleotide was concentrated by ethanol precipitation, and resuspended in TE buffer.

2.26 5' end-labelling of synthetic oligonucleotides

Synthetic oligonucleotides were 5' phosphorylated with γ-[^{32}P]ATP and T4 kinase. The DNA (~20 nmol) was mixed with 1 x T4 kinase buffer (50 mM Tris-HCl pH 7.5, 10 mM $MgCl_2$, 5 mM DTT, 0.1 mM spermidine, 0.1 mM EDTA) along with 0.74 MBq γ-[^{32}P]ATP. 1 unit of T4 kinase was then added and the mixture was incubated at 37 °C for 45 minutes. The reaction was stopped by extracting once with phenol, then once with chloroform, and the phosphorylated DNA was recovered by ethanol precipitation. The 5' phosphorylated DNA was resuspended in TE buffer. In all cases, the top strand was end-labelled and annealed to the unlabelled complementary bottom strand as described in Section 2.15.

2.27 Native polyacrylamide gels for binding and synapsis assays

Non-denaturing PAGE was used specifically for resolvase band-shift assays, i.e. the detection of resolvase-DNA non-covalent bound complexes. The gel was cast as described in Section 2.24, but all equipment was kept scrupulously detergent-free. Two buffer systems were used for the electrophoretic separation of the binding reaction products depending on the purpose of the binding experiment. These are 'TBE binding buffer' (100 mM Tris, 100 mM boric acid, 1 mM EDTA, pH 8.3) and 'TGE binding buffer' (50 mM Tris, 100 mM glycine, 0.1 mM EDTA, pH 9.4). In all cases, the same buffer was used in the gel and in the tanks for the electrophoresis. Gels were pre-run for 30 minutes at 200V constant voltage before loading the samples, and for 3 h at 200 V constant voltage after the samples were loaded. All electrophoretic separations were at 4 °C without recirculation of the buffer.

2.28 SDS-polyacrylamide gels for covalent resolvase-DNA complexes

These gels were used for the analysis of covalent resolvase-DNA complexes. The most frequently used type of gel was a 6.5% polyacrylamide made from a 30% acrylamide solution (37.5: 1 ratio of acrylamide to bisacrylamide). The 'TBE binding buffer' (Section 2.27) to which 0.1% SDS was added was used in forming the gel, and the running buffer. The gel was cast as in Section 2.24 and electrophoresis was at a constant voltage of 200 V at 4 °C for 2 h. In these experiments the DNA was usually radiolabelled, and was visualised by autoradiography (see Section 2.22).

2.29 Discontinuous SDS-polyacrylamide gel electrophoresis

Protein samples were analysed using a discontinuous SDS-PAGE system (Laemmli, 1970). The resolving gels used were prepared from a solution of the following composition: 15-18% polyacrylamide (37.5: 1 ratio of acrylamide to bisacrylamide), 375 mM Tris-HCl (pH 8.8), 0.1% SDS, 0.05% APS, 0.05% (v/v) TMED. The gel was overlaid with 0.5 ml of isopropanol and allowed to polymerise for 30-45 minutes. Following polymerisation of the resolving gel, the overlay was removed and the surface of the gel was rinsed with water to remove any unpolymerised acrylamide. The stacking polyacrylamide gels were prepared from a solution of the following composition: 5%

polyacrylamide (37.5: 1 ratio of acrylamide to bisacrylamide), 125 mM Tris-HCl (pH 6.8), 0.1% SDS, 0.1% APS, 0.2% (v/v) TMED. Stacking acrylamide gel solution was overlaid on the polymerised resolving gel and a comb was added immediately. After polymerisation of the stacking gel, the wells were rinsed with electrophoresis buffer (25 mM Tris base, 250 mM glycine, 0.1% SDS). Laemmli loading buffer (50% glycerol, 5% SDS, 200 mM Tris/HCl (pH 6.8), 0.1 mM EDTA) was added to protein samples (20% of total volume) prior to loading. Samples were boiled for 5 minutes to denature proteins and reduce disulphide bonds before loading on the gel. Polyacrylamide gels were run at 30-40 mA for 2-3 hours.

2.30 *In vitro* binding & synapsis reactions

The resolvase binding and synapsis reaction procedure was modified from that of Arnold *et al.* (1999). The design and sequence of synthetic double-stranded site I oligonucleotides used in binding, synapsis and cleavage reactions are shown in Figure 2.1. The DNA substrates were dissolved in a buffer that contained 20 mM Tris-HCl (pH 7.5, 10 µg/ml poly(dI/dC), and 4% Ficoll. The standard binding reaction mixture contains 50 nM unlabelled and 2.5 nM ^{32}P-labelled duplex DNA to which 400 nM resolvase was added, except where differences are stated. High DNA concentrations (52.5 nM) were used in the binding reactions in order to facilitate observation of synaptic complexes. Resolvase solutions were kept in resolvase dilution buffer (Section 2.33.2). Typically, 2.2 µl of resolvase was added to 20 µl binding buffer containing the site I DNA to bring the final salt concentration of the reaction mixture to approximately 100 mM. The samples were mixed and incubated at 22 °C for 10 minutes, then cooled in ice for 10 minutes and loaded onto a 6.5% native polyacrylamide gel (30:0.8, acrylamide: bisacrylamide) as described in Section 2.27. In order to analyse the covalent products of binding assays, the reaction mixtures were treated with 0.1% SDS for 30 minutes before loading on a SDS-polyacrylamide gel (Section 2.28).

2.31 *In vitro* recombination and cleavage reactions

Resolvase dilutions were made at 0 °C with 1 x resolvase dilution buffer (20 mM Tris-HCl pH 7.5, 1 mM DTT, 0.1 mM EDTA, 1 M NaCl, 50% glycerol). In all reactions with

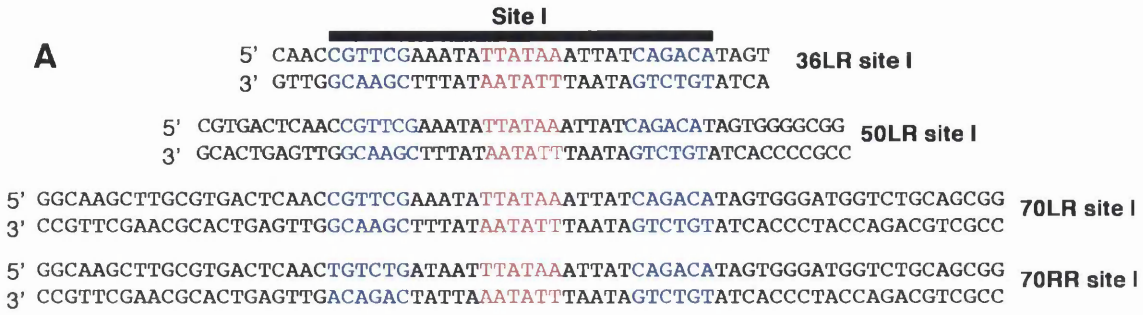

B **Numbering of site I phosphate positions**

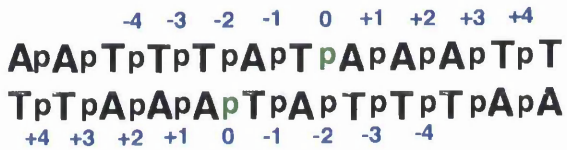

C **Abbreviated names of activated mutants of Tn3 resolvase**

Mutant Name	Mutations in WT resolvase
SY	G101S D102Y
AKSY	R2A E56K G101S D102Y
M	G101S D102Y M103I Q105L
NM	R2A E56K G101S D102Y M103I Q105L

Figure 2.1 Site I oligonucleotides used in resolvase binding, synapsis, and cleavage reactions, and list of activated resolvase mutants used in this study.
Panel A: The thick black line demarcates the 28 bp sequence of site I in the DNA substrates. The central 6 bp are in red, and the outer 6 bp recognised by the C-terminal domains of resolvase are in blue. The oligonucleotide substrates with phosphorothioate modifications at the scissile phosphate on both strands are named as 36LRpth site I and 50LRpth site I. 50LR site I oligonucleotide substrates with methylphosphonate modifications are named with the appropriate modified phosphate positions. e.g. 50LRMeP(-4) site I is modified at the -4 position on both strands. **Panel B** shows the numbering system used in describing the phosphodiester bonds relative to the scissile position (green). **Panel C** lists the abbreviated names of the activated resolvase multiple mutants used in this study.

resolvase, 100 mM NaCl was introduced by the addition of 0.1 volumes of resolvase diluted in this buffer. Two-fold serial dilutions of the resolvase stock solution were made. Generally, 100, 200 or 400 nM of resolvase was required for efficient recombination or cleavage of 20 μg/ml supercoiled substrate DNA. Dilutions were stored indefinitely at -20 °C.

Reactions involving Tn3 resolvase and its mutants were carried out in several reaction buffers that differ only in pH; but all contained 10 mM $MgCl_2$ and 0.1 mM EDTA. The buffers used for the various pH values are: 50 mM sodium phosphate (pH 6.0, 6.5, and 7.0); 50 mM Tris-HCl (pH 7.5, 8.0, and 8.2); 50 mM Tris-glycine (pH 9.5); and 50 mM glycine-NaOH (pH 10.0). The recombination activities of the resolvase mutants were tested on a plasmid with two full *res* sites (pMA21) and a plasmid with two copies of site I (pAL225). A typical reaction (20 μl) contained 0.4 μg of plasmid DNA with 2.2 μl of diluted resolvase. Reactions were carried out at 37 °C, typically for 1 hour, though this could range between 30 minutes to 24 hours. The reactions were terminated by heating at 70 °C for 5 minutes. In general, about 44 μl reactions were carried out and split into two aliquots of 22 μl after incubation. Recombination products were analysed by agarose gel electrophoresis of untreated samples and samples which had been digested with restriction enzymes. A PstI/HindIII restriction digest was generally performed by adding these in 0.5 volumes of NEB 2 buffer. Reactions proceeded for 30-40 minutes at 37 °C. Prior to loading, 5 μl of SDS loading buffer was added to all samples. Figure 2.2 illustrates the PstI/HindIII restriction fragment lengths of resolvase-catalysed recombination reaction products of pMA21 and pAL225. Activated resolvase mutants form intermolecular products in recombination assays (Arnold *et al.*, 1999). The PstI/HindIII restriction products of these intermolecular products along with those of the primary products of intramolecular resolution and inversion reactions are shown in Figure 2.3.

For as yet unclear reasons, inclusion of 15-40% ethylene glycol (EG) in the resolvase reaction system leads to the accumulation of cleaved intermediates (Johnson & Bruist, 1989; Boocock *et al.*, 1995). Cleavage of pAL225 was performed in buffers similar to the

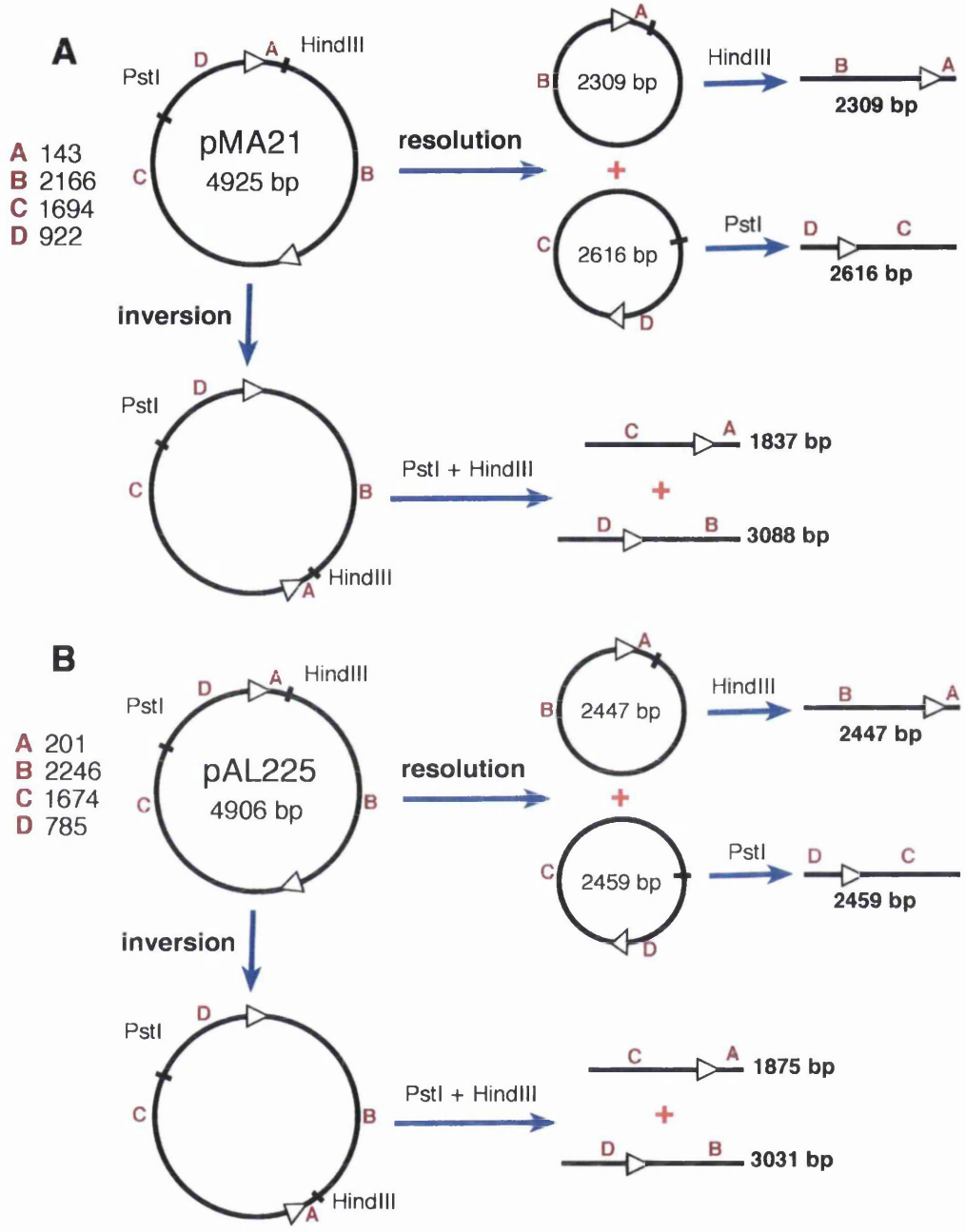

Figure 2.2 Graphic illustrations of PstI/HindIII restriction fragment lengths of resolvase-catalysed intramolecular recombination reaction products of pMA21 (panel A) and pAL225 (panel B)

The white arrowheads represent the crossover sites, *res* in pMA21 and site I in pAL225. The positions of the HindIII and PstI sites relative to the crossover sites are as indicated. The red letters A, B, C, and D represent the segments between the crossover sites and the restriction sites on the plasmids. The lengths of these segments are shown in Figure 2.4.

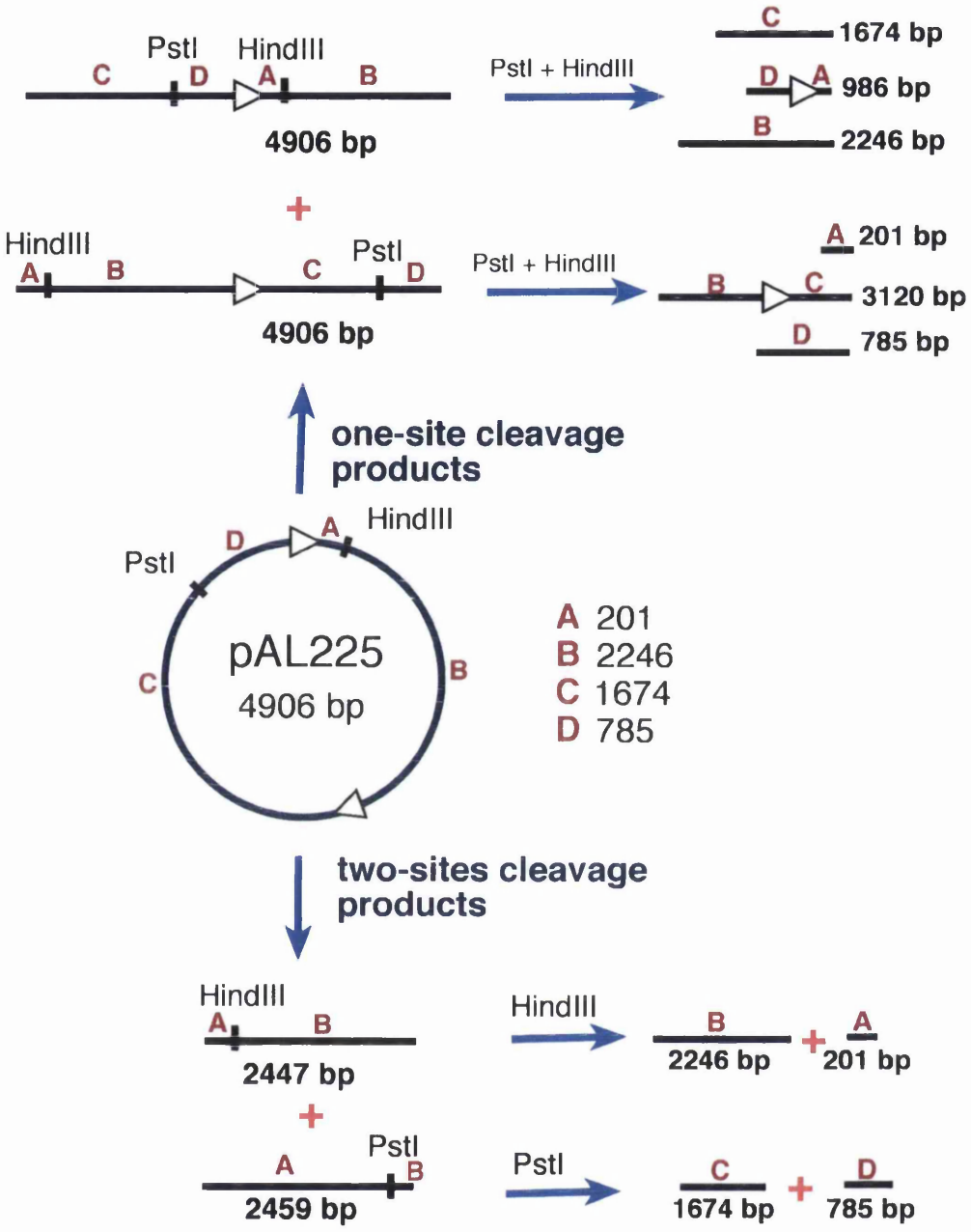

Figure 2.3 Graphic illustration of products of resolvase-catalysed cleavage reaction of pAL225 and the PstI/HindIII restriction fragment lengths of the products
The white arrowheads represent site I in pAL225. The positions of the HindIII and PstI sites relative to the crossover sites are as indicated. The red letters A, B, C, and D represent the segments between the crossover sites and the restriction sites on the plasmids. The lengths of these segments are shown in Figure 2.4.

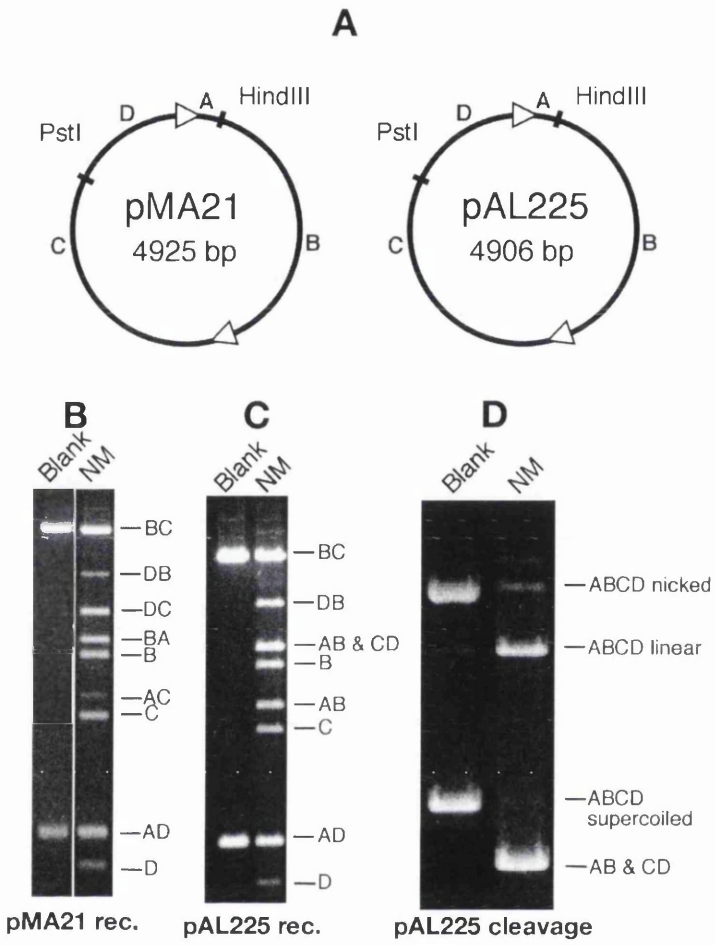

E

Fragments	pMA21	pAL225
Total Size ABCD	4925	4906
Parental DA	1065	986
Parental BC	3860	3620
Resolution DC	2616	2449
Resolution AB	2309	2447
Inversion DB	3088	3031
Inversion AC	1837	1875
Intermolecular AA	286	402
Intermolecular BB	4332	4492
Intermolecular CC	3388	3348
Intermolecular DD	1844	1570
Cleavage A	143	201
Cleavage B	2166	2246
Cleavage C	1694	1674
Cleavage D	922	785

Figure 2.4 Sizes of PstI/HindIII restriction fragments of resolvase-catalysed cleavage, resolution, inversion, and intermolecular products of pMA21 and pAL225. **Panel A** shows the graphic maps of the plasmid substrates pMA21 and pAL225. The symbols are described in Figures 2.2 and 2.3. **Panels B** and **C** show the products of NM-resolvase catalysed recombination of pMA21 and pAL225 respectively after restriction with PstI and HindIII and agarose gel electrophoresis. The products of NM-catalysed pAL225 cleavage reaction in EG buffer (Section 2.31) are shown in **Panel D**. **Panel E** lists all possible products from NM-catalysed cleavage, intramolecular, and intermolecular reactions from pMA21 and pAL225, as illustrated in Figures 2.2 and 2.3.

ones used for recombination assays except that 40% EG was included and $MgCl_2$ was omitted. Cleavage reactions were stopped by adding SDS loading buffer and were analysed without treatment with restriction enzymes. Graphic illustrations of the nature and sizes of reaction products from resolvase-catalysed cleavage of pAL225 and the PstI/HindIII restriction fragment lengths of the cleaved products sometimes observed in recombination reactions are shown in Figure 2.4. The detection of one-site and especially two-sites cleavage products of the right size is diagnostic of site-specific cleavage activity by the resolvase mutants. Cleavage of the site I oligonucleotide substrate (70LR site I, Figure 2.1) was carried out in EG buffer for the quantitative estimation of the effect of mutations on the catalytic activity of NM-resolvase.

2.32 Construction of plasmids encoding resolvase mutants

The cloning and *in vivo* characterisation of NM-resolvase has been described in Burke *et al.* (2004). In order to facilitate the introduction of specific mutations into NM-resolvase, it was necessary to use a version of the expression plasmid with several restriction sites in the resolvase coding sequence. Firstly, the part of the resolvase coding sequence carrying the six mutations in NM-resolvase was swapped from the NM-resolvase over-expression plasmid pJHL-4 (W.M. Stark, unpublished) into pMS140, a pAT5-derived plasmid carrying the ORF of wild-type Tn3 resolvase (Arnold *et al.*, 1999; W.M. Stark, unpublished) to make pFO1 (Figure 2.5). This swapping simplifies the transfer of the whole resolvase coding sequence from one plasmid to another using the NdeI site (unique in pMS140) and the Asp718 site. The unique restriction sites SpeI, EcoRV, and SstI were then introduced into pFO1 by fragment replacement with the MluI-HindIII fragment from pMS140 to create pFO2 (Figure 2.5). The unique restriction site PacI (along with a 'T73C' mutation) was introduced into pFO1 by fragment replacements with the AgeI-ClaI fragment from pSW1511 (Wenwieser, 2001) to create pFO3 (Figure 2.5). Designed mutations were introduced into the resolvase coding sequence of NM-resolvase by cloning appropriate synthetic double-stranded oligonucleotides into pFO2. Figure 2.6 shows the resolvase coding region of the part of pFO2 NM-resolvase ORF where the changes were introduced and the restriction sites used to insert the synthetic oligonucleotides. The ClaI-Asp718 fragment from pMS74, a plasmid carrying the ORF of

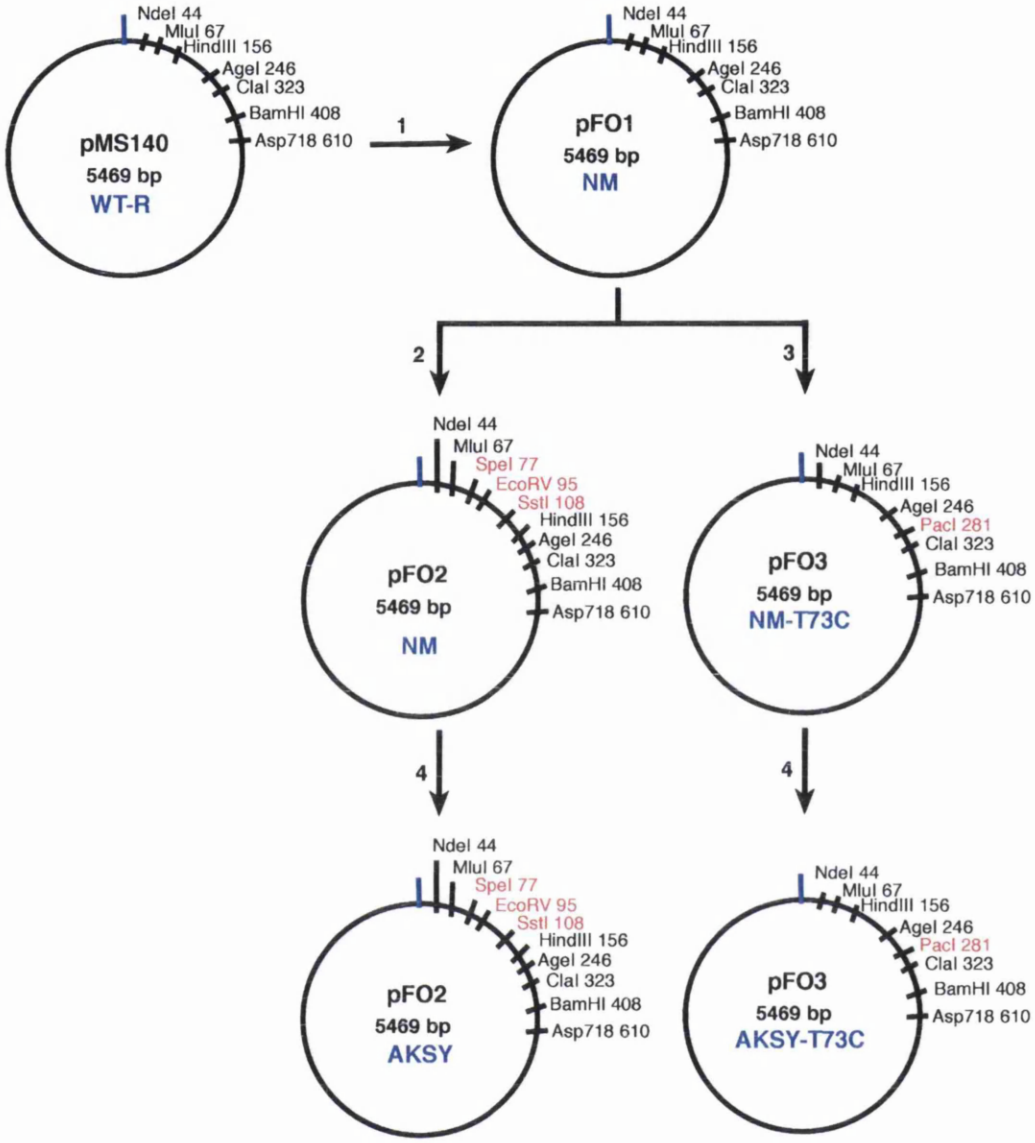

Figure 2.5 Schematic illustration of the construction of pMS140-derived plasmids carrying the coding sequences of Tn3 resolvase activated mutants NM-resolvase and AKSY-resolvase

Step 1. The NdeI-BamHI fragment from pJHL-4, which contains the NM-resolvase mutations (R2A E56K G101S D102Y M103 Q105L) was inserted into pMS140. **Step 2.** A MluI-HindIII fragment from pMS140 was swapped in to introduce the unique sites SpeI, EcoRV, and SstI. **Step 3**. An AgeI-ClaI fragment from pSW1511 was swapped in to introduce the unique site PacI, and the T73C mutation. **Step 4**. A ClaI-Asp718 fragment from pMS74, which contains the G101S and D102Y mutations was swapped in to create AKSY-resolvase (R2A E56K G101S D102Y), and AKSY-T73C.

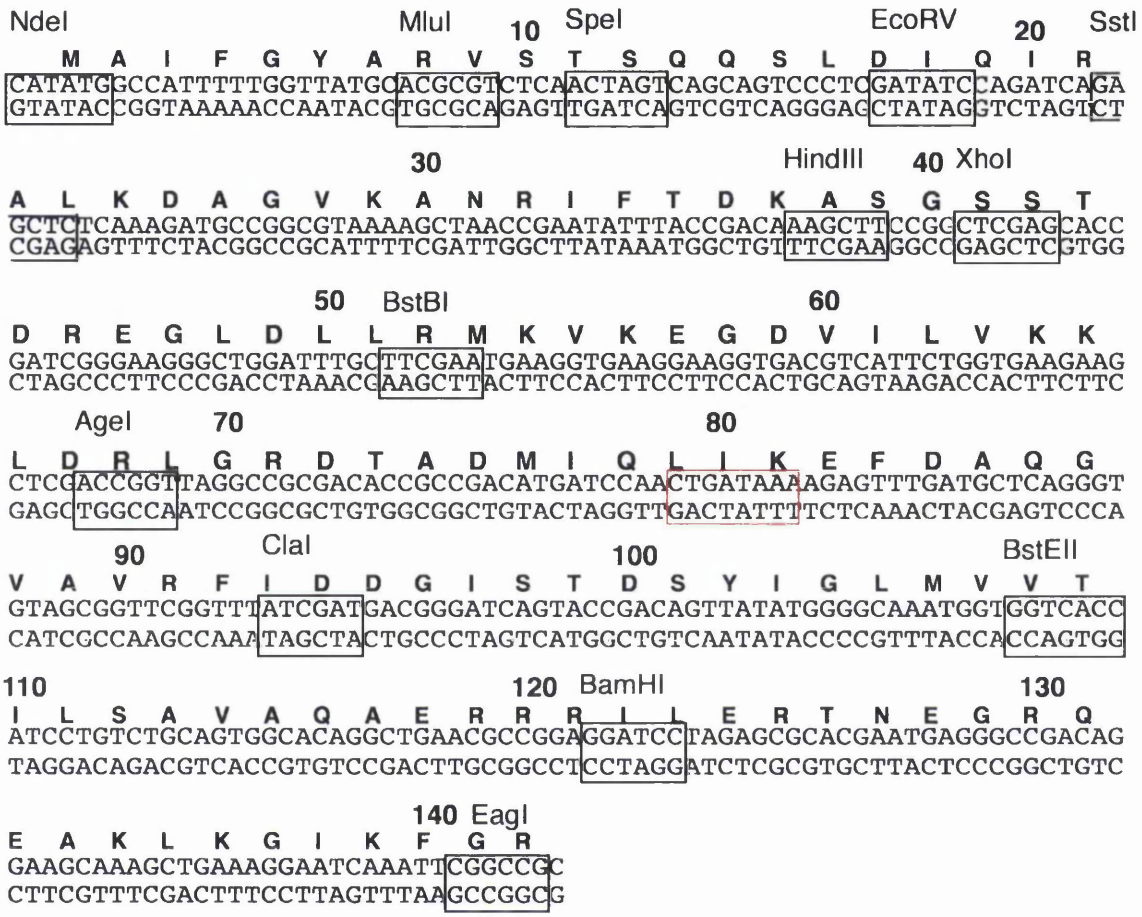

Figure 2.6 Resolvase coding sequence of the N-terminal domain of NM-resolvase in pFO2 showing the restriction sites used for cloning double-stranded synthetic oligonucleotides.

The sequence enclosed within the red box is replaced with TTAATTAA (top strand) and the complementary bottom strand in pFO3 to introduce the unique PacI site.

SY-resolvase (Burke *et al.*, 2004) was swapped into pFO2 (NM-resolvase) and pFO3 (NM-T73C) to create pFO5 (AKSY-resolvase) and pFO6 (AKSY-T73C) respectively (Figure 2.5). The oligonucleotides carrying the desired codon changes were cloned into pFO2, except the ones for D67N, R68K, R68A, R71K, and R71A that were cloned into pFO3. The changes made to the appropriate codons in the resolvase coding sequence of NM-resolvase and AKSY-resolvase are shown in Table 2.2. The resolvase coding sequences (NdeI-Asp718 fragment) of the pMS140-based expression plasmids were transferred into pSA1101 to create overexpression plasmids used in the resolvase purification stage of the study.

2.33 Purification of resolvase mutants

2.33.1 Large scale induction of resolvase mutants

Mini-induction experiments showed that the *E.coli* strain BL21(DE3)pLysS (see Section 2.1) strain was most productive for high amounts of resolvase expression (Arnold, 1997; MacDonald, 1999). BL21(DE3)pLysS is a BL21(DE3) strain containing a T7 lysozyme low-expression plasmid (Studier, 1990). Hence, this strain was used to induce over-expression of Tn3 resolvase mutants.

$CaCl_2$ competent cells of the BL21(DE3)pLysS strain were made and transformed with an expression vector encoding one of the mutant resolvase genes (derived from pSA1101) conferring kanamycin resistance, and the transformed cells were plated on selective agar. Transformed BL21(DE3)pLysS strains were selected on plates containing kanamycin and chloramphenicol. L-broth (20 ml) containing the required antibiotics were then inoculated with colonies from each plate and incubated overnight at 37 °C. Glycerol stocks were then made of each of these cultures. A 1 in 100 dilution of the overnight culture was then made in 800 ml (2 x 400 ml aliquots) of fresh L-broth (plus kanamycin and chloramphenicol), and cells were grown with vigorous shaking to an O.D of 0.4 at 37 °C. Expression of resolvase was then induced by the addition of 0.1 mM IPTG and the cultures were grown for a further 3 hours. Cells were harvested by centrifugation at 10 000 rpm, 4 °C for 10 minutes.

2.33.2 Buffers used in the purification of resolvase mutants

Suspension Buffer: 20 mM Tris-HCl pH 7.5, 10 mM $MgCl_2$, 1 mM DTT, 0.1 mM EDTA, 1.2 mM PMSF, 1% EtOH

Wash Buffer: 20 mM Tris-HCl pH 7.5, 10 mM $MgCl_2$, 1 mM DTT, 0.1 mM EDTA, 1.2 mM PMSF, 1% EtOH, 100 mM NaCl

Solubilisation Buffer: 20 mM Tris-HCl pH 7.5, 1 mM DTT, 0.1 mM EDTA, 1.0 mM PMSF, 1% EtOH, 6 M urea, 1.0 M NaCl

Refolding Buffer I: 20 mM Tris-HCl pH 7.5, 1.0 mM DTT, 0.1 mM EDTA, 1.0 mM PMSF, 1% EtOH, 1.0 M NaCl

Precipitation Buffer: 20 mM Tris-HCl pH 7.5, 10 mM $MgCl_2$, 1 mM DTT, 0.1 mM EDTA, 1.2 mM PMSF, 1% EtOH

Resin Wash Buffer: 50 mM NaCl, 50 mM sodium phosphate pH 7.5.

Urea Buffer A: 50 mM sodium phosphate pH 7.2, 25 mM NaCl, 0.1 mM EDTA, 0.1 mM DTT, 6 M urea.

Urea Buffer B: 50 mM Sodium phosphate pH 7.2, 1.0 M NaCl, 0.1 mM EDTA, 0.1 mM DTT, 6 M urea.

Column Wash Buffer: 2 M NaCl, 25 mM Tris-HCl pH 7.5, 0.1 mM EDTA

Refolding Buffer II: 20 mM Tris-HCl pH 7.5, 1 mM DTT, 0.1 mM EDTA, 2 M NaCl

Resolvase Dilution Buffer: 20 mM Tris-HCl pH 7.5, 1 mM DTT, 0.1 mM EDTA, 1 M NaCl, 50% glycerol.

2.33.3 Extraction and purification of resolvase mutants

The protein purification system was modified from the procedure described in Arnold (1997). The procedure exploited the solubility properties of resolvase. Unlike most proteins, resolvase is insoluble at low salt concentrations but soluble at high salt concentrations (2 M NaCl). The extraction involved a number of low salt (100 mM NaCl) wash steps which kept the resolvase insoluble (i.e. after centrifugation the resolvase remains as an insoluble pellet), followed by treatment with a buffer containing 6 M urea and 1 M NaCl which solubilised the resolvase, but in a denatured state. Renaturation involved a change in buffer conditions, by dialysing out the urea leaving the resolvase in

1 M NaCl. At each step of the procedure, sample aliquots (normally one two-thousandth of the total volume of the mixture; or in the case of pelleted material, a small sample removed by a toothpick) were taken and run on a Laemmli gel to monitor purification.

Following the induction of resolvase expression (see Section 2.33.1), the cells were harvested by centrifugation at 10 000 rpm, 4 °C for 10 minutes in a Beckman centrifuge. On average, approximately 2 g of cells was collected from 800 ml culture. Pellets were then resuspended in 25 ml of Suspension Buffer. Cells were broken using a Vibra-cell VC100 sonicator at 40% power using a micro-probe. Three bursts of 20 seconds were applied, with cooling of the mixture on a mixture of ice and water to 5 °C in between each burst. The crude extract was centrifuged at 20 000 rpm and 4 °C for 15 minutes. The supernatant was removed, and the pellet (which should contain insoluble resolvase) was resuspended in 20 ml of Wash Buffer, homogenised (40 strokes) using a Dounce homogeniser and then re-centrifuged at 20 000 rpm at 4 °C for 15 minutes. This wash step was repeated 3 to 4 times in order to get rid of as much contaminating soluble proteins as possible. The next step involved the addition of 20 ml of Solubilisation Buffer to the pellet. In the presence of 6 M urea and 1 M NaCl, most resolvase mutants were solubilised by vigorous homogenisation after three rounds of 50 strokes each with the homogeniser. Insoluble debris was removed by centrifugation, the supernatant (which now contained the soluble resolvase) was collected and the pellet discarded. The solubilised resolvase in 6 M urea and 1 M NaCl was dialysed against Refolding Buffer I for 5 h at 4 °C. This step ensures that most contaminating proteins and other cell components kept soluble by the 6 M urea are pelleted when the urea is dialysed out. The dialysate was collected and centrifuged to remove the insoluble pellets. The supernatant, which contained the resolvase, was then transferred to fresh dialysis bags and dialysed against the Precipitation Buffer for 6 h. Some resolvase mutants that are difficult to solubilise tend to form substantial precipitates even in the high-salt Refolding Buffer I. In those cases, the dialysis bags and the resolvase contents were transferred directly to the low-salt Precipitation Buffer without centrifuging the dialysates. The precipitated resolvase, which was evident by the appearance of snow-like flakes in the dialysis samples was then collected and centrifuged at 20 000 rpm, 4 °C, for 15 minutes to pellet

the 'snow'. Solubilisation of the precipitated resolvase for the next step was done by vortexing and maceration with a Gilson pipette tip. The solubilised resolvase was centrifuged at 20 000 rpm, 4 °C, for 15 minutes and the supernatant, which contained the resolvase, was collected and kept on ice for the chromatography step.

Removal of the remaining non-resolvase protein, nucleic acid and other contaminating cell components were carried out using an SP sepharose fast flow, ion exchange chromatography column. This cation exchange column should bind positively charged molecules (such as resolvase), whilst concurrently ridding the cell extract of negatively charged molecules (such as DNA, RNA and negatively charged protein molecules) which would wash out as eluate. The chromatography steps were performed at room temperature and the buffers and samples were kept at room temperature throughout the procedure. Approximately 6 ml of the resin was packed into the column, and the packed resin was washed with resin wash buffer and then equilibrated with Urea Buffer A. The column was then loaded with the resolvase-containing supernatant from the final homogenisation and centrifugation using a peristaltic pump at a flow rate of 1 ml/minute, and the column was then re-equilibrated with Urea Buffer A. The column was connected to a Waters^{TM} 650E advanced protein purification system and absorbance values at 260 nm and 280 nm were read using a Waters 490E programmable multiwavelength detector. The readings were recorded on a Millipore chart recorder. The eluate was collected once the extract was loaded, in case the resolvase failed to bind to the column at low salt. Once a second base line was obtained, a programmed gradient of increasing salt concentration (Urea Buffer B) was used to elute the positively charged resolvase:

0-25 min: 100% Urea Buffer A to 75% Urea Buffer A, 25% Urea Buffer B (linear gradient)
25-50 min: 75% Urea Buffer A, 25% Urea Buffer B to 100% Urea Buffer B (linear gradient)

The flow rate was 1 ml/min during the gradient run. 1 ml fractions were collected in Eppendorf tubes and stored on ice. Usually two peaks were recorded, the second being a peak representing the purified resolvase. The resolvase was eluted at about 20-30% Urea Buffer B (i.e. ~400-600 mM NaCl). Fractions corresponding to absorbance peaks were run on a Laemmli gel to determine purity. The column was washed with about 50 ml

Column Wash Buffer. Selected pure fractions from the ion exchange column were then pooled together and dialysed for at least 8 hours in 1 litre of Refolding Buffer II, which contained 2 M NaCl. This concentration of salt ensured that the resolvase would stay soluble. At the same time diffusion of urea from each fraction ensured that the protein would renature into its native conformation. Next, the refolded resolvase was dialysed against 1 litre of resolvase dilution buffer for at least 6 hours. In addition to facilitating the addition of glycerol to the sample for storage at -20 ^{o}C, this step also led to the concentration of the resolvase sample. Estimates of the concentration and purity of the sample were determined by comparing with a standard on a Laemmli gel.

2.34 Estimation of resolvase concentration

The accurate determination of the absolute resolvase concentration has proved difficult because standard protocols, such as the Bradford assay, have given unreliable measurements. Furthermore, amino acid analysis and A_{280} extinction measurements have generated concentration estimates differing by as much as 3-fold. Resolvase concentrations listed here are based upon the amino acid analysis performed by D. Blake (Ph. D. Thesis, 1993) on the wild-type Tn3 resolvase fraction R17 f.47, estimated at 0.4 mg/ml or 20 μM. The Tn3 resolvase fraction was used to standardise an NM-resolvase fraction made by J. He (W.M. Stark & M.R. Boocock, personal communication). This NM-resolvase fraction (estimated concentration, 69.4 μM) was used as the standard in this study. The relative concentrations of other resolvase fractions (Table 2.3) were estimated by comparison with this NM-resolvase fraction on SDS PAGE gels (Section 2.29). The resolvase fractions were diluted until bands were of equal intensity with the standard as measured by visual inspection.

2.35 Molecular Graphics

Molecular graphics were generated from PDB coordinates 2RSL (N-terminal domains of γδ resolvase; Sanderson *et al.*, 1990), 1GDT (γδ resolvase site I-dimer complex; Yang & Steitz, 1995), and 1ZR4 (activated γδ resolvase site I synaptic complex; Li *et al.*, 2005) using the software PyMOL (www.pymol.org).

Table 2.3 List of resolvase mutants purified and used in this study and the estimated concentrations of the fractions. WT Tn3 resolvase (K. Malarkey), SY-resolvase (J. He), and NM-resolvase (J. He) were obtained from W.M. Stark.

Prep No.	Resolvase Mutant & Concentration (μM)	
1	AKSY-resolvase	24.1
2	AKSY-Y6F	20.5
3	AKSY-Q14E	24.6
4	AKSY-Q19E	22.2
5	NM-resolvase	64.8
6	NM-S39A	57.0
7	NM-R45K	129.6
8	NM-Y6F	40.2
9	NM-Q19E	64.8
10	NM-E118Q	58.3
11	NM-S10A	90.7
12	NM-D59N	55.1
13	NM-V9A	208.2
14	NM-R8K	54.4
15	NM-D36N	65.4
16	NM-R119K	91.8
17	NM-D67N	70.6
18	NM-R68K	72.6
19	NM-R71K	53.1
20	NM-Q14E	46.7
21	NM-E124Q	64.8
22	NM-R125K	73.6
23	AKSY-E124Q	97.2
32	AKSY-R125K	154.1
33	M-resolvase	80.2
34	AKSY-V9A	12.8
35	AKSY-R45K	14.2
36	AKSY-D67N	15.7
37	AKSY-D36N	16.4
38	AKSY-E118Q	15.8
40	NM-R8A	40.5
41	NM-R68A	32.8
42	NM-R71A	64.8
Existing resolvase fractions used in this study		
WT Tn3 resolvase	93.7	
SY-resolvase	109.0	
NM-resolvase (J. He)	69.4	

2.36 Binding curves and estimation of apparent dissociation constants

Quantitative imaging of the bandshift data from titration experiments was used for the estimation of K_d(app.) of the mutants. The apparent dissociation constant (K_d(app.)) was taken as the enzyme concentration that converts half the input DNA to bound complexes on the gel, irrespective of the stoichiometry of the complexes formed. Data were fitted to a sigmoidal dose-response curve with variable slopes (West & Austin, 1999) using GraphPad Prism 4.0 data analysis software.

Chapter Three

Binding, synapsis and catalysis by activated Tn3 resolvase mutants

3.1 Introduction

3.1.1 Activating mutations and the biochemical properties of Tn3 resolvase

Several activated mutants of Tn3 resolvase have been isolated and their properties are being studied via biochemical and crystallographic techniques (Burke *et al.*, 2004; Li *et al.*, 2005; Kamtekar *et al.*, 2006). The main objective of studying activated resolvase mutants is to gain a better understanding of the recombination system involving the wild-type enzyme (referred to hereafter as WT-resolvase). This approach has proved very successful since some of these studies are providing relevant insights into the structure and regulation of the site I synapse, the core catalytic unit of the recombination system (Nollmann *et al.*, 2004; Li *et al.*, 2005; Kamtekar *et al.*, 2005). Despite the powerful analytical potential offered by the activated resolvase mutants, the molecular mechanism of the deregulation of resolvase by the mutations remains unclear (Arnold *et al.*, 1999; Burke *et al.*, 2004). Detailed characterisation of the biochemical properties of the activated resolvase mutants have not been carried out. Such analysis could provide interesting insights into how the mutations deregulate site I synapsis, and into the regulatory mechanisms used by the WT-resolvase to control recombination. One of the aims of this chapter is to investigate the effects of activating mutations by comparing the binding and catalytic properties of WT-resolvase with those of some activated resolvase mutants.

3.1.2 Activated resolvase mutants used in this study

The mutant resolvases characterised in this chapter are SY-resolvase (G101S D102Y), M-resolvase (G101S D102Y M103I Q105L), AKSY-resolvase (R2A E56K G101S D102Y), and NM-resolvase (R2A E56K G101S D102Y M103I Q105L). SY-resolvase contains a combination of two adjacent activating mutations, and it resolved site I x site I plasmids *in vivo* (Burke *et al.*, 2004). M-resolvase contains a combination of four activating mutations around D102 (Arnold *et al.*, 1999; Burke *et al.*, 2004; Section 1.9), but it was less efficient than SY-resolvase in resolving the site I x site I plasmids *in vivo* (Burke *et al.*, 2004). The *in vivo* 'hyperactive' phenotypes of certain activated mutants described in

Burke *et al.* (2004) were enhanced by combination with the 2-3' interface mutations, R2A and E56K (Section 1.9). On this basis, the 2-3' interface mutations were combined with the activating mutations in SY-resolvase and M-resolvase to give AKSY-resolvase and NM-resolvase respectively. NM-resolvase resolved the site I x site I plasmids *in vivo* (Burke *et al.*, 2004), and preliminary assays in this study showed that AKSY-resolvase has a similar phenotype (data not shown). Furthermore, NM-resolvase catalyses rapid recombination of a site I x site I plasmid *in vitro* (W.M. Stark, unpublished data) and forms stable synaptic complex with a pair of site I oligonucleotides in polyacrylamide bandshift assays (Nollmann *et al.*, 2004; Section 1.9). The four 'REG residue' (Section 1.9) mutations in these resolvase mutants are found in the N-terminal end of the E-helix, which appears to have some regulatory role in the stabilisation of the synaptic tetramer complex (Burke *et al.*, 2004; Li *et al.*, 2005; Kamtekar *et al.*, 2006). Hence, a comparison of the properties of these activated mutants could further our understanding of how the site I synapse is stabilised in the absence of the *acc* sequences.

3.2 Results

3.2.1 Site I binding properties of Tn3 resolvase and activated mutants

Previous studies showed that wild-type Tn3 resolvase binds isolated site I with a high affinity, to give a stable dimer complex in bandshift assays (Bednarz *et al.*, 1990). However, observation of the site I synapse in binding assays with activated mutants of Tn3 and γδ resolvases is characterised by the absence of the dimer complex (Sarkis *et al.*, 2001; Nollmann *et al.*, 2004). These results suggest that the absence of the dimer complex in these assays might be a characteristic of the activated resolvase mutants that form the site I synapse. This hypothesis was tested by investigating the relationship between the presence of site I synapse and absence of the dimer complex in bandshift assays by four different activated mutants of Tn3 resolvase. In this experiment, the binding properties of WT-resolvase were compared with the activated mutants, SY-resolvase (G101S D102Y), M-resolvase (G101S D102Y M103I Q105L), AKSY-resolvase (R2A E56K G101S D102Y), and NM-resolvase (R2A E56K G101S D102Y M103I Q105L). Binding reactions were set up as described in Section 2.30, and a high DNA concentration (52.5

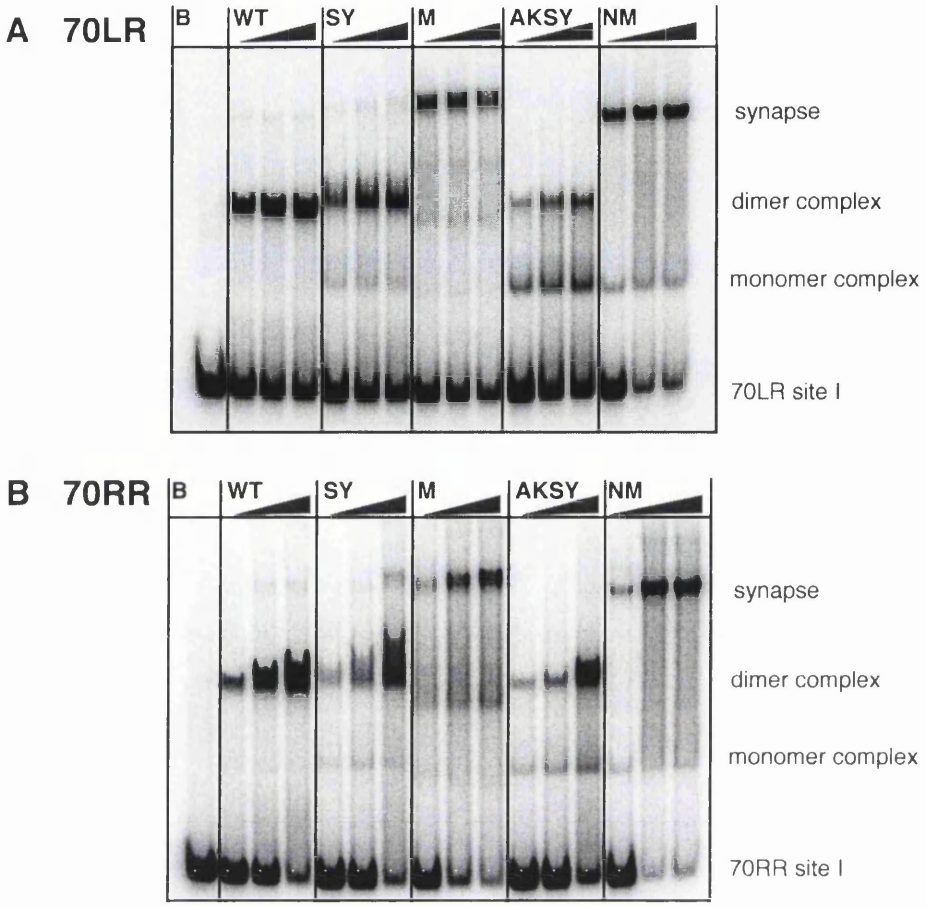

Mutant	Mutations in WT resolvase
SY	G101S D102Y
AKSY	R2A E56K G101S D102Y
M	G101S D102Y M103I Q105L
NM	R2A E56K G101S D102Y M103I Q105L

Figure 3.1 Binding and synapsis of site I substrates by WT resolvase and some activated mutants

Binding reactions were as described in section 2.30: Resolvase concentrations (100, 200, and 400 nM); 70LR site I or 70RR site I (unlabelled, 50 nM; ^{32}P-labelled, 2.5 nM). Electrophoresis was on a 6.5% TBE gel (Section 2.27). The SY-resolvase used in this and other experiments in this study carries a His-tag in the C-terminal domain. This might account for the slower migration of its dimer complex than that of WT-resolvase.

nM of 70LR site I) was used to encourage the formation of the site I synapse. The results are shown in Figure 3.1.

The identities of the complexes formed by WT-resolvase and the mutants in these assays were determined based on their known mobilities. WT-resolvase forms a complex containing two resolvase subunits and one site I DNA that can be observed in polyacrylamide bandshift assays (Bednarz *et al.*, 1990; Blake *et al.*, 1995). The assignment of the retarded band formed by NM-resolvase and M-resolvase as the site I synapse is based on the results of mixing experiments involving NM-resolvase and NM-GFP (Sarkis *et al.*, 2001; W.M. Stark, unpublished data). NM-GFP is a tagged version of NM-resolvase in which the green fluorescent protein (GFP) is attached to the C-terminal domain of resolvase. NM-GFP is bigger than NM-resolvase. Hence, a resolvase-DNA complex formed by NM-GFP is more retarded than the NM-resolvase complex of the same stoichiometry in bandshift assays. It was shown that the retarded band formed by NM-resolvase in this assay contains four resolvase subunits and two site Is (Nollmann *et al.*, 2004; W.M. Stark, unpublished data; see Figure 3.5).

The results of the bandshift experiments show that little or no dimer complex was observed in assays with the mutants that formed stable site I synapse (M-resolvase and NM-resolvase) (Figure 3.1, Panel A). In addition, these mutants formed significant amounts of monomer complex. Conversely, WT-resolvase and the activated mutants (SY-resolvase and AKSY-resolvase) that did not make stable site I synapse formed dimer complexes. AKSY-resolvase formed approximately equal amounts of monomer and dimer complexes. In order to investigate whether the absence of the dimer complex in the gel patterns of M-resolvase and NM-resolvase is due to a binding defect caused by the mutations, binding assays were carried out with 70RR site I. In this substrate, the base sequence of the left half of site I is replaced with the sequence of the right half (Figure 2.1). The right end sequence (TGTCTG) of the outer 6 bp of site I recognised by the DNA-binding C-terminal domain of resolvase binds with a higher affinity than the left end sequence (CGTTCG) (Bednarz *et al.*, 1990). If the absence of dimer complexes in the M-resolvase and NM-resolvase bandshift assays were due to an inherent defect in binding

to site I, the high-affinity 70RR site I could compensate for this defect and encourage the formation of dimer complexes. As expected, WT-resolvase and the activated mutants bind 70RR site I more tightly than 70LR site I, especially at the higher resolvase concentrations (Figure 3.1, Panel B). The binding pattern of WT-resolvase is not altered by 70RR site I since mainly dimer complexes are formed. SY-resolvase forms more synapse with 70RR site I than it does with 70LR site I. However, the streaky nature of the dimer complex suggests that it could be formed from synaptic complexes that disassembled during electrophoresis. M-resolvase seems to form more fuzzy dimer complex with 70RR site I than it does with 70LR site I. The 70RR site I substrate led to the formation of significantly less monomer complex by AKSY-resolvase, but still no synapses were found. NM-resolvase made less monomer complexes with 70RR site I than with 70LR site I. However, no dimer complex was observed despite the presumed higher affinity of the 70RR site I (Figure 3.1, Panel B).

3.2.2 Effects of electrophoretic conditions and catalytic activity on the bandshift pattern of WT-resolvase and NM-resolvase

The chemical nature and ionic strength of the electrophoresis buffer can affect the stability of certain complexes in bandshift experiments (Lane *et al.*, 1992). High-ionic strength buffers tend to favour the stability of higher order protein-DNA complexes over intermediate species. Hence, the binding properties of NM-resolvase were analysed on the low-ionic strength TGE buffer (Section 2.27) to see if dimer complexes of the activated mutants are formed. NM-resolvase was used in this experiment since it formed the most stable site I synapse among the activated resolvase mutants compared in Figure 3.1.

NM-S10A, a catalytically inactive mutant of NM-resolvase (Section 1.8) was included in this experiment as a control to determine the effect of catalytic activities on the nature of complexes formed. For the same reason, binding reactions of NM-resolvase and NM-S10A were set up with the modified 50LRpth site I substrate (Figure 2.1) that contains a phosphorothioate modification at both scissile phosphodiesters. This modification significantly inhibits the cleavage of site I by NM-resolvase (Nollmann *et al.*, 2004). The

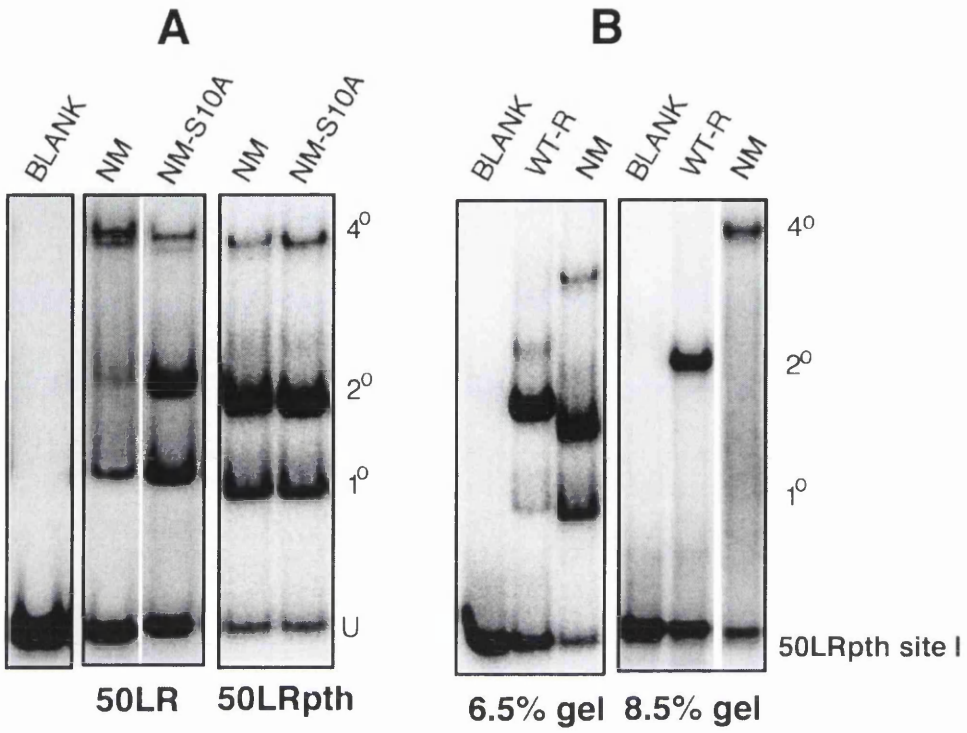

Figure 3.2 Effect of Tris-glycine electrophoresis buffer conditions on bandshift properties of WT-resolvase and NM-resolvase

Binding reactions and electrophoretic separations are as described in Sections 2.30 and 2.27 respectively. Resolvase (400 nM); 50LR site I or 50LRpth site I (unlabelled, 50 nM; ^{32}P-labelled, 2.5 nM). Electrophoresis was on 6.5% TGE gels (Section 2.27) except for the rightmost panel (8.5% gel). The symbols U, 1°, 2°, and 4° represent unbound DNA, monomer complex, dimer complex and synaptic complex respectively. **Panel A**: Binding/synapsis reactions of NM-resolvase and NM-S10A with unmodified 50LR site I and phosphorothioate-modified 50LRpth site I. **Panel B**: Effect of polyacrylamide gel percentage on bandshift patterns in the binding reactions of WT-resolvase and NM-resolvase with phosphorothioate-modified 50LRpth site I, analysed using Tris-glycine buffer.

unmodified 50LR site I (Figure 2.1) was used as the substrate here rather than the 70LR site I used in Section 3.2.1 in order to facilitate comparisons with the 50LRpth site I. The results shown in Figure 3.2 (Panel A) indicate that NM-resolvase forms mainly monomer and synaptic complexes with the unmodified 50LR site I, similar to the results of the binding with 70LR site I analysed under TBE electrophoresis buffer condition (Figure 3.1, Panel A). However, more monomer complexes were found under the TGE buffer conditions than the TBE conditions. In addition, a weak band corresponding to the dimer complex of NM-resolvase was formed on the TGE gel (Figure 3.2, Panel A, lane 2). The binding of NM-S10A (inactive mutant) with 50LR site I resulted in the formation of significant amounts of monomer and dimer complexes, along with the site I synapse (Figure 3.2, Panel A, lane 3). Binding of NM-resolvase and NM-S10A with 50LRpth site I also resulted in the formation of monomer and dimer complexes on TGE polyacrylamide gels (Figure 3.2, Panel A, lanes 4 and 5). These results show that the nature of the electrophoresis buffer affects the outcome of bandshift assays of NM-resolvase. It was also observed that two species that migrate close to one another are formed by NM-resolvase and NM-S10A in the bands that correspond to the site I synapse (Figure 3.2, Panel A).

It is known that polyacrylamide gel concentration could affect the stability of protein-DNA complexes in bandshift experiments (Lane *et al.*, 1992). Hence, the effect of polyacrylamide gel concentration on the distribution of the complexes formed by WT-resolvase and NM-resolvase under TGE electrophoresis buffer condition was investigated. The modified 50LRpth site I substrate was used in this experiment so that any monomer and dimer complexes formed can be observed. WT-resolvase formed mainly the dimer complex, and to a lesser extent some monomer complex when the binding reaction was analysed on a 6.5% polyacrylamide gel. In addition, a band that migrates slower than the dimer complex but faster than the NM-resolvase synapse was seen. The dimer complex of NM-resolvase migrates faster on the gel than the WT-resolvase dimer complex (Figure 3.2, Panel B, lanes 2 and 3). Increasing the polyacrylamide gel concentration to 8.5% under the same TGE buffer conditions changed the bandshift pattern obtained. WT-resolvase formed exclusively the dimer complex, and

only the synaptic complex is seen in the NM-resolvase lane (Figure 3.2, Panel B, lanes 5 and 6).

3.2.3 Analysis of the DNA stoichiometries of the two site I synapse bands

The bandshift assays used in this study usually give two bands corresponding to the synapse (e.g. Figure 3.2, panel A). The sites used in these assays are symmetrical in length; hence, the two bands are unlikely to be synapses with 'parallel' and 'anti-parallel' arrangements of the DNA. Such complexes are observed with DNA fragments in which site I is off-centre (M.R. Boocock & W.M. Stark, unpublished data). The appearance of the two bands is not dependent on catalytic activity since the two bands were still seen with inactive NM-S10A, and in assays in which the 50LRpth site I substrate that inhibits catalysis is used (Figure 3.2, Panel A). Titration of site I with NM-resolvase shows that there is a gradual reduction of the faster migrating species and increase of the slower one as the resolvase concentration in the binding mixture is increased (Figure 3.3, panel A). The possibility that one of the two bands is a a tetramer of resolvase bound to a single site I DNA was tested by investigating the DNA stoichiometries of the two species in a binding experiment involving a short ^{32}P-labelled 36LRpth site I and a long unlabelled 70LR site I.

In this experiment (Figure 3.3, panel B), standard binding reaction mixtures (Section 2.30) that contained 50 nM unlabelled and 2.5 nM ^{32}P-labelled 36LRpth site I were used for the assays, except that 50 nM of unlabelled 70LR was added to the reactions in the third and fourth lane. NM-D36N, another mutant of NM-resolvase was used in this experiment because it forms stable monomer, dimer and synaptic complexes in TBE bandshift assays (see Section 4.2.2; Figure 4.4), which is necessary for an unambiguous analysis of the data. In addition, the separation of the two bands is more distinct in binding assays of NM-D36N than those of NM-resolvase. The results show that the two species both contain two bound site Is since the synapse that contains the ^{32}P-labelled 36LRpth site I and the unlabelled 70LR site I (36/70 synapses in Figure 3.3, panel B) also

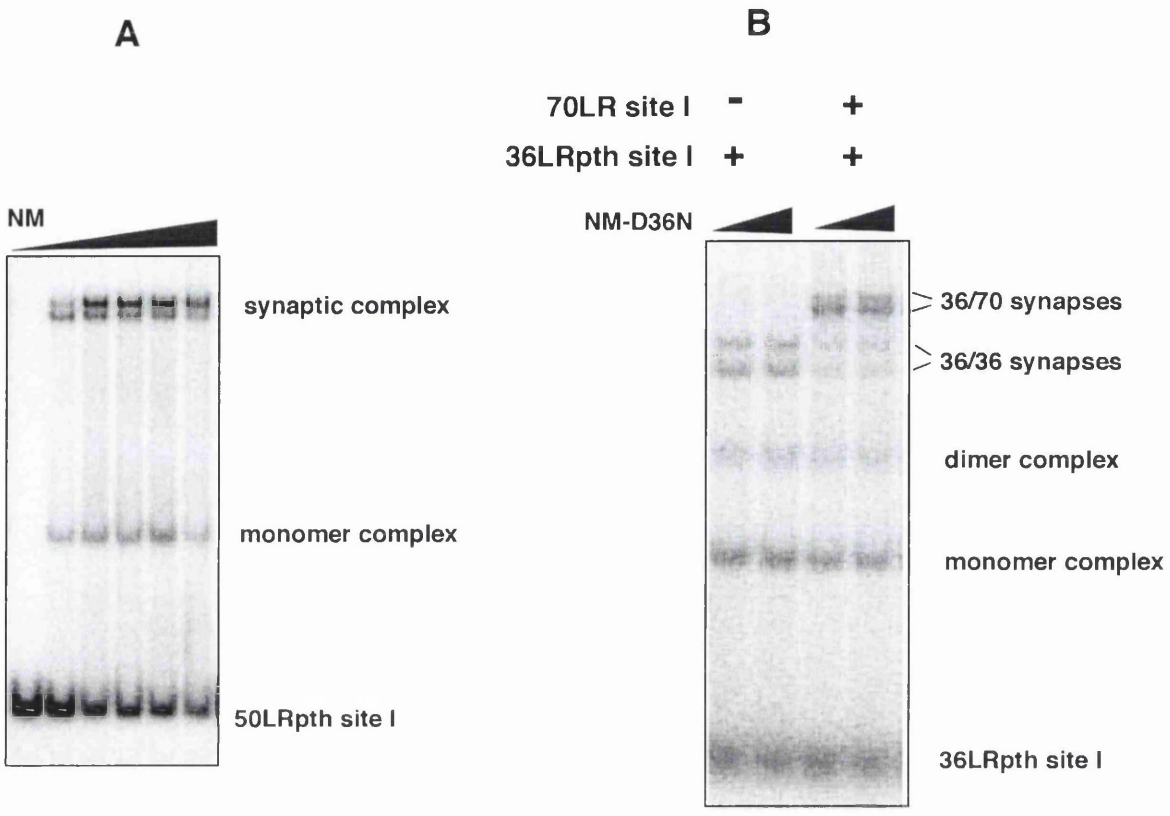

Figure 3.3 Characterisation of two synaptic complexes of NM-resolvase.
Panel A: Two bands with the mobility expected for the synapse can be observed. Increasing concentration of NM resolvase shifts the equilibrium in favour of the slower migrating species. The concentrations of NM resolvase used were 50, 100, 200, 400, and 800 nM. Binding reactions were as described in section 2.30: Resolvase (400 nM); 50LRpth (unlabelled, 50 nM; ^{32}P-labelled, 2.5 nM). Electrophoresis was on a 6.5% TBE gel (Section 2.27). **Panel B:** Bandshift experiment providing evidence that the two close bands are both true synaptic complexes containing two site Is. In this experiment, standard binding reaction mixtures (Section 2.30) that contained 50 nM unlabelled and 2.5 nM ^{32}P-labelled 36LRpth were used for the assays, except that 50 nM of unlabelled 70LR was added to the reactions in the third and fourth lane. NM-D36N at 400 and 800 nM concentrations was used.

splits into two visible bands. The two bands might differ in their resolvase content. For instance, the slower one might have an extra subunit, but this question was not resolved.

3.2.4 Subunit interactions in the assembly of the site I synapse by activated resolvase mutants

An attempt was made to detect the intermediate complexes of NM-resolvase on a TBE gel by investigating the time course of the formation of the site I synapse in a binding experiment with 50LRpth site I. Ice-cooled NM-resolvase and the DNA-containing buffer were mixed to initiate the binding reaction on ice. At timed intervals, aliquots were withdrawn from the scaled-up reaction and loaded directly onto a TBE polyacrylamide gel running at 200 V. Due to the practical limitations of this experiment, the earliest time point assayed was 20 seconds. The results show that the assembly of the site I synapse is a fast process with the maximum yield of the complex happening within 30 seconds at 0 ^{o}C (Figure 3.4). Apart from the synapse, monomer complexes were detected at all time points assayed. However, no band corresponding to the dimer complex was observed.

The pathway of synapse assembly in activated mutants was investigated using protein mixing experiments with NM-resolvase and NM-GFP. If NM-resolvase were mainly tetrameric in solution (as is reported for similar γδ resolvase mutants (Sarkis *et al.*, 2001; Grindley *et al.*, 2006), rapid mixing of NM-resolvase and NM-GFP with site I DNA should lead to the formation of two distinct synaptic complexes containing NM-resolvase tetramers and NM-GFP tetramers. However, formation of three mixed synapses (with 1:3, 2:2, and 3:1 resolvase stoichiometries) would prove that NM-resolvase exists mainly as monomers in solution, or is in rapid equilibrium as monomers and multimers. Stable dimers in solution would lead to formation of one mixed complex. In the experiment shown in Figure 3.5 (panel A), equal concentrations of NM-resolvase and NM-GFP were added to the 36LRpth site I substrate and the binding reaction was analysed in a bandshift assay. In order to exclude pre-binding mixing of NM-resolvase and NM-GFP, the two protein samples and the 36LRpth site I were added simultaneously. The results show that NM-resolvase and NM-GFP formed three mixed synapses in addition to the

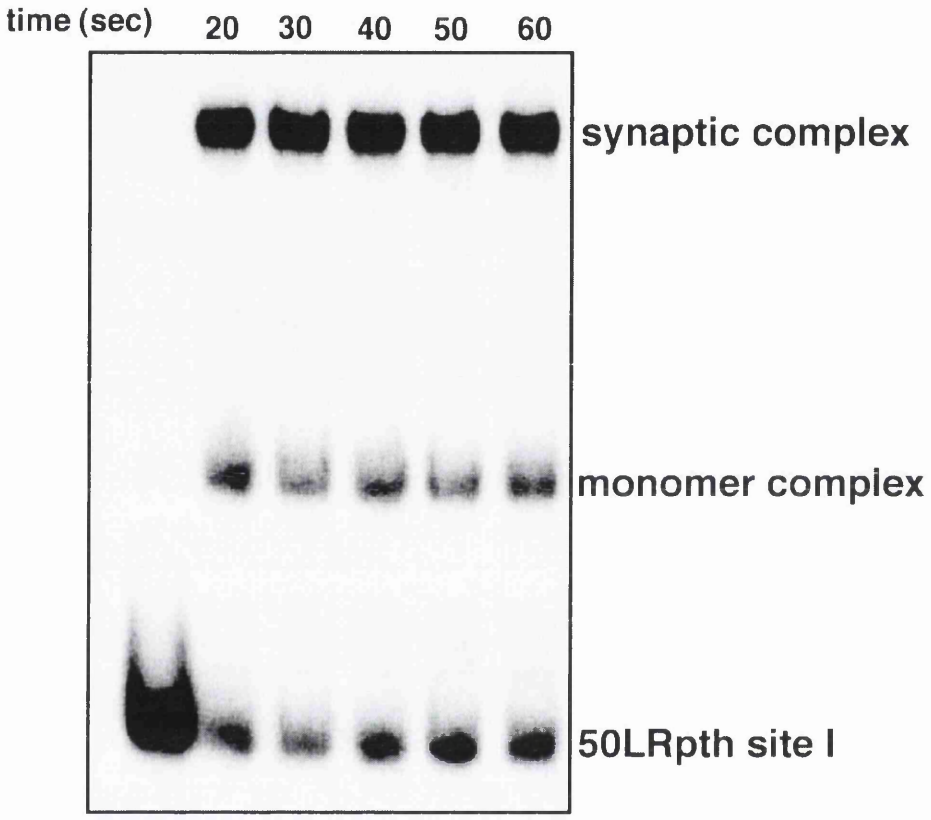

Figure 3.4 Time course of assembly of the site I synapse by NM-resolvase
At timed intervals, aliquots were withdrawn from a scaled-up binding reaction mixture at 0 °C and loaded on a running gel. Binding reactions were as described in section 2.30: Resolvase (400 nM); 50LRpth site I (unlabelled, 50 nM; ^{32}P-labelled, 2.5 nM). Electrophoresis was on a 6.5% TBE gel (Section 2.27).

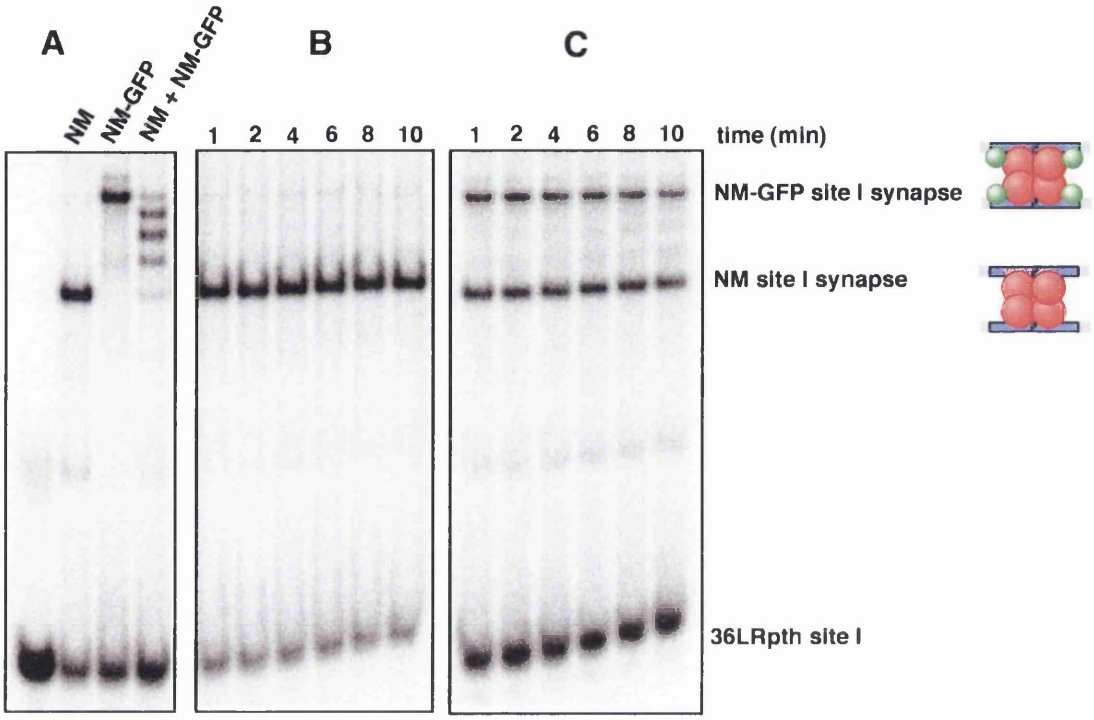

Figure 3.5 Assembly of the site I synapse from resolvase subunits and site I DNA
Panel A: The difference in the sizes of NM-resolvase synapse and NM-GFP synapse results in different rates of migration in bandshift assays. Mixing both proteins and the DNA simultaneously resulted in the formation of three mixed complexes. Binding reactions were as described in section 2.30: Resolvase concentration (400 nM); 36LRpth site I (unlabelled, 50 nM; ^{32}P-labelled, 2.5 nM). Electrophoresis was on a 6.5% TBE gel (Section 2.27). **Panel B**: A scaled-up binding reaction was set up with 400 nM of NM-resolvase and 36LRpth site I for 5 minutes to form the synapse, after which 400 nM of NM-GFP was added, and the mixture was vortexed. At timed intervals, aliquots were withdrawn from the scaled-up reaction mixture and loaded onto a running gel. **Panel C**: Scaled-up binding reactions (Section 2.30) of NM-resolvase and NM-GFP with 36LRpth were set up for 5 minutes to ensure that synapsis reached equilibrium, after which the two mixtures containing pre-formed synapses were mixed and vortexed. At timed intervals, aliquots were withdrawn from the mixture and loaded onto a running gel.

homotetramer synapses formed by the individual resolvases (Figure 3.5, panel A, lane 4), in amounts consistent with a mainly monomeric solution state for NM-resolvase.

A solution of pre-formed synapse of NM-resolvase was challenged with an equimolar concentration of free NM-GFP to ask if mixed synapses of the two resolvases are formed, and thus if subunits in the synapse can exchange readily with resolvase in solution (Figure 3.5, Panel B). In a different assay, separate pre-formed synapses of NM-resolvase and NM-GFP were mixed to encourage any possible re-distribution of subunits in the complexes (Figure 3.5, Panel C). In both experiments, the expected subunit redistribution was monitored for ten minutes at timed intervals. The results show that once the NM-resolvase site I synapse is formed, it is resistant to subunit exchange with resolvase subunits in solution, or with subunits from another synaptic complex (Figure 3.5, Panels B and C).

3.2.5 Site I cleavage activities of activated resolvase mutants

Time course analysis shows that NM-resolvase forms the site I synapse rapidly even at ice temperature (Figure 3.4). In order to see if the activation of the catalytic steps happens on a similar time scale, the cleavage of 70LR site I by NM-resolvase under the conditions in which the binding and synapsis reactions were carried out was investigated. Standard binding reactions were set up at 0 and 37 °C, and aliquots were withdrawn at timed intervals, then added to an SDS-containing stop buffer (Section 2.30). Addition of SDS to the binding reaction denatures and traps the resolvase if it has formed a covalent linkage to the site I DNA. The covalent intermediates can be visualized on a denaturing gel (Section 2.28). The results of the cleavage assay of NM-resolvase shows that only single strand cleavage products of 70LR site I are formed after 300 seconds when the reaction is incubated at 0 °C (Figure 3.6, Panel A). In addition, only a fraction of the total DNA in the reaction mixture is covalently attached to NM-resolvase. However, it takes only about 30 seconds to bind most of the input DNA in a similar time course analysis of the assembly of the synapse (Figure 3.4). The reaction proceeds at a faster rate at 37 °C to form both single strand and double strand cleaved products (Figure 3.6, Panel A).

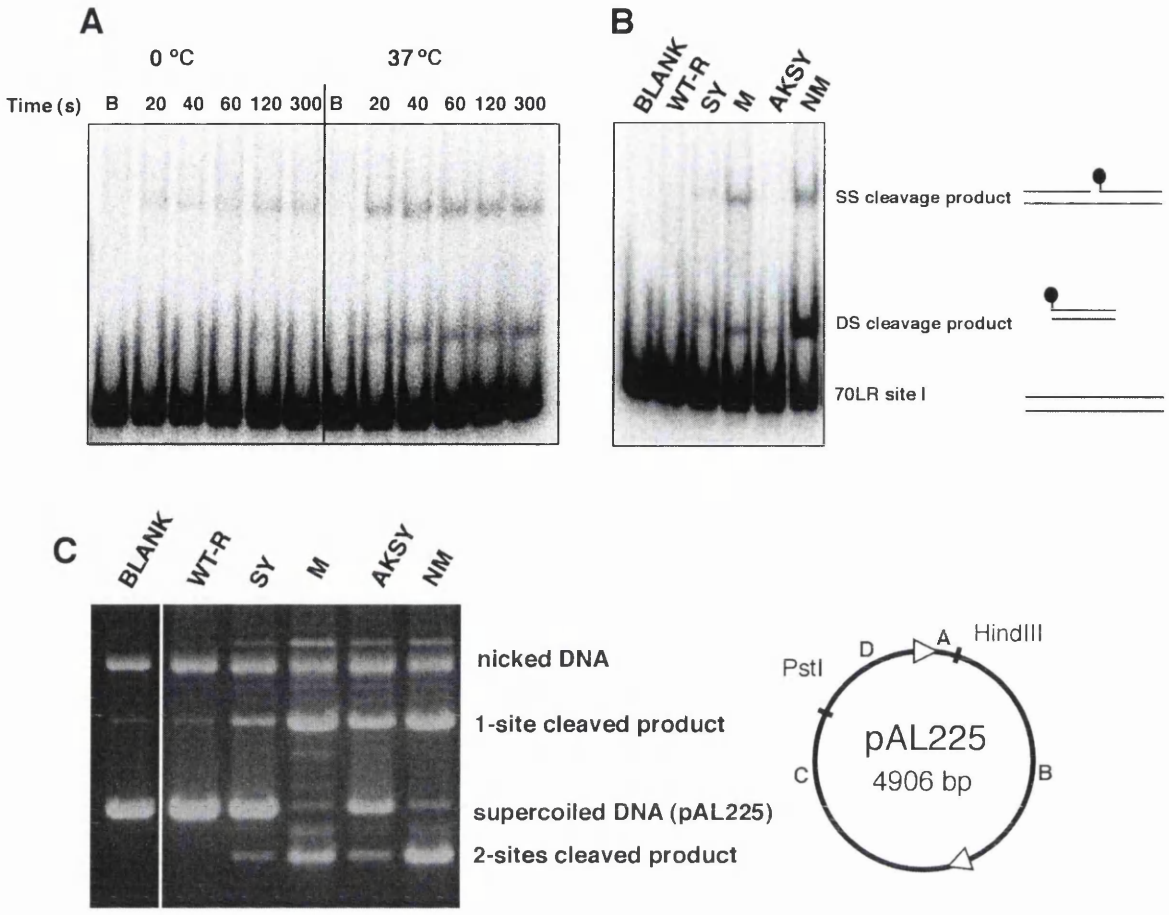

Figure 3.6 Cleavage activities of activated resolvase mutants on site I substrates
Panel A: Time course of the 70LR site I cleavage activity of NM-resolvase in binding/synapsis buffer (Section 2.30) at 0 and 37 °C. Scaled-up binding reaction mixtures were set up at 0 and 37 °C as described in Section 2.30: Resolvase (100 nM); 70LR site I (unlabelled, 50 nM; ^{32}P-labelled, 2.5 nM). At timed intervals, aliquots were withdrawn from the mixture and immediately treated with 0.1% SDS for 10 min at room temperature (Section 2.18). Electrophoresis was on a 6.5% TBE SDS gel (Section 2.28). **Panel B:** 70LR site I cleavage activities of activated resolvase mutants in binding/synapsis buffer. Binding reactions were set up as described in Panel A for 30 minutes and then treated with 0.1% SDS for 10 minutes. Electrophoresis was on a 6.5% TBE SDS gel (Section 2.28). The cartoons illustrate the single strand and double strand cleavage products formed. The grey lines represent the DNA strands, and the lollipops represent resolvase covalently attached to the DNA strand at the scissile phosphate. **Panel C:** pAL225 cleavage activities of activated resolvase mutants in EG buffer (Section 2.31). Each reaction contained 100 nM resolvase and 0.4 μg DNA in each 22 μl reaction mixture. The reactions were incubated for 20 minutes. SDS/protease K loading buffer was added to stop the reactions, after which the products were separated on a 1.2% agarose gel (Section 2.17). A graphic map of pAL225, the site I x site I plasmid substrate used is shown in Panel C (see Section 2.31).

The correlation between the ability of an activated resolvase mutant to form site I synapse in bandshift assays and ability to catalyse strand cleavage on oligonucleotide substrates was investigated using 70LR site I. Binding reactions of WT-resolvase, SY-resolvase, M-resolvase, AKSY-resolvase, and NM-resolvase with 70LR site I were incubated for 30 minutes at 37 °C and analysed for the formation of resolvase-site I covalent complexes after treatment with SDS (Figure 3.6, Panel B). The results show that WT-resolvase is completely inactive, while traces of single strand cleavage products are formed by SY-resolvase and AKSY-resolvase. In contrast, M-resolvase and NM-resolvase that form stable site I synapses in bandshift assays (Figure 3.1) generated significant amounts of single-strand and double-strand cleavage products.

The cleavage activities of the activated resolvase mutants were further tested on a site I x site I plasmid substrate, pAL225 (Section 2.31). The reactions were set up in EG buffer (Section 2.31), which favours the formation of cleaved intermediates (Johnson & Bruist, 1989; Boocock *et al.*, 1995). Protease K was added to the stopped reaction to digest resolvase molecules that are covalently attached to the cleaved plasmid substrate in order to facilitate the migration of the reaction products on agarose gels. Figure 3.6 (Panel C) shows the cleavage activities of WT-resolvase and the activated mutants on pAL225. WT-resolvase was completely inactive in cleavage of the site I x site I substrate. However, the activated mutants formed single-site and double-site cleavage products to different extents. The mutants that formed stable site I synapse in bandshift assays (Figure 3.1), M-resolvase and NM-resolvase, were significantly more active than SY-resolvase and AKSY-resolvase, which did not form detectable synaptic complexes.

3.2.6 Recombination of *res* x *res* substrate (pMA21) by WT-resolvase and activated resolvase mutants

In order to gain further insights into the effects of activating mutations on the properties of WT-resolvase, the recombination activities of the four activated resolvase mutants (SY-resolvase, M-resolvase, AKSY-resolvase, and NM-resolvase) along with WT-resolvase were tested on a *res* x *res* substrate, pMA21. The effect of pH variation on the recombination activities of the mutants were also investigated to see if the activating

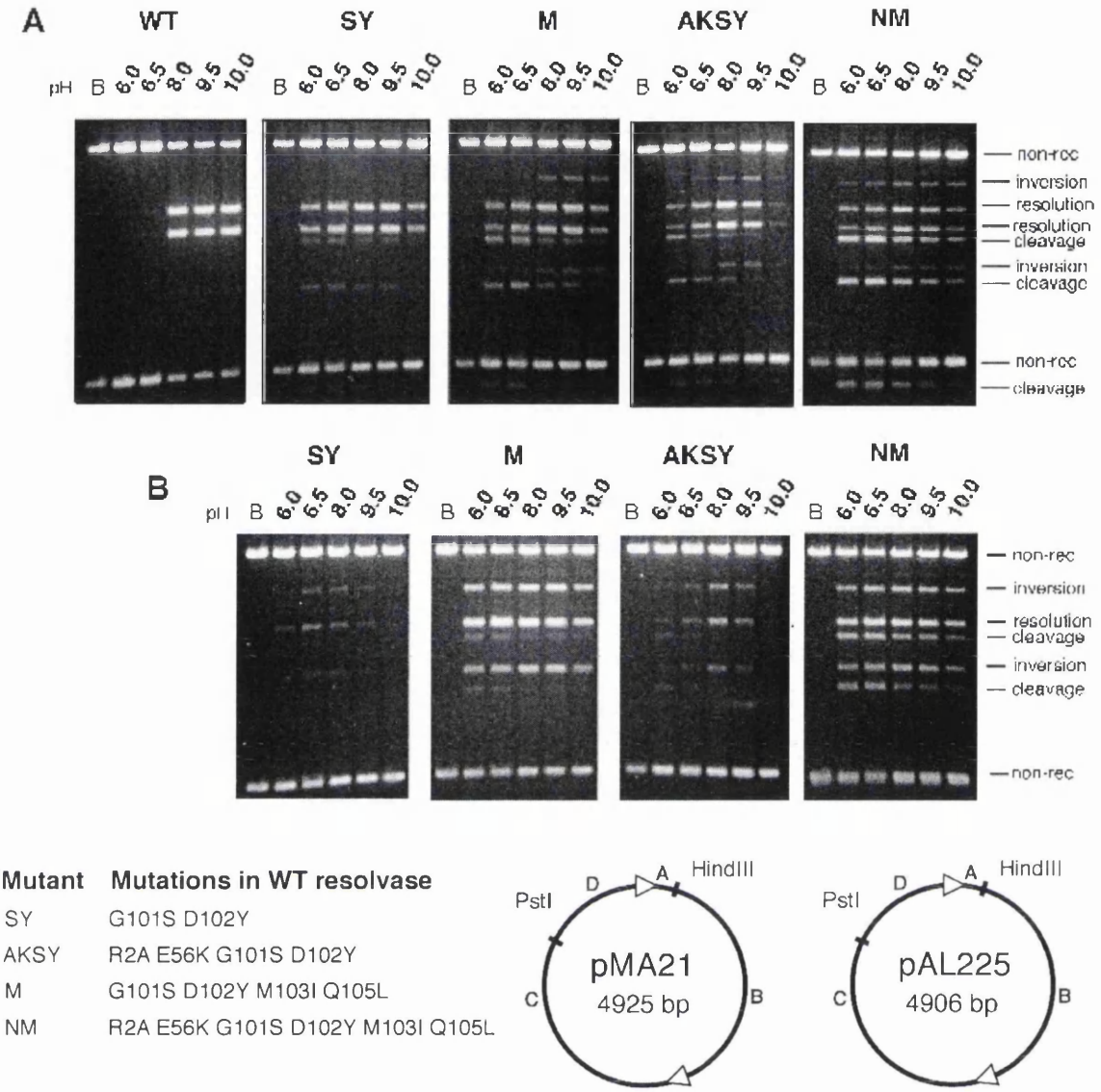

Mutant	Mutations in WT resolvase
SY	G101S D102Y
AKSY	R2A E56K G101S D102Y
M	G101S D102Y M103I Q105L
NM	R2A E56K G101S D102Y M103I Q105L

Figure 3.7 Recombination activities of WT-resolvase and activated resolvase mutants.

Panel A: Recombination activities on *res* x *res* substrate, pMA21. Reactions were in recombination buffer at the indicated pH (Section 2.31). Reactions were set up in the following buffer systems: Sodium phosphate (pH 6.0 and 6.5); Tris-HCl (pH 8.0); Tris-glycine (pH 9.5); Glycine-NaOH (pH 10.0). Each reaction contained 100 nM resolvase and 0.4 μg DNA in each 22 μl reaction mixture. The reactions were incubated at 37 °C for 1 hour. Reaction products were treated with HindIII and PstI, and were separated on a 1.2% agarose gel after treatment with SDS and Protease K (Section 2.17). The specific mutations in each of the mutant resolvases are listed in Figure 2.1. **Panel B:** Recombination activities on site I x site I substrate, pAL225. Reaction conditions and treatment of the reaction products are as described in Panel A. The sizes of the bands are as summarised in Figures 2.2-2.4.

mutations have any effects on the catalytic mechanism of resolvase. The recombination reaction was investigated at pH 6.0, 6.5, 8.0, 9.5, and 10.0 at 37 °C.

As shown in Figure 3.7 (Panel A), the activated mutants were less efficient in catalysing the recombination of pMA21 than WT-resolvase. In addition, WT-resolvase formed exclusively resolution products while the mutants (other than SY-resolvase) formed both resolution and inversion products. Another characteristic difference between WT-resolvase and the activated mutants is that all the mutants generated unligated cleaved intermediate products. This feature of activated mutants has been reported by Arnold *et al.* (1999). Furthermore, the activated resolvase mutants were more active at neutral to slightly acidic pH and less active at pH 9.5 and 10.0, in contrast to the pattern of WT-resolvase. There was also a change in the product profile of the reactions by the activated resolvase mutants at lower pH. Reactions catalysed in the acidic range resulted in the formation of more unligated cleaved intermediates. M-resolvase and AKSY-resolvase, and NM-resolvase to a lesser extent, formed less inversion products at pH 6.0 and 6.5.

3.2.7 Recombination of site I x site I substrate (pAL225) by activated resolvase mutants

The results presented in Section 3.2.5 suggest that activated resolvase mutants that form site I synapses in bandshift assays are more active in cleavage of oligonucleotide and plasmid site I substrates. The recombination activities of the activated resolvase mutants were tested on pAL225 (site I x site I plasmid substrate) to investigate if there is a correlation between formation of stable site I synapse and catalysis of site I recombination. In order to see if the difference in the pH dependence of recombination of pMA21 by WT-resolvase and the activated mutants (Figure 3.7, Panel A) is due to the effect of the accessory sites in that substrate, recombination of pAL225 (site I x site I substrate) was also assayed at different pH values. WT-resolvase was not included in this assay since it does not catalyse recombination of site I x site I substrates (Bednarz *et al.*, 1990; Figure 3.6). The results of the pAL225 recombination assays show that M-resolvase and NM-resolvase catalysed the recombination of pAL225 efficiently, while SY-resolvase and AKSY-resolvase were less efficient (Figure 3.7, Panel B). M-resolvase

and NM-resolvase were more active at lower pH and they formed more cleaved intermediates at pH 6.0 and 6.5 as was the case in the reaction with the *res* x *res* substrate, pMA21 (Figure 3.7, Panel A).

3.3 Discussion

Some biochemical properties of activated resolvase mutants were compared with those of WT-resolvase in this chapter with the aim of understanding how activating mutations deregulate site I synapsis and catalysis by Tn3 resolvase. The findings from this investigation and their implications are discussed below.

3.3.1 Catalysis of *res* x *res* recombination by activated mutants

While activating mutations confer the capacity for *acc*-independent synapsis and catalysis on resolvase, the efficiency with which the enzyme catalyses the *res* x *res* recombination reaction has been reduced (Figure 3.7). The residues that produce activating effects when mutated (REG residues) are not highly conserved among the serine recombinases (Burke *et al.*, 2004; Section 1.9) suggesting that they are unlikely to participate directly in the catalysis process. Hence, the effects of the activating mutations on the efficiency of *res* x *res* recombination might not be due to a direct effect on the chemical steps of catalysis. One possibility is that activating mutations disrupt an important element of wild-type *res* synapsis that regulates catalysis, thereby 'compromising' the efficiency of recombination.

3.3.2 Activating mutations and pH dependence of recombination

The differences in the pH dependence of *res* x *res* recombination by WT-resolvase and activated resolvase mutants (Section 3.2.6) suggest that the activating mutations have altered certain aspects of catalysis in the wild-type reaction. The same pattern of pH dependence is seen in site I x site I recombination reactions by the activated mutants (Section 3.2.7). Hence, the inability of WT-resolvase to catalyse recombination at low pH may be due to control mechanisms that regulate synapsis and/or catalysis at the site I synapse, and not necessarily due to the dependence of formation of the *res* synapse on high pH. Mutation of residues either near or distal to the active site can modify internal

enzyme motions with consequent effects on catalysis (Tousignant & Pelletier, 2004). Such mutations could lead to changes in the local environment of some active site residues whose functions are pH-sensitive. Hence, it is possible that the altered pH dependence of recombination by activated mutants from the WT-resolvase pattern could be due to subtle changes in the active site. Certain residues that produce activating effects when mutated (REG residues) including A117, R121 and E124 have their side chains contacting active site residues S10, D67, R68, and R71 of the partner subunit in the γδ resolvase dimer complex (Yang & Steitz, 1995). In addition, it was suggested that mutation of the REG residues L66 and G70 could perturb the neighbouring side chain configurations of D67, R68, and R71 (Burke *et al.*, 2004).

3.3.3 Formation of site I synapse and efficiency of site I x site catalytic activities by activated resolvase mutants

Comparison of the binding properties (Section 3.2.1) and catalytic activities (Sections 3.2.5 and 3.2.7) of the activated resolvase mutants clearly show that there is a correlation between observation of site I synapse in polyacrylamide bandshift assays and efficient catalysis of site I recombination. These results suggest that the initiation of catalytic events by resolvase happens in the synapse rather than at the level of the monomer or dimer complex. Since all the catalytic residues in the active site are believed to be provided by the same resolvase subunit (Boocock *et al.*, 1995; Grindley *et al.*, 2006), it is possible that specific synaptic interactions are required to initiate catalysis. Hence, efficient catalysis of site I x site I recombination by the activated resolvase mutants might depend on the assembly of a stable site I synapse. However, the assembly of the synapse might not be the only factor that determines catalysis of site I x site I recombination. Comparison of the time courses of formation of the site I synapse (Figure 3.4) and of catalytic products (Figure 3.6) shows that activation of catalysis lags behind synapse assembly. While NM-resolvase binds and synapses site I rapidly, there could be certain steps after the assembly of the synapse that are important for the initiation of catalysis (Parker & Halford, 1991).

3.3.4 Assembly of the site I synapse by activated resolvase mutants

The observation that activated mutants that form site I synapse formed little or no dimer complex on TBE polyacrylamide gels (Section 3.2.1) suggests that the mutants might form dimer complexes that are structurally and functionally distinct from the dimer complex of WT-resolvase. This might account for the faster migration of the dimer complex of NM-resolvase than that of WT-resolvase on TGE polyacrylamide gel (Figure 3.2, Panel B). The failure to detect the dimer complex band in the time course experiment (Figure 3.4) suggests that once the dimer complexes are formed, they rapidly associate to form the synapse. Hence, the activating mutations might modify the WT-resolvase dimer-site I complex from a conformation that is not competent for synapsis into a form that readily associates to form the synapse. This might explain why SY-resolvase and AKSY-resolvase form dimer complexes but fail to form synapses on TBE polyacrylamide gels (Section 3.2.1; Figure 3.1). Li *et al.* (2005) invoked Ramachandran plot considerations to suggest that the G101S and E102Y changes in γδ resolvase could destabilise the pre-synaptic dimer complex and stabilise the site I synapse. The equivalent mutations G101S and D102Y are present in all the activated mutants studied in this chapter (see Section 3.1.2). An altered structure of the dimer complex of NM-resolvase might be less stable, and thus account for the monomer complexes formed by this mutant in bandshift assays (Figures 3.1 and 3.2). The near absence of monomer-site I complex is characteristic of bandshift assays of WT-resolvase (Bednarz *et al*, 1990; Arnold *et al.*, 1999). The cooperative binding of WT-resolvase to site I to form mainly the dimer complex could have significance for the regulation of catalysis. The inability of WT-resolvase to form a synapse with isolated site Is might serve to ensure that catalytic events are confined to DNA substrates with full *res* sites.

Solution and crystal structures provide interesting insights into the nature of the site I synapse (Nollmann *et al.*, 2004; Li *et al.*, 2005; Kamtekar *et al.*, 2006; Section 1.9). However, the structures do not reveal how the synapse is assembled from resolvase subunits and site I. The assembly of the site I synapse might occur via two different pathways (Figure 3.8). In the 'resolvase dimer pathway', the association of two dimer-site I complexes leads to the assembly of the synaptic complex (Figure 3.8, Panel A). The

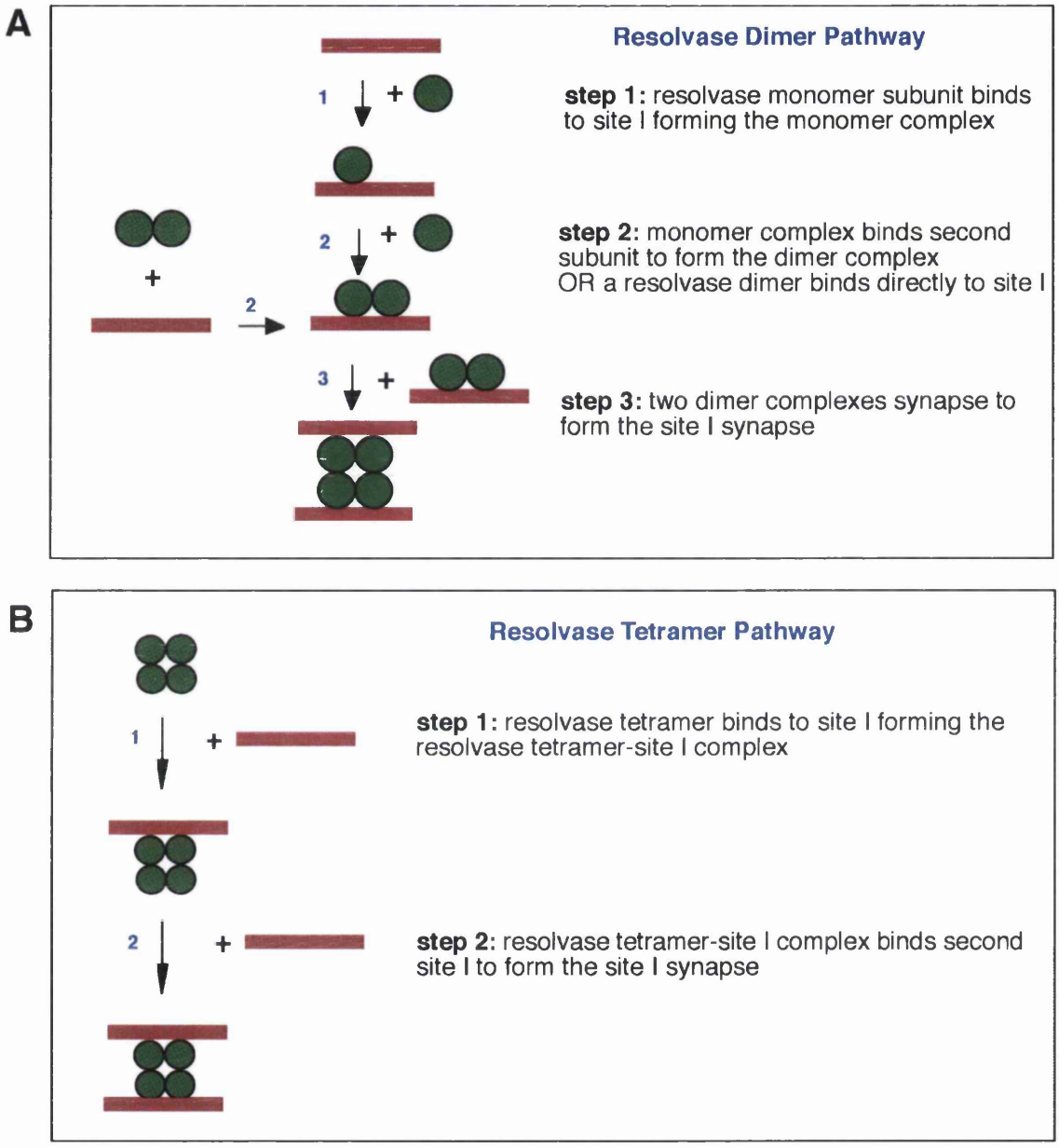

Figure 3.8 Hypothetical pathways for the assembly of the site I synapse by activated resolvase mutants

dimer complex can be formed by the sequential binding of resolvase monomers to site I or by the binding of a resolvase dimer to site I (Blake *et al.*, 1995; Nollmann *et al.*, 2005). It has been suggested that the activating mutations could stabilise a pre-assembled resolvase tetramer in solution (Sarkis *et al.*, 2001; Grindley *et al.*, 2006; Kamtekar *et al.*, 2006). If the resolvase tetramer is stable in solution it could form the synapse by sequentially binding two site Is using the 'resolvase tetramer pathway' (Figure 3.8, Panel A).

The mixing experiments with NM-resolvase and NM-GFP (Figure 3.5, Panel A) show that the main solution species of NM-resolvase are apparently monomers; any multimers formed in solution are not stable. The synapse mixing experiments (Figure 3.5, Panels B and C) confirm that the synaptic tetramers of NM-resolvase are stable in solution. These results are different from the findings of Sarkis *et al.* (2001), whose data suggest that an activated γδ resolvase mutant (R2A E56K G101S E102Y M103I K105L E124Q) forms stable tetramers in solution, that then bind DNA to form the site I synapse. Furthermore, a crystal structure of a tetramer of the N-terminal domains of this activated mutant without DNA has been solved (Kamtekar *et al.*, 2006). In contrast to the γδ resolvase mutant, sedimentation velocity data show that NM-resolvase is mainly monomeric in solution (Nollmann *et al.* 2005).

The hypothetical pathways shown in Figure 3.8 predict different sets of resolvase-site I complexes that may be observed in bandshift experiments. The 'resolvase dimer pathway' involves monomer, dimer and synaptic tetramer complexes. On the other hand, in the 'resolvase tetramer pathway', the synaptic tetramer complex and the tetramer bound to a single site would be the two major protein-DNA species. WT-resolvase forms mainly the dimer complex and NM-resolvase form monomer, dimer and synaptic complexes (Figures 3.1 and 3.2). This pattern is consistent with the resolvase dimer pathway for the assembly of the site I synapse (Figure 3.8) by activated resolvase mutants. It is significant that no band corresponding to a resolvase tetramer bound to only one site I has been found under any electrophoretic conditions with either Tn3 or γδ resolvase mutants (Section 3.2.3; Sarkis *et al.*, 2001). Figure 3.2 (Panel A) shows that significant amounts of

dimer complexes of NM-resolvase were observed on 6.5% TGE polyacrylamide gels under conditions in which catalysis was inhibited (binding assays with NM-S10A, and binding of NM-resolvase with 50LRpth). In contrast, less dimer complexes were observed in the binding assay of NM-resolvase with 50LR (Figure 3.2, Panel A). These results suggest that inability to initiate catalysis facilitates the dissociation of the synapse to intermediate complexes on the low ionic-strength TGE gel (Lane *et al.*, 1992). The absence of the monomer and dimer complexes of NM-resolvase on the TGE 8.5% polyacrylamide gel (Figure 3.2, Panel B) might be due to the caging effect of the higher percentage gel (Lane *et al.*, 1992). An interpretation that would account for the results is that in solution, nearly all dimers efficiently go into the synapse, which is reflected in TBE (Figure 3.1) and 8.5% TGE (Figure 3.2, Panel B) gels. The synapse however is less stable on the 6.5% TGE gels, and dissociates to give dimer and monomer complexes (Figure 3.2, Panel A). The disassociation of the synapse into dimer complexes on 6.5% polyacrylamide TGE gels supports the argument that the synapse is assembled via the association of two dimer complexes (see Section 5.3.2).

Chapter Four

Mutational analysis of the role of putative active site residues of Tn3 resolvase in site I synapsis and catalysis

4.1 Introduction

4.1.1 Mutational analysis of conserved residues to probe their contributions to catalysis

Mutagenesis of conserved and/or putative active site residues is a standard approach used to investigate how amino acid residues are involved in the reaction mechanism of enzymes. The initial step in identifying the key residues involved in catalysis is selection of candidate residues based on sequence conservation among a protein family, and the polar character of such residues. This is followed by mutagenesis of the residues and characterisation of the mutant proteins to see the effect on the catalytic process. Generally, mutation of residues that are essential to the chemistry of catalysis leads to complete or partial loss of activity. Information that is more useful can be obtained when the created changes lead to specific defects in the catalytic pathway. This can reveal previously unidentified or unanticipated routes in the reaction mechanism, and the residue mutated to generate the observed effect is likely to be involved in events at and/or downstream of the arrested step. Identification and successful characterisation of step-arrest mutants is a potentially powerful tool in elucidating the mechanism of reactions involving multiple components and multiple steps. This approach is facilitated if there are specific and relatively independent assays for each of the steps in the reaction pathway. The principle of elucidating reaction mechanisms via mutagenesis of active site residues is illustrated in Figure 4.1.

4.1.2 Analysis of the role of putative active site residues in NM-resolvase

The strategy in this chapter was the construction and characterisation of conservative mutations of a set of residues in the N-terminal domain of resolvase. The mutations were created mainly in the background of NM-resolvase, an activated mutant of Tn3 resolvase (Section 1.9). Unlike WT-resolvase, NM-resolvase does not require accessory sites and catalyses recombination on oligonucleotide substrates. Hence, effects of mutations can be more reliably ascribed to events at site I (binding, synapsis, and catalysis), and not regulatory functions (see Section 1. 9).

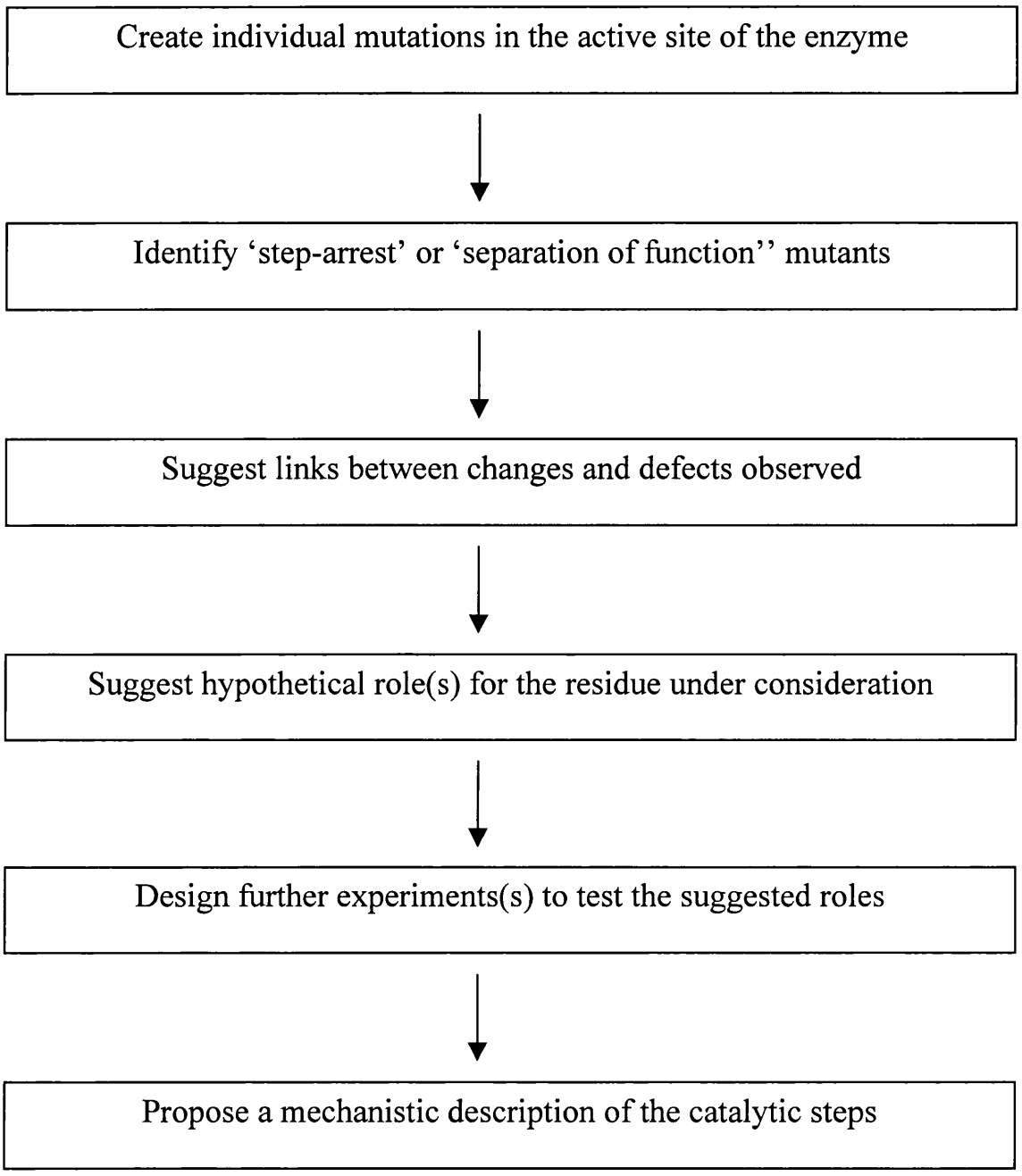

Figure 4.1: Schematic illustration of the use of site-directed mutagenesis of putative catalytic residues to study enzyme catalytic mechanism

The residues chosen for mutation in this study are highly conserved in the serine recombinase family and are hypothesised either to be part of the active site, or required for maintaining the structure of the active site, or have other crucial roles in catalysis. They are: Y6, R8, V9, Q14, Q19, D36, S39, R45, D59, D67, R68, R71, E118, R119, E124 and R125. Some of these residues have been previously mutated in Tn3 and γδ resolvase and shown to affect binding and the recombination reaction (Grindley, 2002). The positions of these residues in the crystal structure of an activated γδ resolvase site I synapse (Li *et al.*, 2005) are shown in Figure 4.2. Table 4.1 contains a summary of published structural information and results of mutational analysis of these conserved residues in serine recombinases. The data from the literature shows that mutation of R8, S10, R68, and R71 in γδ resolvase (and equivalent residues in other serine recombinases) results in abolition of catalytic activities. This suggests that these residues may be involved in the chemical steps of catalysis. In addition, they are found to interact closely with the scissile phosphate in crystal structures of γδ resolvase (Table 4.1).

Alanine scanning mutagenesis is an approach used for identifying residues involved in the catalytic mechanism of enzymes. It involves changing the amino acid residues in a part of the protein to alanine, the assumption being that alanine has a simple, small hydrocarbon side chain that will not introduce new functional groups at the position of interest. The approach adopted in this study is different since the initial replacements made were chosen to conserve the steric bulk of the original residue in order to minimise changes to the global structure of resolvase. The substitutions made were Y→F, S→A, V→A, R→K, D→N, E→Q, and Q→E. Table 4.2 is a summary of the predicted effect of the changes on the functionality of the amino acid residues and the likely side effects that the changes could have on the structure and function of the protein. Such conservative replacements appear to be more suitable for a catalytic system such as resolvase that involves multiple protein subunits and some steps involving conformational changes. The mutant resolvases were made and their *in vitro* binding and catalytic properties were compared with the parent NM-resolvase using the procedures described in Chapter 3.

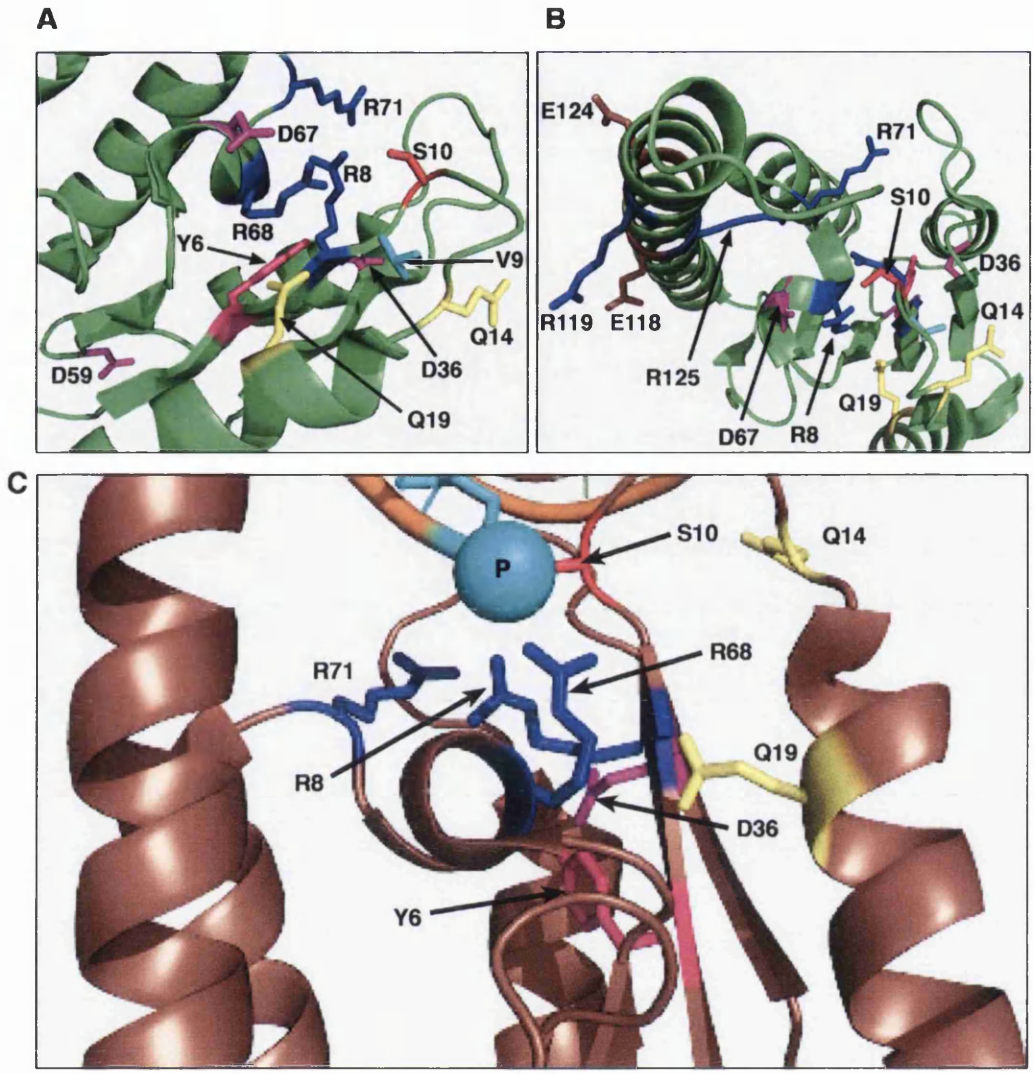

Figure 4.2 N-terminal domain of γδ resolvase activated mutant in the site I synapse showing the positions and relative orientations of conserved residues mutated in this study.

Two different views of the same structure are shown in **Panels A** and **B**. The polypeptide backbone of the molecule is represented as green cartoons, while the side chain of the residues are shown as sticks with the following colouring representations: Arg (blue), Ser (red), Asp (purple), Glu (brown), Gln (yellow), Tyr (pink), and Val (cyan). The DNA is not shown in these pictures. **Panel C** shows a close-up view of some putative active site residues close to the scissile phosphate. In this picture, S10 is covalently attached to the scissile phosphate (cyan sphere), while R8 and R68 are close to this phosphate group. The pictures were generated from PDB coordinates of 1ZR4 (Section 2.35).

Table 4.1: Summary of published structural and *in vitro* mutational data on resolvase putative catalytic residues

Residue	Structural information	Mutational Analysis	References
Y6	Forms part of the hydrophobic core; H-bonds to D36	Tn3 Y6F: Bind+, Rec-, γδ Y6F: Bind+, Rec-, Cat+	2,10,17,19
R8	Within 5 Å of S10 in the dimer; interacts with the post cleavage non-bridging oxygen of the 5'-phosphoserine	γδ R8Q: Cat- Hin R8Q: Cat- Hin R8W: Bind+, Cat-	4,9,11,12,19
V9	Forms part of the hydrophobic core of the N-terminal domain	Hin V9M: Cat-	12,17,19
S10	Covalently attached to the DNA in the cleaved synaptic complex	Tn3 and γδ S10A: Bind+, Rec-, Cat- γδ S10L: Site I Bind- β S10A: less cooperative binding	4,5,7,11,15
Q14	Near the active site in all structures; no definite contact seen	β Q14R: monomeric, weak binding, poor site I bending, Rec- γδ Q14R: Bind+, Rec- (in vivo) γδ Q14L: Bind+, Cat-	5,6,11,17,19
Q19	H-bond network with D67, R68, & E124 in 1GDT	No mutants characterised	18
D36	H-bonds to Y6 and N terminus of helix αB in the dimer complex	No mutants characterised	18
S39	Forms part of the mobile loop between β2 and αB helices	γδ S39C: Rec+	7,9,11,16,17,19
R45	Forms part of the mobile loop between β2 and αB helices; may control access to Y6	Hin R43H: Weak cleavage & inversion activities Hin R43L: Cat-, extended binding specificity Hin R43C: Cat-, extended binding specificity Hin R43S: Extended binding specificity	1,16,16
D59	Close to the 2-3' interface in 2RSL; far from the active site	β D55N: weak binding, Rec-	5,17
D67	Forms part of the H-bond network with R8, S10, R68 & E124 of the partner subunit; interacts with R68 in the post-cleavage complex	γδ D67G: Bind+, Cat- Hin D65N: Bind+, Cat-	6,11,13,19

R68	Within 5 Å of S10 in the dimer; interacts with the post-cleavage non-bridging oxygen of the 5'-phosphoserine	γδ R68H: Bind+, Cat- γδ R68C: Bind+, Cat-	4,6,11,19
R71	Coordinates the scissile phosphate and the one 5' to it in the dimer complex; interacts with S43 of the mobile loop in the post-cleavage complex	γδ R71H: Bind+, Cat- Hin R69C: weak cleavage & inversion activities, extended binding specificity Hin R69S: Cat- Hin R69P: Cat-	1,4,6,11,19
E118	Stabilises the dimer interface	β E121K: monomeric, weak binding, poor site I bending, Rec- γδ E118K: Rec-, poor site I bending	5,8,19
R119	E-helix residue; far from the pre-cleavage active site; makes DNA contact near the scissile bond	No mutants characterised	19
E124	Interacts with S10 and R68 of the partner subunit in the pre-cleavage dimer complex	Tn3 & γδ E124Q & E124A have activating phenotypes	2,3,18,19
R125	Close to the pre-cleavage scissile bond and the post-cleavage 3'OH; ionic contacts with D96 on the post-cleavage hydrophobic interface	Hin R123Q: Bind+, Cat- γδ R125Q: Rec+	11,12,13,19

References:

1. Adams *et al.*, 1997
2. Arnold, 1997
3. Arnold *et al.*, 1999
4. Boocock *et al.*, 1995
5. Canosa *et al.*, 1997
6. Grindley, 1994
7. Hatfull & Grindley, 1986
8. Hatfull *et al.*, 1987
9. Hatfull *et al.*, 1989
10. Leschziner *et al.* 1995
11. Li *et al.*, 2005
12. Nanassy & Hughes, 1998
13. Nanassy & Hughes, 2001
14. Newman & Grindley, 1984
15. Nollmann *et al.*, 2004
16. Rice & Steitz, 1994b
17. Sanderson *et al.*, 1990
18. Sarkis *et al.*, 2001
19. Yang & Steitz 1995

Bind: indicates binding to a *res* site
Cat: indicates cleavage activity
Rec: indicates complete recombination activity
Hin: Hin recombinase
β: β recombinase

2RSL: γδ resolvase PDB coordinates (18)
1GDT: γδ resolvase PDB coordinates (20)
1ZR4: γδ resolvase PDB coordinates (11)

Table 4.2: Potential usefulness and possible drawbacks of the changes made to the putative catalytic residues

Mutations made at the chosen residues	Potential usefulness and possible drawbacks of the mutations
S10A S39A	Probes any role of the hydroxyl group in catalysis and H-bond interactions in binding and synapsis.
R8K R45K R68K R71K R119K R125K	Replacement of arginine with lysine probes the specific requirement for the guanidinium side chain, while preserving some positive charge and the bulk of the side chain. The flexible lysine side chain is a potential drawback since it could make new interactions.
Q14E Q19E	Probes any role of the amino functional group of the amide side chain in protein-DNA interactions, while conserving the isosteric properties of the glutamine residue. The replacement of a neutral side chain with a negatively charged one could lead to repulsion of the DNA phosphate backbone.
D36N D59N D67N E118Q E124Q	Tests the specific contribution of the carboxylate functional group. The changes are expected to conserve steric effects if the original residues are solvent exposed. Complete loss of the negative charge may generate new interactions.
Y6F	Useful for probing any binding and catalytic role of the hydroxyl group. Preserves the hydrophobic contacts made in the crystal structures.
V9A	Probes the role of the hydrophobic interactions made by the residue in maintaining the structure of the active site. The absence of two methylene groups results in a large loss of hydrophobic interactions and may lead to the collapse of neighbouring side chains into the cavity.

4.2 Results

4.2.1 Construction and purification of resolvase mutants

The strategy used for the introduction of the active site mutations into NM-resolvase is described in Section 2.32. The procedures for the expression and purification of the mutant resolvases are described in Section 2.33. In all cases except one, the mutant resolvases were expressed and purified in amounts sufficient for experimental-scale purification as desired for this project. NM-D59N was more difficult to solubilise and tended to precipitate at lower NaCl concentrations. However, it remained soluble under the storage conditions of 1 M NaCl and 50% glycerol. The concentrations of purified resolvase mutants were estimated by comparing their band intensities on an SDS PAGE Laemmli gel with that of a resolvase standard of known concentration (Section 2.34). Visual examinations of the bands on the gel were used to assess protein purity. In all cases, only trace amounts of impurities could be seen. Figure 4.3 shows a sample Laemmli gel. The estimated stock concentrations (Section 2.34) of the purified resolvases and other preparations previously made in the laboratory and used in this study are shown in Table 2.3.

4.2.2 Effect of mutation of putative active site residues on binding and synapsis properties of NM-resolvase

Bandshift assays were used to test the binding and synapsis properties of the mutants relative to the parent NM-resolvase using the 70LR site I substrate (Figure 2.1). The electrophoretic buffer systems for the analysis of the binding and synapsis properties of the mutants are described in Section 2.27. The bandshift assays shown here were carried out using the high ionic strength TBE buffer since it favours the formation of the site I synapse on polyacrylamide gels (Sections 3.2.1 and 3.2.2). Figure 4.4 (Panel A) shows that NM-resolvase and most of the tested mutants bind 70LR site I to form the site I synapse. The bandshift patterns of NM-V9A, NM-S10A, NM-S39A, NM-D67N, NM-E118Q, and NM-E124Q were similar to that of NM-resolvase since most of the bound DNA is in the synapse. NM-Y6F, NM-Q14E, NM-Q19E, NM-D36N, and NM-R125K formed significantly less synapse than the parent NM-resolvase did. Rather, these mutants

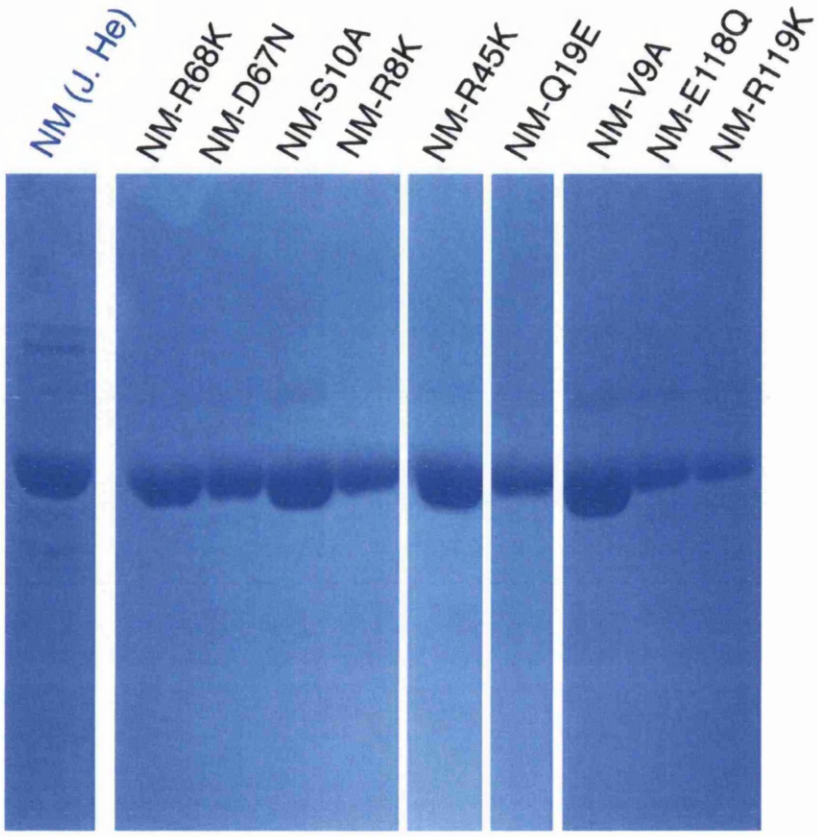

Figure 4.3 Laemmli SDS PAGE analysis of some of the resolvase preparations made and used in this study.
An older fraction of NM-resolvase (J. He) was used as the standard to assess purity and estimate protein concentration (Section 2.34; Table 2.3)

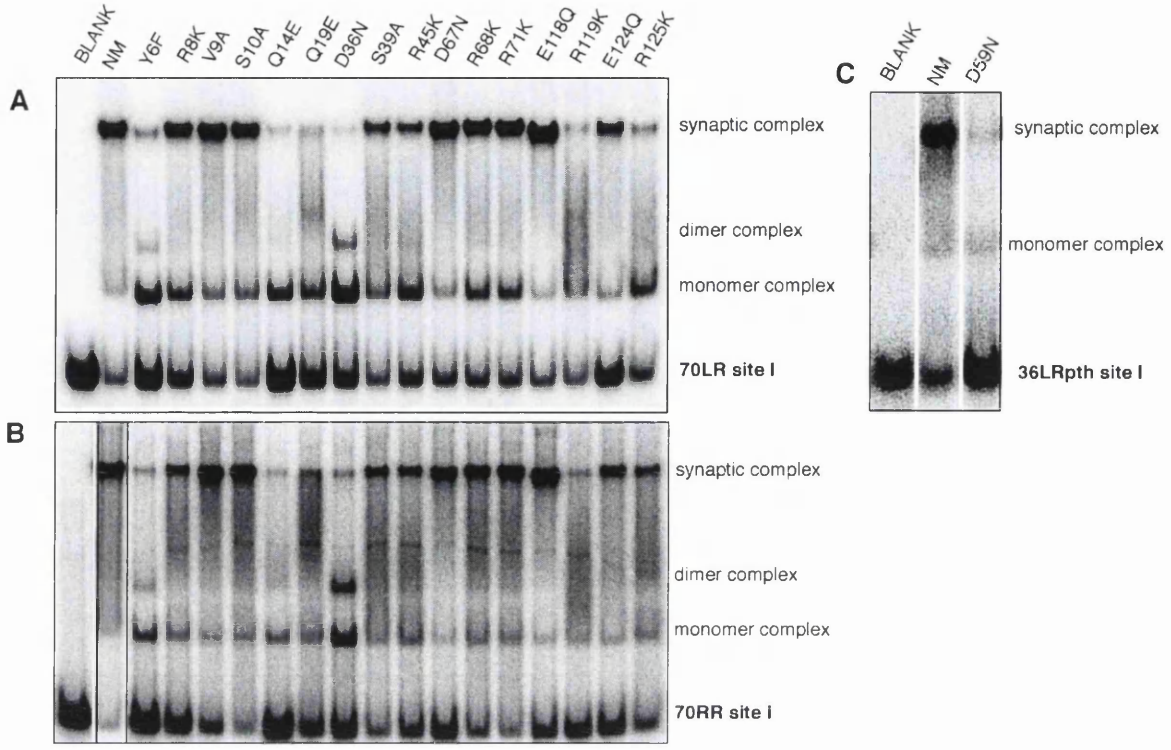

Figure 4.4 Binding and synapsis assay of NM-resolvase mutants.
Binding reactions were as described in section 2.30: Resolvase (400 nM); 70LR site I or 70RR site I (unlabelled, 50 nM; ^{32}P-labelled, 2.5 nM). Electrophoresis was on a 6.5% TBE gel (Section 2.27). In the Q14E, R119K, and R125K assays, 800 nM of resolvase was used since very weak binding was seen with 400 nM resolvase as used in the assays for NM-resolvase and the other mutants. **Panel A:** Binding reaction with 70LR site I. **Panel B:** Binding reaction with 70RR site I. **Panel C:** Comparison of the binding properties of NM-resolvase and NM-D59N. The binding reactions were carried out as described for the ones shown in Panels A and B except that the substrate was 36LRpth site I.

formed large amounts of monomer complex. In addition, NM-Y6F and NM-D36N had bands that correspond to the dimer complex. NM-Q19E and NM-R119K gave fuzzy patterns that are indicative of the assembled synapses falling apart during electrophoretic separation of the binding reaction mixtures. While NM-R8K, NM-R68K, and NM-R71K formed synaptic complexes similar in amount to that of NM-resolvase, these mutants also formed some monomer complexes. NM-D59N was a rather insoluble protein. The mutant repeatedly precipitated out of solution during protein purification even at the high NaCl concentration (1 M) that sufficed to keep most resolvase mutants soluble. This poor solubility might account for the weak intensity of the complex bands in binding assays with NM-D59N (Figure 4.4, Panel C).

The binding and synapsis properties of the NM-resolvase mutants were further investigated using the 70RR site I substrate, since NM-resolvase formed more site I synapse with this substrate than with 70LR site I (Section 3.2.1). In 70RR site I, the base sequence of the left half of site I is replaced with the sequence of the right half (Figure 2.1). The right end sequence binds with a higher affinity than the left end sequence (CGTTCG) (Bednarz *et al.*, 1990). The results of the binding assay of NM-resolvase mutants with 70RR site I were essentially similar to that seen with 70LR site I (Figure 4.4, Panel B). The 70RR site I assay provided more details on the specific binding defects seen with some of the mutants in the 70LR site I assay. NM-R8K, NM-R68K, NM-R71K, and NM-R125K formed less monomer complex with 70RR site I than they did with 70LR site I. The streaking pattern formed by NM-Q19E and NM-R119K in the 70LR site I assay was also seen in the 70RR site I assay. The 70RR site I substrate did not improve the binding properties of NM-Y6F and NM-Q14E, since the main bound species were monomer complexes. However, NM-D36N formed more dimer complexes with 70RR site I than it did with 70LR site I.

As shown in Figure 4.4, mutation of the conserved residues affected the binding and synapsis properties of NM-resolvase to different extents. Hence, an attempt was made to describe the effects in quantitative terms. This was done by titrating each mutant with 70LR site I under standard binding conditions (Section 2.30). A typical titration assay and

the binding isotherm used to estimate the apparent dissociation constant, K_d(app.) are shown in Figure 4.5. The K_d(app.) was taken as the resolvase concentration that converts half the input site I DNA as bound complexes on the gel, irrespective of the stoichiometry of the complexes formed. The K_d(app.) values determined (Table 4.3) showed that most of the mutations have modest effects on binding and synapsis by NM-resolvase. However, NM-Y6F, NM-Q14E, NM-Q19E, and NM-D36N had a substantially reduced affinity for 70LR site I (Table 4.3).

While the K_d(app.) value provides an indication of the affinity of a resolvase mutant for the 70LR site I, it gives no indication as to whether the DNA is bound as monomer, dimer, or synaptic complexes. Indeed, mutants having similar K_d(app.) values could display different distribution patterns of the bound complexes. For instance, while NM-D67N and NM-R71K have comparable K_d(app.) values of 291 nM and 294 nM respectively (Table 4.3), NM-R71K had more monomer complexes than NM-D67N (Figure 4.4, Panel A). Bar charts showing the distribution of bound complexes for sets of mutants at equal resolvase concentration were used to describe this effect in quantitative terms (Figure 4.6). The distributions showed that mutations of some putative active site residues in NM-resolvase reduced the amount of synapse formed, with the appearance of monomer and dimer complexes, even on TBE polyacrylamide gels.

4.2.3 Effect of mutation of putative active site residues on binding properties of AKSY-resolvase

Since some putative active site mutations in NM-resolvase were found to affect the amount of the synapse formed (Figure 4.4), a similar investigation was conducted in the context of AKSY-resolvase, which has the four mutations R2A E56K G101S D102Y. The objective was to identify changes that alter the binding or synapsis properties of AKSY-resolvase. Mutants of AKSY-resolvase with the individual changes Y6F, V9A, Q14E, Q19E, D36N, R45K, D67N, E118Q, E124Q, and R125K were made and purified as described earlier for similar mutants of NM-resolvase (Section 4.2.1). Binding assays of AKSY-resolvase with 70LR site I show monomer and dimer complexes in approximately equal proportions, while most of the bound species are the dimer complex

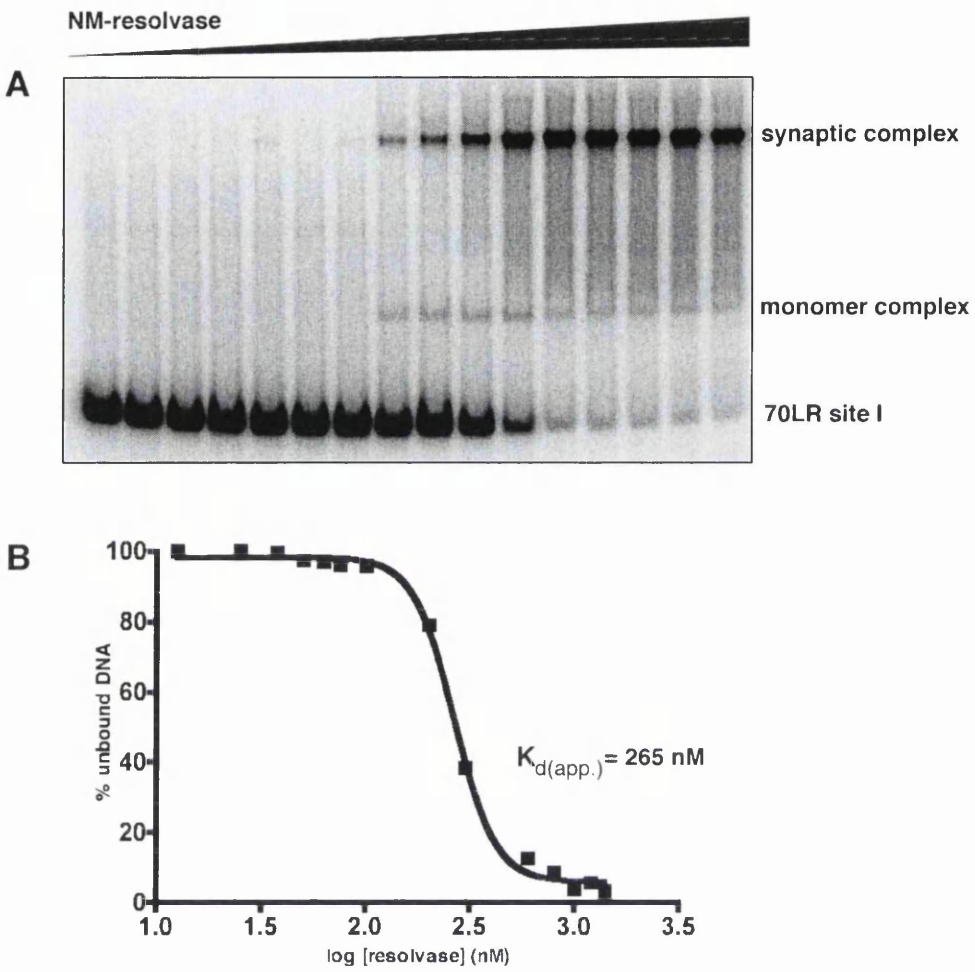

Figure 4.5 Representative binding isotherm for the estimation of apparent dissociation constant (K_d(app.)) from a binding assay of NM-resolvase and 70LR site I
Binding reactions were as described in Section 2.30: 70LR site I (unlabelled, 50 nM; ^{32}P-labelled, 2.5 nM). Electrophoresis was on a 6.5% TBE gel (Section 2.27). NM at 0, 12.5, 25, 37.5, 50, 62.5, 75, 100, 200, 300, 600, 800, 1000, 1200, and 1400 nM was used for the titration assays. **Panel A:** Phosphorimage of the gel. **Panel B:** Quantitation of the bands on the phosphorimage was used to plot the binding curve and estimate the K_d(app). (Section 2.36).

Table 4.3 $K_{d(app.)}$ values of NM-resolvase and its derived active site mutants.
The apparent dissociation constant values were determined from binding isotherms similar to the one shown in Figure 4.3 (Section 2.36). The standard errors for the $K_{d(app.)}$ values range from 12 to 18% for NM-resolvase and the mutants.

mutant	$K_{d(app.)}$
NM	265 nM
Y6F	513 nM
R8K	354 nM
V9A	257 nM
S10A	272 nM
Q14E	820 nM
Q19E	467 nM
D36N	446 nM
S39A	274 nM
R45K	341 nM
D67N	291 nM
R68K	302 nM
R71K	294 nM
E118Q	252 nM
R119K	331 nM
E124Q	263 nM
R125K	310 nM

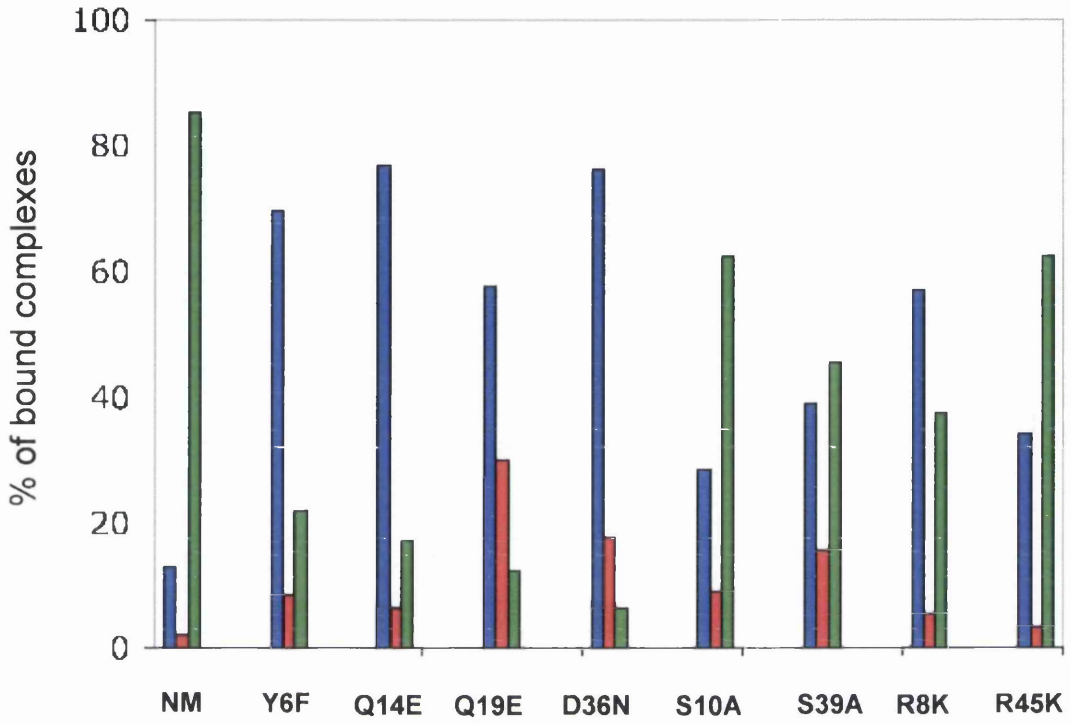

Figure 4.6 Quantitative analysis of the profile of protein-DNA complexes formed by selected mutants of NM-resolvase.

The bands corresponding to the bound complexes on the phosphorimage in Figure 4.4, panel A were profiled to determine the fraction of the input DNA bound as monomer (blue bars), dimer (red bars) and site I synapse (green bars) complexes. The profile of NM-resolvase was compared with the Y6F, Q14E, Q19E, and D36N mutants that formed relatively large amounts of monomer and dimer complexes. NM-S10A, NM-S39A, NM-R45K, and NM-R68K are included in the figure as control mutants that formed less monomer and dimer complexes.

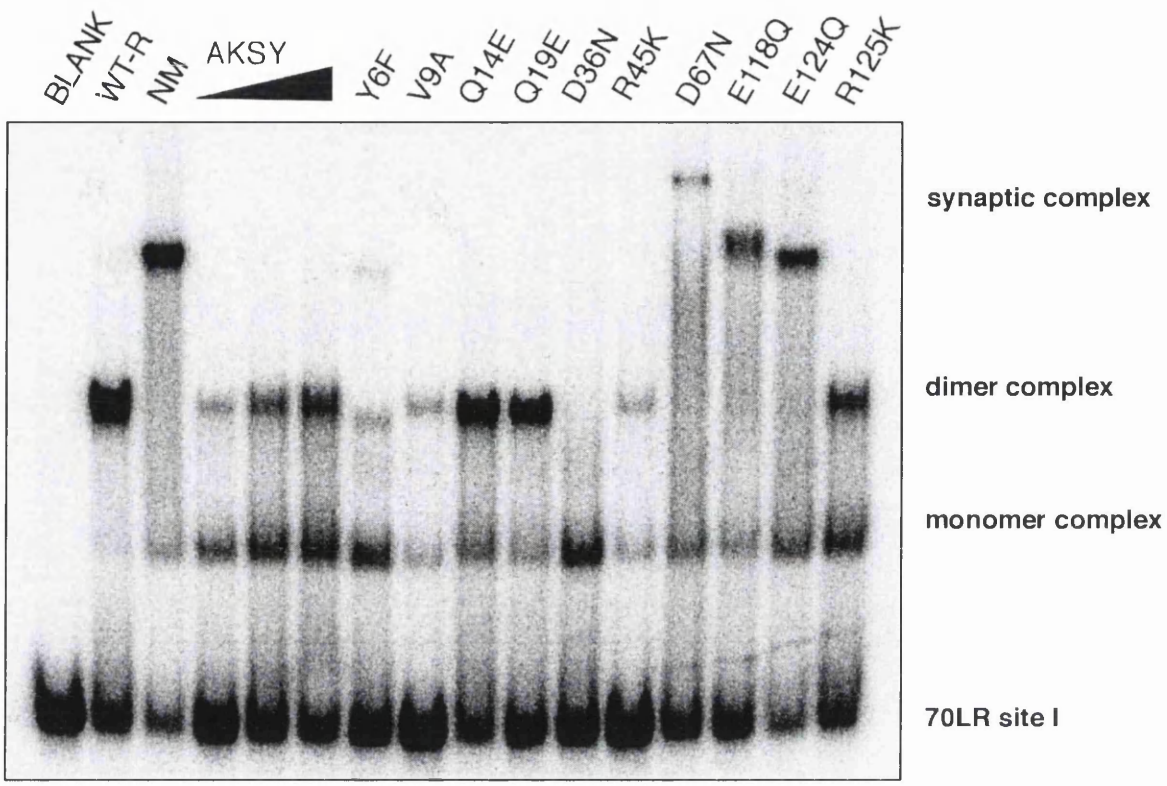

Figure 4.7 Effects of active site mutations on binding properties of AKSY-resolvase
Binding reactions were as described in section 2.30: 70LR (unlabelled, 50 nM; ^{32}P-labelled, 2.5 nM); Resolvase concentrations were 200, 400, and 800 nM for AKSY-resolvase, and 400 nM for the rest. Electrophoresis was on a 6.5% TBE gel (Section 2.27).

with the high-affinity 70RR site I (Section 3.2.1; Figure 3.1). The effects of the mutations on the binding properties of AKSY-resolvase were investigated in binding assays with 70LR site I. The results show that the individual mutations Y6F, D67N, E118Q, and E124Q in AKSY-resolvase led to the observation of synaptic complexes (Figure 4.7). However, the synaptic complexes formed by AKSY-Y6F, AKSY-D67N, and AKSY-E118Q had mobilities different from that of NM-resolvase on the polyacrylamide gel. AKSY-Q14E and AKSY-Q19E formed mainly dimer complexes similar to WT-resolvase. The mutants AKSY-V9A, AKSY-R45K, and AKSY-R125K bound 70LR site I to different extents, but formed approximately equal amounts of monomer and dimer complexes as did the parent AKSY-resolvase.

4.2.4 Effect of mutation of putative active site residues on catalytic activities of NM-resolvase

Cleavage activities on site I x site I plasmid substrate (pAL225)

In order to identify which of the conserved residues chosen for mutation are important for the catalytic activities of NM-resolvase, the cleavage activities of the NM-resolvase mutants on a site I x site I plasmid substrate, pAL225, were investigated. The reactions were in EG buffer (Sections 2.31 and 3.2.5) at 37 °C for 20 minutes. The results shown in Figure 4.8 (Panel A) indicate that in contrast to the generally mild effects on binding and synapsis, the catalytic activities of NM-resolvase were affected more by mutation of the conserved residues. The mutants NM-Y6F, NM-R8K, NM-S10A, NM-Q14E, NM-Q19E, NM-D36N, NM-R68K, and NM-R71K were found to be inactive in this assay. In contrast, NM-S39A, NM-R45K, NM-D67N, NM-E118Q, NM-R119K, NM-E124Q, and NM-R125K, formed the characteristic one-site and two-sites cleavage products to different extents. NM-V9A showed a topoisomerase-like activity, characterised by conversion of the supercoiled substrate pAL225 mainly into the one-site cleavage product and a series of topoisomers (Figure 4.8, Panel A). In spite of its poor solubility and binding (Figure 4.4), NM-D59N showed site-specific cleavage activity to a limited extent (Figure 4.8, Panel A).

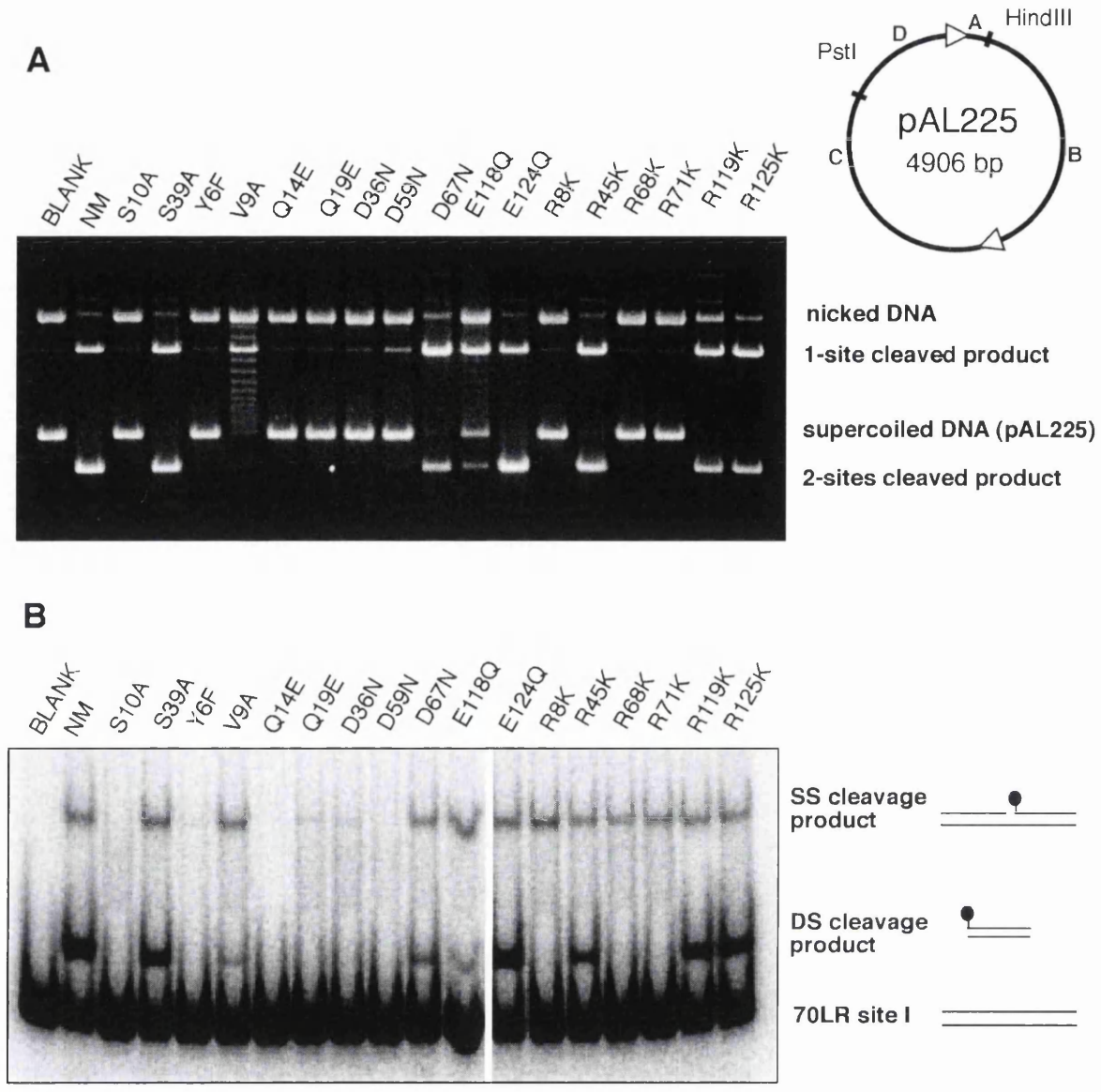

Figure 4.8 Cleavage activities of NM-resolvase and mutants.
Panel A: Cleavage of pAL225 in EG buffer (Section 2.31). Each reaction contained 100 nM resolvase and the reactions were incubated for 20 minutes at 37 °C. Reaction products were separated on a 1.2% agarose gel after treatment with SDS and Protease K (Section 2.17). The sizes of the bands are as summarised in Figures 2.2-2.4. **Panel B:** Cleavage of 70LR site I in binding/synapsis buffer at 37 °C. Binding reactions were as described in Section 2.30: Resolvase (100 nM); 70LR site I (unlabelled, 50 nM; ^{32}P-labelled, 2.5 nM). The binding reactions were set up for 22 h at 37 °C and treated with 0.1% SDS for 10 minutes (Section 2.18). Electrophoresis was on a 6.5% TBE SDS gel (Section 2.28). The cartoons illustrate the single strand and double strand cleavage products formed. The lines represent the DNA strands, and the lollipops represent resolvase covalently attached to the DNA strand at the scissile point.

Cleavage activities on 70LR site I oligonucleotide substrate

Since some mutants of NM-resolvase that formed the site I synapse in bandshift assays (Figure 4.4) were inactive in the pAL225 cleavage assay (Figure 4.8, Panel B), the ability of the mutants to form covalent complexes with 70LR site I under binding and synapsis conditions was investigated (Sections 2.30 and 3.2.1). The formation of covalent complexes is a more sensitive assay of catalytic activity since trace amounts of the complex formed with the radioactively labelled DNA can be readily detected by autoradiography. The reactions were incubated for 22 hours at 37 °C to allow even very slow strand cleavage to be observed. The results shown in Figure 4.8 (Panel B) reveal that the mutants NM-V9A, NM-S39A, NM-R45K, NM-D67N, NM-E118Q, NM-R119K, NM-E124Q, and NM-R125K which were active in the pAL225 cleavage assay (Figure 4.8, Panel A) form single-strand and double-strand cleavage products to different extents. The mutants NM-R8K, NM-R68K, and NM-R71K that were apparently inactive in the pAL225 cleavage assay (Figure 4.8, Panel A) formed significant amounts of single-strand cleavage products (Figure 4.8, Panel B). Similarly, trace amounts of single-strand cleavage products were formed by NM-Q19E and NM-D36N. No cleavage products were observed with NM-S10A, NM-Y6F, NM-Q14E, and NM-D59N.

Quantitative assays of 70LR site I double-strand cleavage by NM-E124Q, NM-S39A, NM-V9A, NM-D67N, NM-E118Q, NM-R119K, and NM-R125K in EG buffer were carried out, as described in Section 2.31. These NM-resolvase mutants are the ones found to be active in the pAL225 cleavage assay (Figure 4.8, Panel A). A time course of the formation of double-strand cleavage product by NM-resolvase (Figure 4.9, Panel A) shows that the reaction progress was roughly linear over the first five minutes (Figure 4.9, Panel B). Hence, the cleavage activities of the mutants were assayed after five minutes to obtain estimates of the initial rates of the formation of double-strand cleavage products. The results shown in Figure 4.9 (Panels C and D) reveal that NM-R119K was as active as the parent NM-resolvase, while NM-E124Q and NM-S39A showed about half the activity of NM-resolvase. Among the mutants assayed in this experiment, NM-V9A and NM-E118Q were the least active, showing less than 20% of the activity of NM-resolvase (Figure 4.9, Panels C and D).

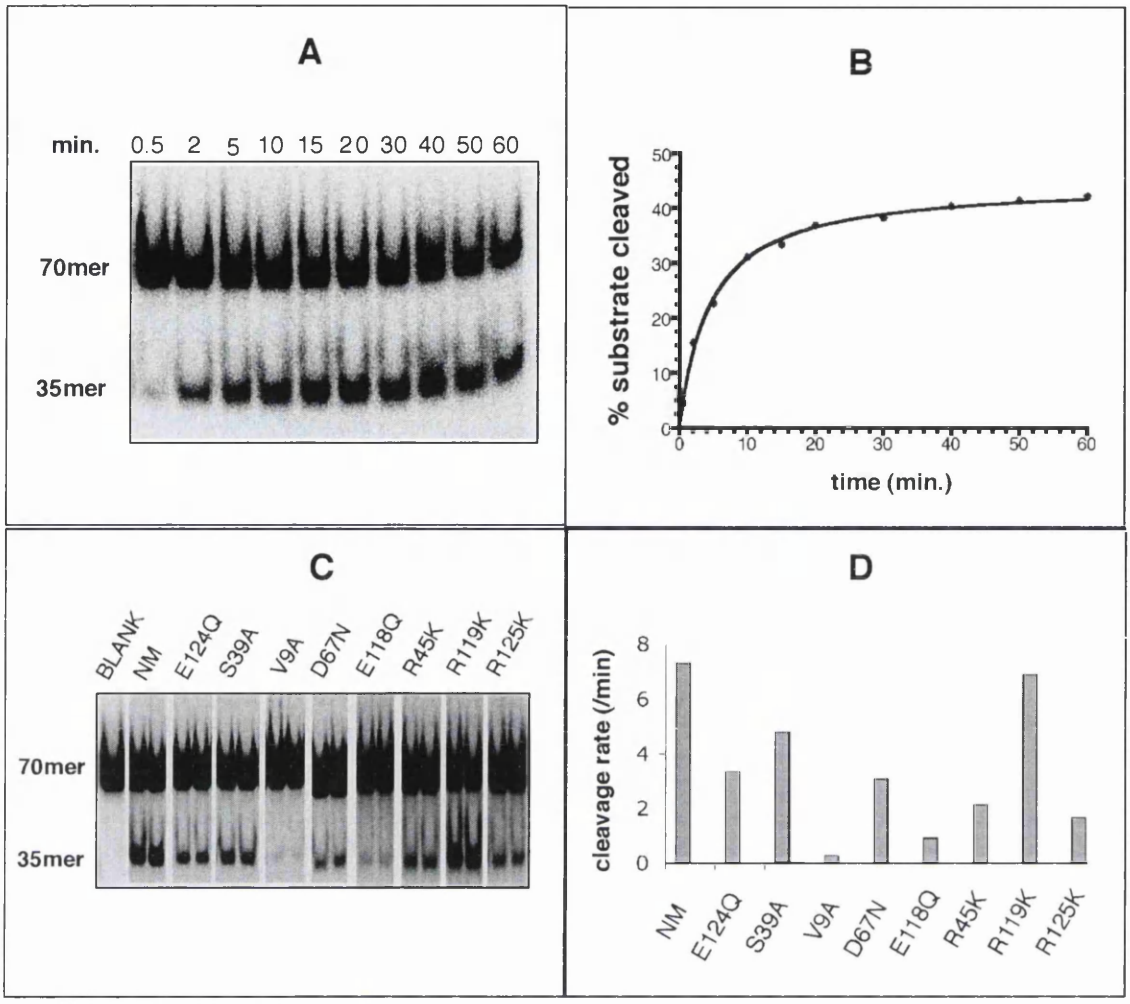

Figure 4.9 Quantitative assay of site I oligonucleotide cleavage activities of NM-resolvase mutants Cleavage reactions were as described in section 2.31: Resolvase (100 nM); 70LR site I (unlabelled, 50 nM; ^{32}P-labelled, 2.5 nM); EG buffer. The top strand of the duplex DNA was labelled at the 5' end, and annealed to an unlabelled bottom strand (Section 2.26). The reaction products were separated on a 6.5% polyacrylamide gel (Section 2.27). **Panel A:** Time course of the cleavage activity of NM-resolvase in EG buffer (Section 2.31) at 37 °C. At timed intervals, aliquots were withdrawn from a scaled-up reaction mixture and SDS/protease K loading buffer was added to stop the reaction. **Panel B:** Quantitative graphical representation of the time course analysis. The percentages of the input substrate DNA converted to the 35mer double-strand cleavage product at the indicated time points are shown. **Panel C:** NM-resolvase mutants that were active in the pAL225 cleavage reaction (Figure 4.8, Panel A) were assayed to obtain quantitative estimates of the reaction rates. The reactions were for 5 minutes at 37 °C, and 100 nM of resolvase was used. The two lanes are replicates of each assay. **Panel D:** The bars represent the cleavage rates (percentage substrate converted per minute determined by quantitating the phosphorimage shown in panel C.

Recombination activities on site I x site I plasmid substrate (pAL225)

The reaction products formed by NM-resolvase and other activated mutants in the pAL225 recombination assay include resolution and inversion products as well as cleaved intermediate products (Figures 2.2, 2.3, and 2.4). Comparison of the recombination activities of the mutants with that of the parent NM-resolvase at the same protein concentration reveals some differences in the profile of reaction products. Figure 4.10 shows the pAL225 recombination activities of NM-resolvase mutants that were found to be active in the cleavage assays (Figure 4.8). The mutants NM-S39A, NM-R45K, NM-R119K and NM-E124Q catalysed the complete recombination reaction, forming products similar to those of the parent NM-resolvase. These mutations did not seem to affect the distribution of reaction products formed by NM-resolvase. In contrast, NM-V9A, NM-D67N, NM-E118Q, and NM-R125K formed mainly cleaved products. The mutants that were inactive in the cleavage assays (NM-S10A, NM-Y6F, NM-Q14E, NM-Q19E, NM-D36N, NM-R8K, NM-R68K, and NM-R71K) and NM-D59N were also tested in the pAL225 recombination assay and found to be inactive (data not shown).

4.2.5 Further analysis of the effects of R8, R68 and R71 mutations on synapsis and catalytic properties of NM-resolvase

The binding and synapsis properties of NM-resolvase and AKSY-resolvase mutants indicate that some putative active site residues could be involved in synapsis (Sections 4.2.2 and 4.2.3). However, mutation of S10, R8, R68, and R71 residues that are considered to form the catalytic centre of resolvase (Grindley *et al.*, 2006), did not seriously affect the synapsis properties of NM-resolvase (Figure 4.4). If the arginine residues had any roles in the pre-catalytic binding and synaptic steps, the positively charged lysine in the R→K mutants could potentially still provide the needed interactions. Hence, the possible involvements of R8, R68, and R71 in synaptic interactions were investigated further by replacing these residues with alanine in NM-resolvase. The premise is that an arginine-to-alanine mutant in NM-resolvase that is significantly affected in synapsis would suggest an essential synaptic role for the residue mutated. The mutants NM-R8A, NM-R68A, and NM-R71A were made and purified. The

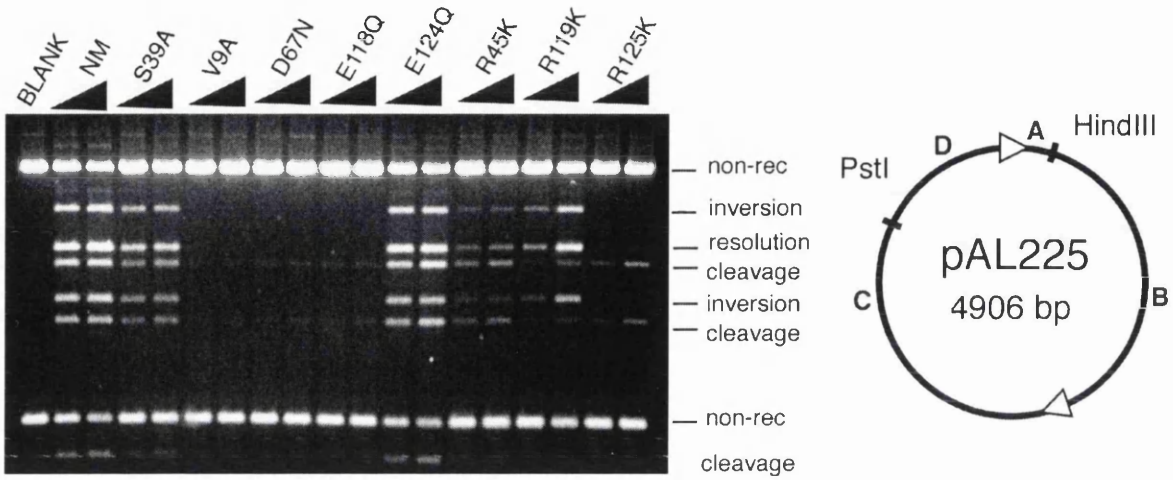

Figure 4.10 Recombination activities of NM-resolvase mutants
The mutants that were active in the pAL225 cleavage assay in EG buffer (Figure 4.8) were tested for recombination activity on pAL225. Reactions were in sodium phosphate recombination buffer, pH 6.5 (Section 2.31). Reactions contained 100 and 200 nM resolvase and were incubated at 37 °C for 1 hour, and stopped by heating at 70 °C for 5 minutes. The reaction products were treated with HindIII and PstI, and separated on a 1.2% agarose gel after treatment with SDS and Protease K (Section 2.17).

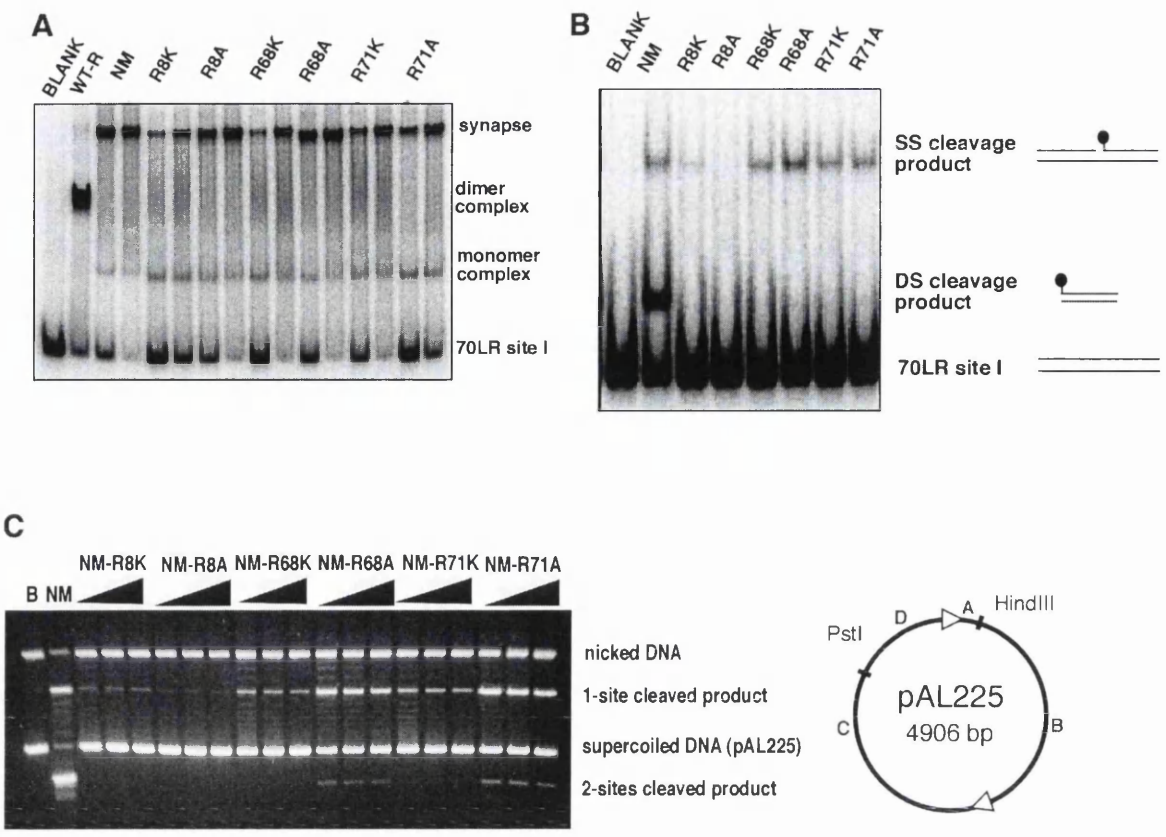

Figure 4.11 Effects of R8, R68, and R71 mutations on binding/synapsis and cleavage activities of NM-resolvase

Panel A: Binding/synapsis properties of R8, R68, and R71 mutants of NM-resolvase. Binding reactions were as described in section 2.30: 70LR (unlabelled, 50 nM; ^{32}P-labelled, 2.5 nM). 400 and 800 nM resolvase concentrations were added to the reaction mixtures for NM-resolvase and the mutants. The WT-resolvase reaction contained 400 nM resolvase. Electrophoresis was on a 6.5% polyacrylamide TBE gel (Section 2.27). **Panel B:** 70LR site I cleavage activities of NM-resolvase and the mutants in binding/synapsis buffer. Binding reactions were set up as described in Panel A for 22 h at 37 °C and then treated with 0.1% SDS for 10 minutes. Resolvase concentration was 100 nM in all cases. Electrophoresis was on a 6.5% polyacrylamide TBE SDS gel (Section 2.28). The cartoons illustrate the single-strand and double-strand cleavage products formed. The lines represent the DNA strands, and the lollipops represent resolvase covalently attached to the DNA strand at the scissile point. **Panel C**: Cleavage of pAL225 by NM-resolvase and the R8, R68, and R71 mutants. Reactions were in EG buffer (Section 2.31). The concentrations of resolvase used were 100, 200 and 400 nM (NM-resolvase, 100 nM only) and the reactions were incubated at 37 °C for 22 h, except for NM-resolvase, which was stopped after 1 hour. Reaction products were separated on a 1.2% agarose gel after treatment with SDS and Protease K (Section 2.17).

binding and synapsis properties, as well as the cleavage activities of these mutants were investigated along with the analogous R→K mutants of NM-resolvase. The results show that the R→A mutations did not affect the ability of NM-resolvase to form the site I synapse any more than the R→K mutations did (Figure 4.11, Panel A). The only subtle difference observed in the bandshift assay is the slightly faster rate of migration of the NM-R68A synaptic complex compared to that of other resolvase mutants.

The cleavage activities of the R→K and R→A mutants on 70LR site I substrate were compared and the results are shown in Figure 4.11 (Panel B). While covalent complexes are formed with NM-R8K, NM-R68K, NM-R68A, NM-R71K, and NM-R71A, no evidence of covalent complex formation was found with NM-R8A after 22 h incubation at 37 °C (Figure 4.11, Panel B). Figure 4.11 (Panel C) shows the cleavage activities of the mutants on pAL225. While cleavage products were formed by NM-R8K, NM-R68K, NM-R68A, NM-R71K, and NM-R71A, no evidence of catalytic activity was found with NM-R8A after 22 hours incubation at 37 °C. Surprisingly, the R→A mutants of R68 and R71 were more active in the pAL225 cleavage assay than the seemingly conservative R→K mutants (Figure 4.11, Panel C).

4.2.6 Comparison of the cleavage activities of mutants on NM-resolvase and AKSY-resolvase

The results presented in Figures 4.4 and 4.7 show that mutation of putative active site residues in NM-resolvase and AKSY-resolvase affected the binding properties of the activated mutants. However, the mutations did not necessarily have similar effects in the context of the two activated mutants. Hence, a comparison of the effects of some of the putative active site residue mutations on cleavage of pAL225 in the context of the two activated mutants were carried out (Figure 4.12). In contrast to their mild effects on the cleavage activity of NM-resolvase, the individual changes V9A, R45K, D67N, E118Q and R125K significantly reduced the cleavage activity of AKSY-resolvase. The mutants AKSY-Y6F, AKSY-Q14E, AKSY-Q19E, and AKSY-D36N were found to be completely inactive (data not shown) like their NM-resolvase equivalents, and were not included in this experiment.

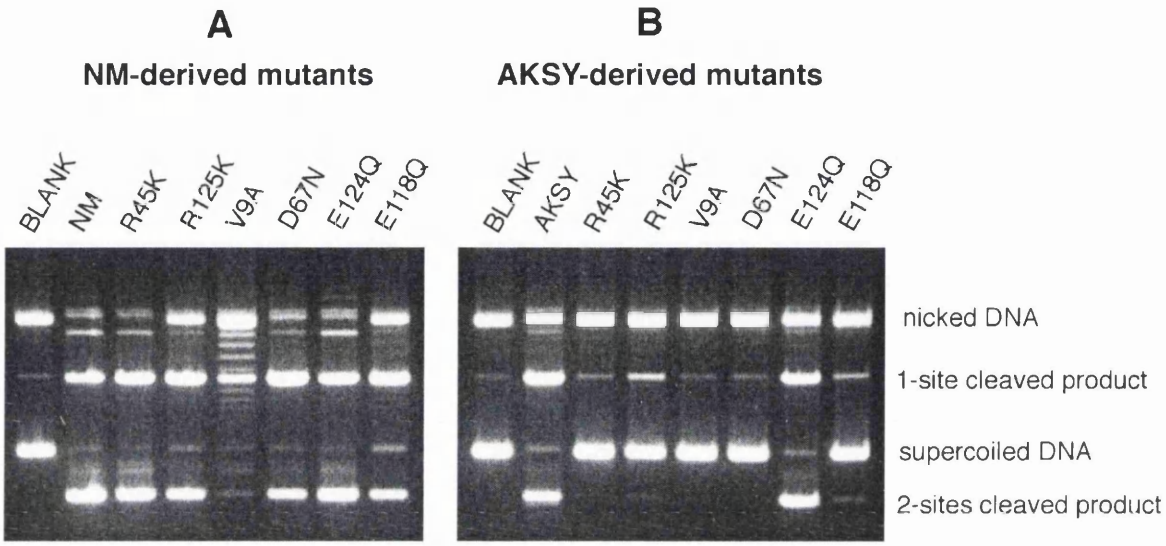

Figure 4.12 Comparison of the effects on pAL225 cleavage of mutations in conserved residues in the context of AKSY-resolvase and NM-resolvase.
The figures show cleavage of pAL225 by NM-resolvase and its derived mutants (Panel A) and by AKSY-resolvase and its derived mutants (Panel B) in EG buffer (Section 2.31). Each reaction contained 100 nM resolvase and the reactions were incubated for 20 minutes. Reaction products were separated on a 1.2% agarose gel after treatment with SDS and Protease K (Section 2.17).

4.3 Discussion

4.3.1 Effect of the mutations on site I binding

The binding/synapsis properties of putative active site residue mutants of NM-resolvase were studied using polyacrylamide gel bandshift assays (Sections 4.2.2 and 4.2.3). The ability of the mutant resolvases to bind site I and form (at least) stable monomer complex showed that those mutations did not seriously affect the global structure of the parent NM-resolvase. The exact mechanistic significance of this K_d(app.) value is uncertain since there are multiple steps in the assembly of the synapse. One of its uses is that it gives a simple indication of the affinity of the resolvase mutant for site I, and provides a simple quantitative way of comparing the effects of the individual mutations.

4.3.2 Role of putative active site residues in site I synapsis

The finding that mutation of several of the putative active residues in NM-resolvase reduced the amount of site I synapse observed in bandshift assays (Figure 4.4) invites the suggestion that the residues could be involved in the assembly and/or stabilisation of the synapse. The data in Table 4.3 show that these reductions in the amount of synapse observed are not simply due to weaker binding. Some of the mutations (especially Q14E and D36N) do not affect the ability of NM-resolvase to form monomer and dimer complexes, but do apparently affect a post-binding step necessary for assembling the synapse (Figure 4.4, Panel A). This conclusion is supported by the observation that binding with the high affinity 70RR site I substrate did not cause a large increase in the amount of synapse formed by NM-Q14E, NM-Q19E, NM-Y6F, NM-D36N, and NM-R119K (Figure 4.4, Panel B). Further evidence for the involvement of the putative active site residues in synapsis is found in binding assays of AKSY-resolvase and its derived mutants. The individual changes Y6F, D67N, E118Q, and E124Q in AKSY-resolvase resulted in the observation of synaptic complexes (Figure 4.7). Mutating resolvase carboxylate residues (D67, E118, and E124) to equivalent amide residues could enhance protein-DNA interactions. Interestingly, each of these three carboxylate residues have a well-conserved arginine residue occurring next to it in the primary structure of resolvase

(D67/R68, E118/R119, and E124/R125). In the crystal structure of the activated γδ resolvase mutant (1ZR4), D67 appears to position R68 close to the scissile phosphate (Li *et al.*, 2005). Hence, each carboxylate residue and its neighbouring arginine residue might form a network of interactions that are involved in stabilisation of the synapse. There are insufficient data at present to account for the observed synapse-stabilising effect of the Y6F mutation in the context of AKSY-resolvase (Figure 4.7), since the same mutation shows an opposite effect in NM-resolvase (Figure 4.4). In contrast to the effects of mutating Y6, Q14, Q19, D36, and R119, changes to S10, R8, R68, and R71 did not lead to a reduction in the amount of site I synapse formed by NM-resolvase in bandshift assays (Figures 4.4 and 4.11). These residues seem to make little or no contribution to the stabilisation of the site I synapse in NM-resolvase.

The residues that affect the synapsis properties of NM-resolvase and AKSY-resolvase could be involved in making direct contacts with the DNA in the synapse, or in maintaining the structure of a protein interface involved in synapsis. The finding that stable tetramerisation of NM-resolvase is dependent on site I synapsis (Section 3.3.4), along with the finding here that putative active site residues are involved in the formation and/or stabilisation of the synapse suggests that site I synapsis may be coupled to specific interaction of residues with the DNA. This could serve as a mechanism for ensuring that the active site residues engage with the DNA substrate only when the two recombining sites are brought together in a synapse. Such DNA-dependent orientation of active site residues only within the context of a synaptic complex can be viewed as an induced-fit type of control mechanism for confining catalytic activation to the synapse. Substrate-induced reorganisation of an enzyme's active site could be a common paradigm in phosphoryl transfer reactions. Using structural evidence and biochemical experiments with modified DNA substrates, Kurpiewski *et al.* (2004) showed that the assembly of the functional active site of EcoRI endonuclease is dependent on DNA binding. Structural evidence has also been presented for the dependence of active site assembly in MutH on DNA and cofactor binding (Lee *et al.*, 2005). In both examples, the proposed model is that of the enzymes using DNA-dependent assembly steps to couple site recognition to catalysis as a mechanism of ensuring the specificity of the endonuclease.

4.3.3 Active site residues that are essential to catalysis

The catalytic activities of NM-resolvase mutants were investigated in order to identify the residues that are involved in catalysis. Cleavage assays of NM-resolvase mutants (Figure 4.8) show that among the residues investigated in this study, S10, Y6, and Q14 are essential to catalytic activity of NM-resolvase. The highly conserved R68 and R71 are important for catalytic activity, but are not essential since covalent complexes with 70LR site I are formed by NM-R68A and NM-R71A (Figure 4.11). The finding that NM-R8K showed some catalytic activities and that NM-R8A did not (Figure 4.11) suggest that the guanidinium functional group of R8 might make an interaction that could be partially substituted for by the positively charged lysine side chain. Hence, R8 might be more important in the activation of catalysis than R68 and R71. However, these findings do not pinpoint the exact roles of the arginine residues in catalysis. The side chains of R8 and R68 are close to the scissile phosphate in the dimer and synapse structures of γδ resolvase (Yang & Steitz, 1995; Li *et al.*, 2005; Figure 4.2) suggesting that they could be involved in the stabilisation of the transition state during catalysis.

The finding that Y6 plays important roles in site I synapsis (Figure 4.4) and is essential for catalysis in Tn3 resolvase (Figure 4.8) is not in agreement with the reported effect of the same mutation in γδ resolvase. Leschziner *et al.* (1995) reported that the γδ resolvase Y6F mutant, though defective in recombination, formed covalent resolvase-DNA complex and could rejoin the cleaved ends. However, the Y6F mutation in wild-type Tn3 resolvase led to complete loss of activity (Arnold, 1997). The significance of this difference, and the role of Y6 in catalysis, are still unclear. It has been speculated that D67 is the general base in the activation of S10 at the cleavage step of recombination (Pan *et al.*, 2001). The results shown in Figure 4.8 suggest that the residue is not likely to play this role since NM-D67N was active in pAL225 and 70LR site I cleavage assays. In comparison, NM-D36N and NM-D59N in which conserved aspartate residues are similarly mutated to asparagine were less active in catalysis than NM-D67N (Figure 4.8). The slow catalytic activity of NM-D59N might be due to the protein precipitating out of

solution at the lower salt concentration (100 mM) at which binding, cleavage and recombination reactions are set up.

Mutation of V9, S39, R45, D67, E118, R119, E124, and R125 did not have serious effects on the cleavage activities of NM-resolvase (Figure 4.8). NM-V9A, NM-D67N, NM-E118Q, and NM-R125K were active in pAL225 cleavage assays (Figure 4.8). However, they did not form significant amounts of recombination products from the plasmid substrate, and cleaved intermediates were observed (Figure 4.10). This might be the consequence of the low activities of the mutants (Figure 4.9) and not necessarily due to a defect in catalysing the ligation step required to form recombinant products. This investigation shows that while these residues (V9, S39, R45, D67, E118, R119, E124, and R125) are well conserved and close to the putative active site region of resolvase, they do not participate directly in the chemical steps of catalysis. They could have structural or regulatory functions in resolvase catalysis that are less obvious in the context of an activated mutant such as NM-resolvase. In fact, mutations of some of these residues (V9A, R45K, D67N, E118Q, and R125K) led to significant reduction in the cleavage activity of AKSY-resolvase (Figure 4.12). Apparently, these residues are more important for cleavage in AKSY-resolvase than they are in NM-resolvase (Figure 4.12). The highly deregulated properties of NM-resolvase could have resulted in the active site having a relaxed specificity, and hence, able to tolerate mutations that significantly reduced the activity of the less 'hyperactive' AKSY-resolvase (Section 3.3.3).

Chapter Five

Interactions of Tn3 resolvase and activated resolvase mutants with site I DNA

5.1 Introduction

5.1.1 Use of methylphosphonate substitutions to probe the contribution of phosphate contacts in synapsis and catalysis

The finding that mutation of residues in the active site affected the synapsis properties of NM-resolvase (Section 4.2.2) prompted an investigation into the roles of protein contacts with DNA phosphodiesters in the synaptic complex. Replacements of specific non-bridging phosphate oxygens at and around the scissile phosphate with methyl groups (i.e, by substituting phosphate with methylphosphonate) were used to probe the role of phosphate contacts in the assembly and activation of the synapse (Figure 5.1). The experimental goal was the identification of methylphosphonate substitutions that affected synapsis (in bandshift assays) and catalytic activation (in oligonucleotide cleavage assays). Substitution of a methylphosphonate at a putative phosphate contact position might destabilise the protein-DNA complex by neutralising the phosphate charge (Stivers & Nagarajan, 2006). In contrast to the ethylated phosphodiester also used in probing DNA contacts, methylphosphonate substituents are almost isosteric with oxygen (Stivers & Nagarajan, 2006). Hence, methylphosphonate replacements generally do not cause serious steric clashes either within the DNA or with the protein in the assembled protein-DNA complex. Methylphosphonate substitutions induce local bending in the double-helical DNA axis via neutralisation of phosphate charge. Each methylphosphonate substitution is estimated to induce a bending angle of about 3.6° (Tomky *et al.*, 1998), which is comparable to the sequence-specific bending of duplex DNA (Goodsell *et al.*, 1993). Thus, any experimental effect observed on binding, synapsis, and catalysis caused by methylphosphonate substitutions could be ascribed mainly to the loss of the ionic or H-bond interactions rather than steric effects. One of the consequences of methyl substitution of the non-bridging phosphate oxygen is the acquisition of chirality by the phosphorus atom, and thus there are two stereoisomers of the methyl-modified DNA (Figure 5.1, Panel A).

Racemic mixtures of methylphosphonate DNA (as obtained by chemical oligonucleotide synthesis) have been used to map phosphate positions contributing to the stabilisation of

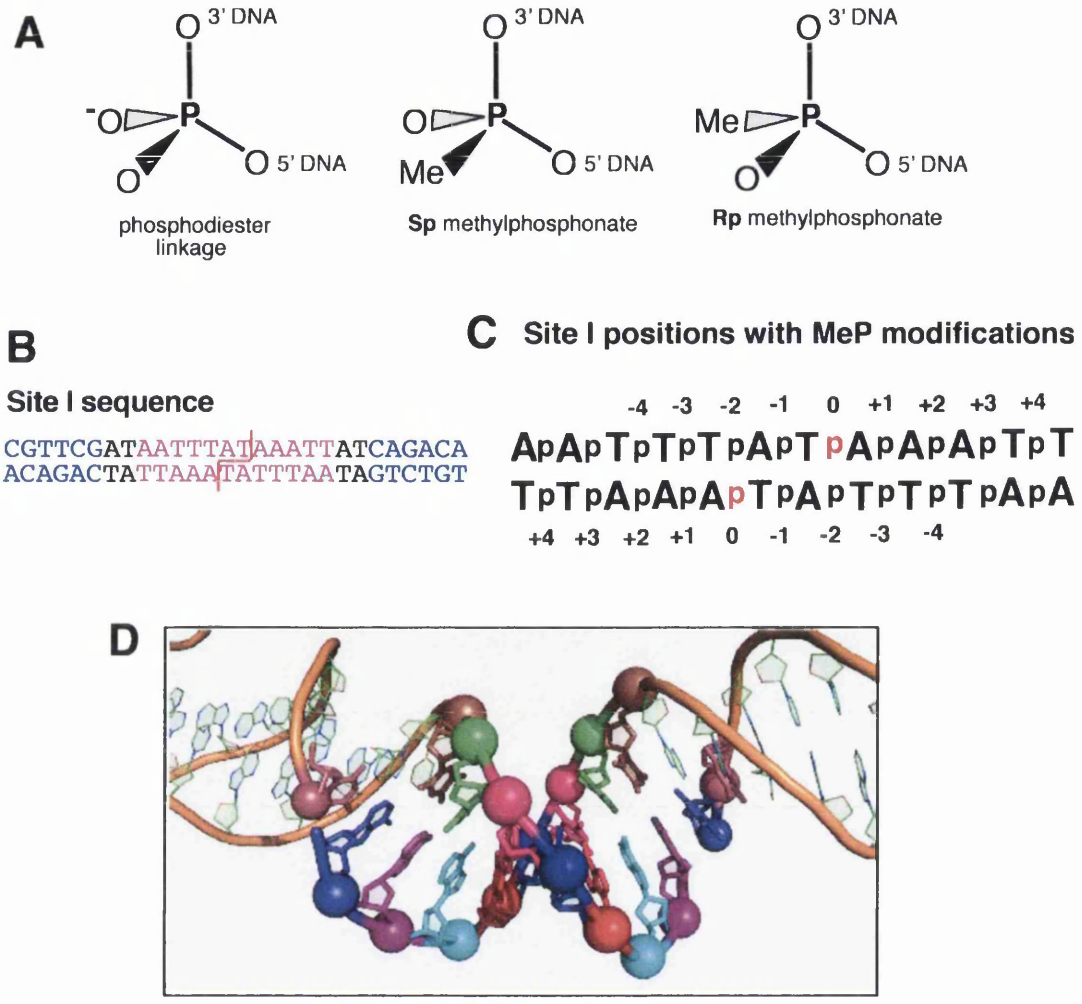

Figure 5.1 Strategy used in the methylphosphonate substitution assay
Panel A: Replacement of one of the phosphate oxygen atoms with a methyl group makes the phosphorus atom a chiral centre, resulting in two stereoisomers of the methylphosphonate-substituted DNA. **Panel B**: Sequence of site I of *res*. The six-base sequences recognised by the C-terminal domain of resolvase are shown in blue and the centre of the site where the methylphosphonate groups were introduced is in purple. The staggered line indicates the points of strand cleavage and rejoining. **Panel C**: The nomenclature adopted for the phosphate positions in the methylphosphonate interference experiments. The scissile phosphates are coloured red, and the numberings are relative to these positions. **Panel D**: Representation of the centre of site I, highlighting the modified phosphate positions. The picture was generated from PDB coordinates of 1GDT (Section 2.35) The phosphate backbone of the DNA is represented as an orange tube, while the phosphate groups and the bases are shown as spheres and sticks respectively. The colouring corresponds to the numberings shown in panel C as follows: -4 (brown), -3 (green), -2 (pink), -1 (blue), 0 (red), +1 (cyan), +2 (purple), +3 (deep blue), and +4 (magenta).

protein-DNA complexes and their catalytic activation (Allawi *et al.*, 2003; Dertinger & Uhlinbeck, 2001, Xu *et al.*, 2001). However, in order to obtain more detailed information on the nature of molecular contacts in protein-nucleic acid complexes, it is often necessary to use chirally pure isomers of the methylphosphonate-modified DNA (Stivers & Nagarajan, 2006). Methylphosphonate substitutions have been used to determine protein-DNA contact sites in several systems including the *lac* repressor (Nobles *et al.*, 1984), the lambda repressor (Batfield & Weiss, 1994), and uracil DNA glycosylase (Jiang *et al.*, 2003). Significant insights into the catalytic mechanisms of topoisomerase I (Tian et. al., 2003; Tian et. al., 2005) and EcoRI endonuclease (Kurpiewski *et al.*, 2004) have been obtained using methylphosphonate substitutions at phosphate positions involved in catalysis.

5.1.2 Experimental design and strategy

In this chapter, single methylphosphonate substitutions were introduced on both strands of the 50LR site I substrate at the -4, -3, -2, -1, 0, +1, +2, +3, and +4 positions to give the corresponding doubly modified 50LRMeP site I substrates (Figure 5.1, Panels B and C). The modified duplexes were made such that the top and bottom strands have the methylphosphonate groups at the symmetry-related positions. For instance, the MeP(-4) duplex was made by annealing the MeP(-4) top strand with the MeP(-4) bottom strand (Figure 5.1, Panel C). Each single-stranded oligonucleotide contained about equal amounts of the Rp and Sp methylphosphonate stereoisomers, since they were made by chemical synthesis. Thus, there are four isomers of the double-stranded modified sites (i.e. RR, RS, SR, and SS). The RS and SR isomers might be expected to behave similarly in their effects on the tested parameters. The unmodified 50LR site I was used as the control. Based on the resolvase-site I dimer structure (Yang & Steitz, 1994), any synapsis- and catalysis-specific contacts of the N-terminal domain with site I should involve the phosphodiester bonds close to the scissile position (Figure 1.11; Figure 5.1, Panel D).

5.2 Results

5.2.1 Effects of methylphosphonate substitutions on binding and synapsis by WT-resolvase and NM-resolvase

Figure 5.2 (Panel A) shows the effects of the methylphosphonate substitutions on the binding properties of WT-resolvase and NM-resolvase. In order to assess these effects relative to the unmodified 50LR site I substrate, the complexes formed by WT-resolvase and NM-resolvase with each of the modified 50LRMeP site I substrates were quantitated to determine the percentage of the input DNA bound as monomer, dimer and synaptic complexes (Figure 5.2, Panels B and C). Methylphosphonate substitution at the -2 position, and to a lesser extent +3 and +4, led to significant decreases in the amount of the dimer complex formed by WT-resolvase (Figure 5.2, Panel A). The modifications at the -4, -3, 0, +1, and +2 positions did not produce effects that are significantly different from the binding pattern with the control 50LR site I substrate (Figure 5.2, Panel A).

Methylphosphonate subsitutions at the -2, -1 and 0 positions led to decreases in the amount of the synapse formed by NM-resolvase, and significant increase in the amounts of monomer complexes observed (Figure 5.2, Panels A and C). The +3 and +4 modifications also affected the amount of the synapse formed to a lesser extent. The effects of the MeP(-1) and MeP(0) modifications are specific to the NM-resolvase synapse, since the binding of WT-resolvase was not significantly affected by these substitutions (Figure 5.2, Panels A and B). The MeP(-4) modification did not affect the amount of the site I synapse observed, but selectively inhibited the monomer complex (Figure 5.2, Panels A and C). The methylphosphonate substitutions at the -3, +1, and +2 positions did not have significant effects on the formation of the synapse by NM-resolvase.

5.2.2 Effects of scissile position methylphosphonate substitution on binding and synapsis properties of activated mutants

The results shown in Figure 5.2 indicate that some methylphosphonate substitutions that reduced the amount of synapse led to the accumulation of monomer complexes, without

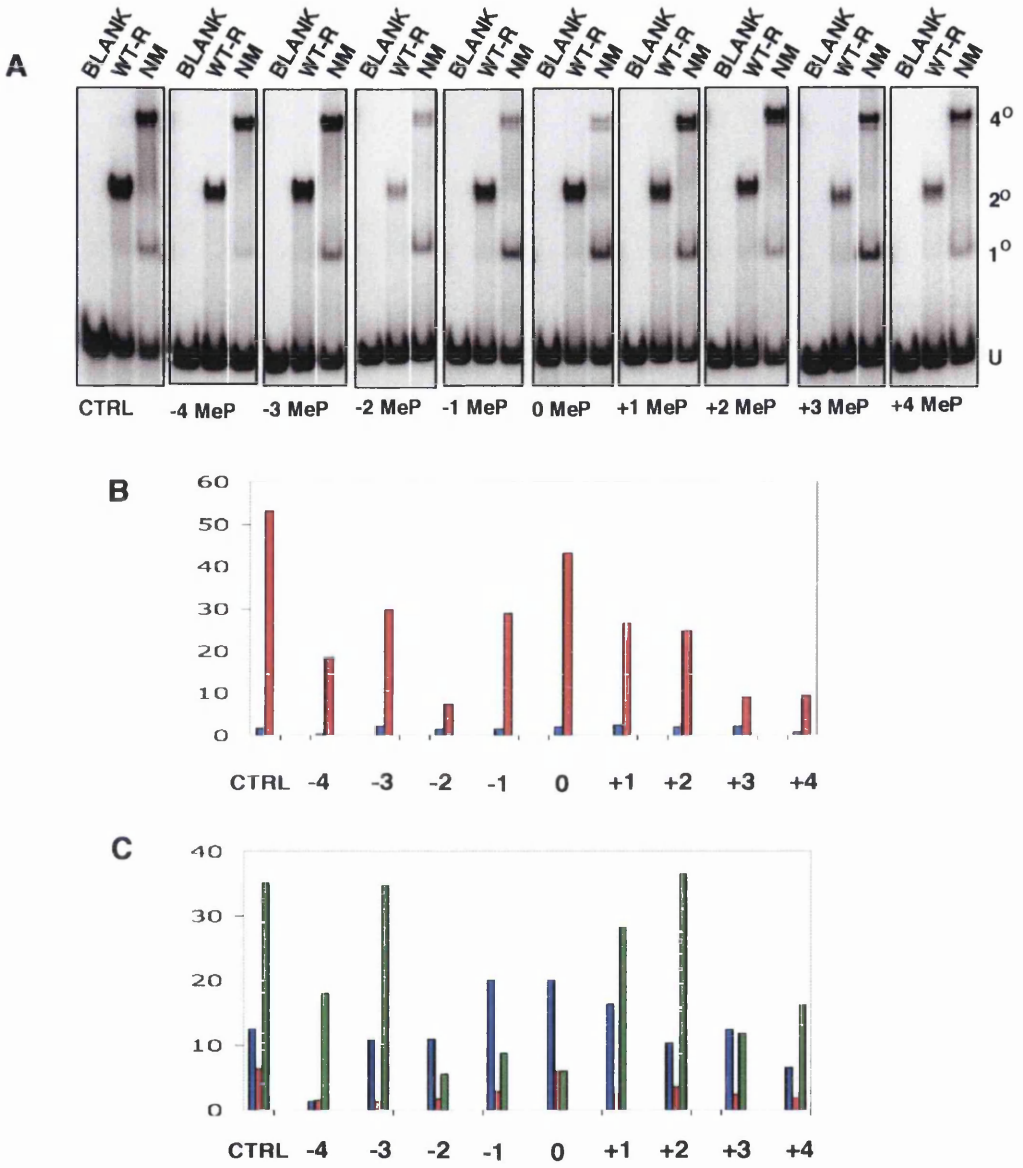

Figure 5.2 Methylphosphonate substitution assay of the role of phosphate ionic contacts at site I in resolvase binding and synapsis

Panel A: Binding reactions were as described in section 2.30: Resolvase (400 nM); 50LR site I or the appropriate 50LRMeP site I (unlabelled, 50 nM; ^{32}P-labelled, 2.5 nM). Electrophoresis was on a 6.5% polyacrylamide TBE gel (Section 2.27). The symbols U, 1°, 2°, and 4° represent unbound DNA, monomer complex, dimer complex and the synapse respectively. **Panels B** and **C**: The complexes formed by NM-resolvase with each of the modified 50LRMeP site I were quantitated to determine the percentage of the input DNA bound as monomer (blue bar), dimer (red bar) and synaptic (green bar) complexes, and are shown in Panel B for WT-resolvase and Panel C for NM-resolvase.

the appearance of the dimer complex. The results presented in Section 3.2.2 (Figure 3.3) show that dimer complexes of NM-resolvase are observed on TGE polyacrylamide gels when catalysis is inhibited by use of a site I with phosphorothioate substitutions of the scissile phosphates. Hence, the effects of 50LRMeP(0) site I and the phosphorothioate-modified 50LRpth site I on the nature of complexes formed by WT-resolvase, and the activated mutants SY-resolvase and NM-resolvase were compared on TBE and TGE polyacrylamide gels. The scissile position methylphosphonate-substituted substrate was used in this experiment since it had the most effect on the formation of NM-resolvase synapse (Figure 5.2, Panels A and C). As shown in Figure 5.3 (Panels A and B), the phosphorothioate-modified 50LRpth site I did not cause a significant difference in the binding properties of WT-resolvase and the mutants, compared with the unmodified 50LR site I, when the reactions were analysed on TBE gels. In addition, scissile position methylphosphonate substitution did not have a significant effect on the binding properties of WT-resolvase, SY-resolvase, and AKSY-resolvase on both TBE and TGE gel conditions (Figure 5.3, Panels A, C, and E). It is noteworthy that these two activated mutants (SY-resolvase and AKSY-resolvase) did not form significant amounts of the site I synapse in the bandshift assays described in Figure 3.1. In agreement with the results shown in Section 5.2.1 (Figure 5.2, Panel A), the 50LRMeP(0) site I significantly reduced the amount of the synapse by NM-resolvase when the binding reaction was analysed on both TBE and TGE gels (Figure 5.3, Panels C and E). In contrast to the result with 50LRpth site I, where large amounts of the dimer complex of NM-resolvase were observed (Figure 5.3, Panel D), only a faint band corresponding to the dimer complex was found in the reaction with 50LRMeP(0) site I (Figure 5.3, Panel E).

5.2.3 Effects of methylphosphonate substitutions on site I cleavage

The effects of the methylphosphonate substitutions that affected the amount of synapse observed in bandshift assays (Section 5.2.1) on the cleavage of site I by NM-resolvase were investigated. These are MeP(-2), MeP(-1), and MeP(0). In order to rule out the inhibitory effects of the modifications on binding and synapsis from any observed effect on catalysis, the 50LRMeP(+1) site I was included as a control in this experiment. The assays were carried out in EG buffer (Section 2.31) to favour the formation of double-

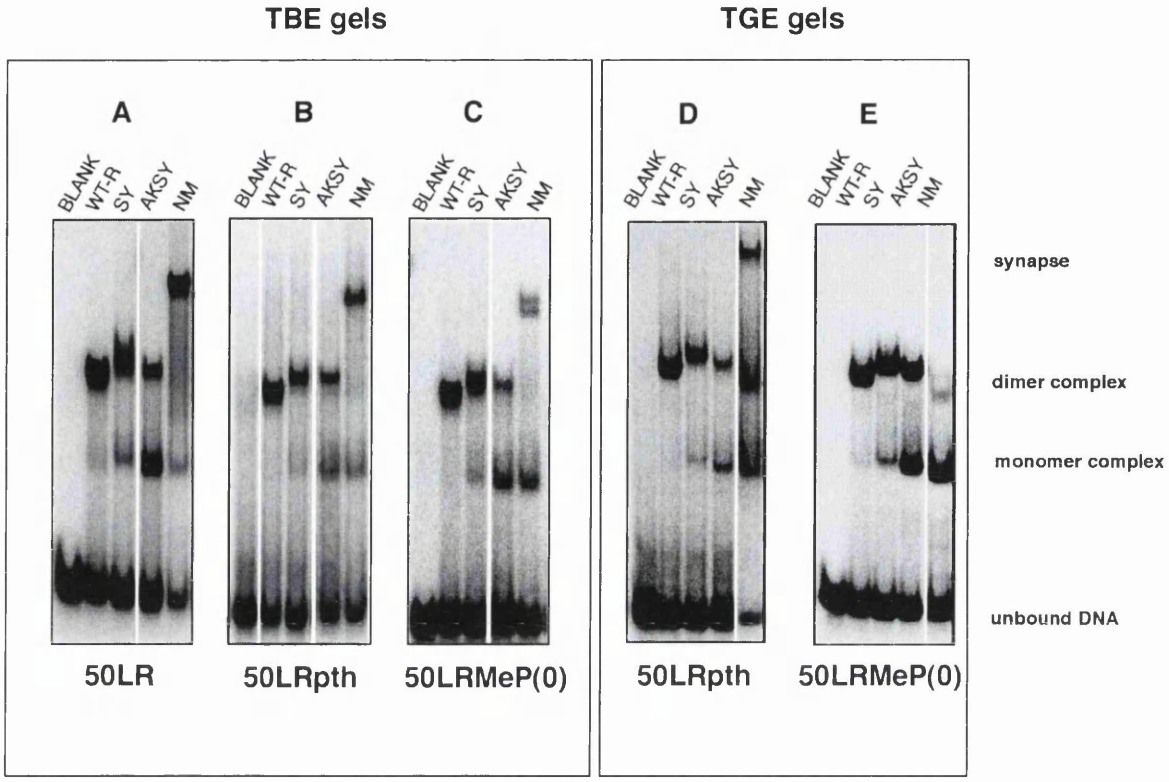

Mutant	Mutations in WT resolvase
SY	G101S D102Y
AKSY	R2A E56K G101S D102Y
NM	R2A E56K G101S D102Y M103I Q105L

Figure 5.3 Comparison of effects of phosphorothioate and methylphosphonate substitutions on binding/synapsis properties of WT-resolvase and some activated mutants

Binding reactions were as described in section 2.30: Resolvase (400 nM); 50LR, 50LRpth or 50LRMeP(0) (unlabelled, 50 nM; ^{32}P-labelled, 2.5 nM). Electrophoresis was on 6.5% TBE or TGE polyacrylamide gels (Section 2.27).

stranded cleavage products. The results (Figure 5.4, Panel A) show that methylphosphonate substitution at the scissile position (MeP(0)) completely inhibited the formation of double-stranded cleavage products, while modifications at the -2 and –1 positions that led to significant reduction in the amount of the synaptic complex formed in bandshift assays (Figure 5.2), had modest effects on catalysis. The surprising result from this experiment came from the MeP(+1) modification that did not have a significant effect on synapsis (Figure 5.2), but inhibited catalysis (Figure 5.4). A summary of the effects of methylphosphonate substitutions at phosphate positions -2, -1, 0, and +1 in the synapsis (Figure 5.2) and cleavage assays (Figure 5.3, Panel A) is shown in Figure 5.4, Panels B and C.

The effects of the methylphosphonate modifications on the cleavage reaction were further investigated by characterising the nature of the covalent complexes formed with the modified substrates. Despite their effects on binding and synapsis (Figure 5.2), the methylphosphonate modifications at the -4, -3, -2, -1, +2, +3, and +4 positions did not have significant effects on the extent of cleavage and the distribution of the covalent complexes formed (Figure 5.5, Panels A and B). The modification at the scissile phosphodiester, MeP(0), had the most serious effect on catalysis, since products were only barely detectable. In the 50LRMeP(+1) site I assay, single strand-cleaved covalent complexes are formed to the same extent as that seen with the control and other methylphosphonate-modified site I substrates, but the amount of double strand-cleaved products formed was significantly reduced (Figure 5.5, Panels A and B).

Since racemic mixtures of the methylphosphonate-modified DNAs are used in these experiments, the limited formation of double-strand cleavage products with the MeP(+1) substrate might be due to a preference for one stereoisomer at this position (see Section 5.1.2). If that were the case, double strand-cleaved products would be obtained only when both strands of the DNA are of the preferred stereoisomer. DNA molecules having the inhibitory stereoisomer on both strands will not be cleaved at all, and a duplex having both stereoisomers will form only single strand-cleaved products. This hypothesis was investigated by using a hybrid substrate that consists of a 50LRMeP(+1) site I DNA (top

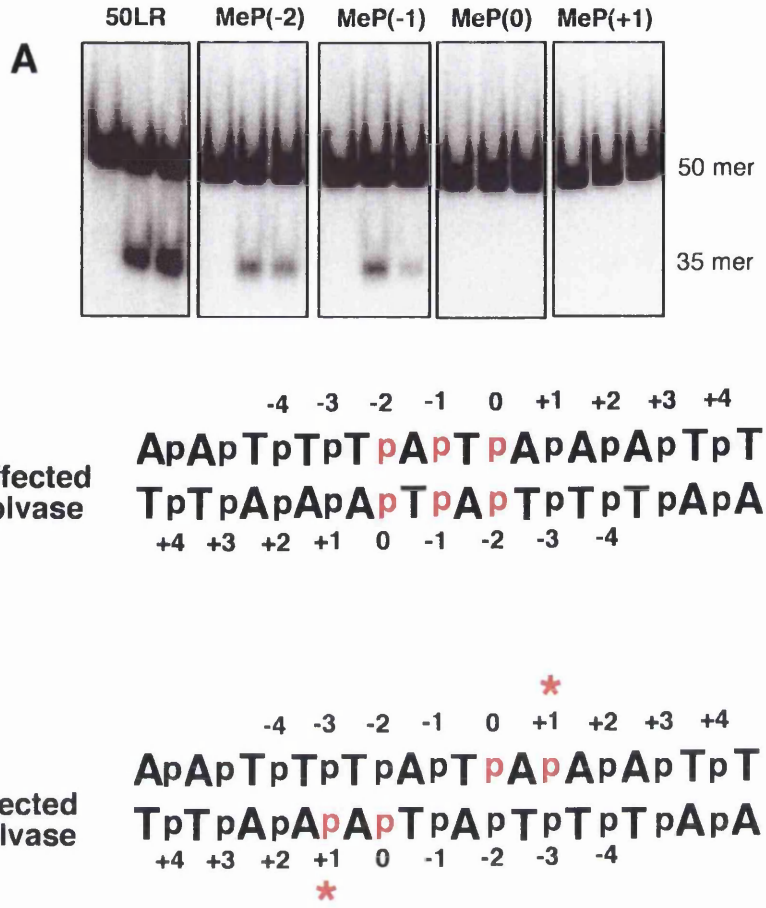

Figure 5.4 Effect of methylphosphonate substitutions on DNA cleavage by NM-resolvase

Panel A: Cleavage of 50LR, 50LRMeP(-2), 50LRMeP(-1), 50LRMeP0), and 50LRMeP(+1) site Is by NM-resolvase. Cleavage reactions were as described in section 2.31: Resolvase (100 nM); 50LR or the appropriate 50LRMeP (unlabelled, 50 nM; ^{32}P-labelled, 2.5 nM); EG buffer. The top strand of the duplex DNA was labelled at the 5' end, and annealed to an unlabelled bottom strand (Section 2.26). The reactions were for 30 minutes and SDS/protease K loading buffer was added to stop the reaction. The reaction products were separated on a 6.5% gel (Section 2.27). **Panels B** and **C** compare the phosphate positions (red) whose substitution affected the formation of double-strand cleavage products in the assay shown in panel A with those that affected synapsis in the assays shown in Figure 5.2. The +1 (*) position is unique in having an effect on cleavage without affecting binding and synapsis.

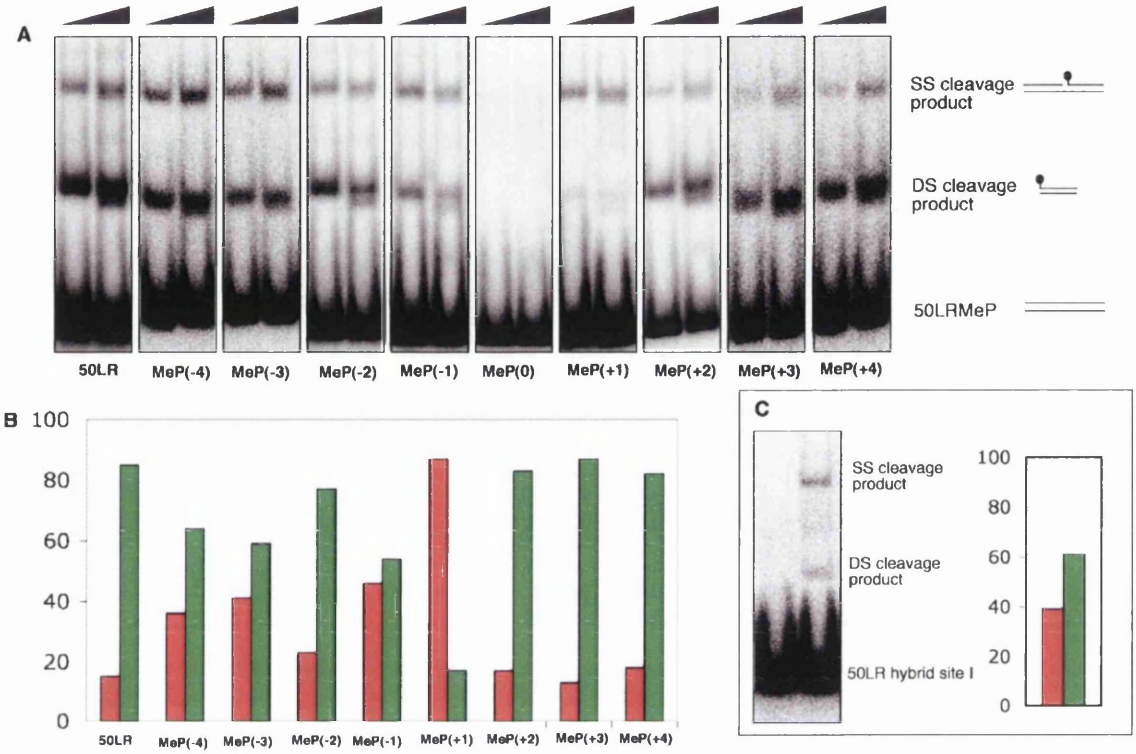

Figure 5.5 Analysis of the effect of methylphosphonate substitutions on DNA cleavage by NM-resolvase

Panel A: Binding reactions were as described in section 2.30: Resolvase (100 and 200 nM); 50LR site I or the appropriate 50LRMeP site I (unlabelled, 50 nM; ^{32}P-labelled, 2.5 nM). The binding reactions were set up for 30 minutes and then treated with 0.1% SDS for 10 minutes (Section 2.18). Electrophoresis was on a 6.5% polyacrylamide TBE SDS gel (Section 2.28). **Panel B:** The bands from the samples treated with 200 nM resolvase were quantitated to determine the percentage of the reaction products trapped as single-strand (red bar) and double-strand (green bar) cleaved products. **Panel C:** Cleavage of a hybrid site I substrate by NM-resolvase. The hybrid substrate consists of a 50LRMeP(+1) site I DNA (top strand and ^{32}P-labelled) annealed to an unmodified 50LR site I DNA (bottom strand).

strand) annealed to an unmodified 50LR site I DNA (bottom strand). The results (Figure 5.5, Panel C) show that NM-resolvase forms roughly twice the amount of double-strand cleavage products from the hybrid substrate as it did with the 50LRMeP(+1) site I (Figure 5.5, Panel B), but cleavage is still less efficient compared to the unmodified 50LR site I.

5.3 Discussion

5.3.1 Resolvase-DNA contacts at the centre of site I that are important for binding and synapsis

The effects of methylphosphonate substitutions on site I binding by WT-resolvase are consistent with the contacts seen in the crystal structure of the resolvase-site I dimer complex (Yang & Steitz, 1995). Binding of WT-resolvase was affected by methylphosphonate substitutions at -2, +3, and +4 positions (Figure 5.2). Neutralisation of the phosphate oxygen at the -2 position may affect the base-pair interactions that seem to be important for the minor groove base-specific contacts made by R130 in the dimer complex (Yang & Steitz, 1995). This minor groove interaction appears to be important for the stable binding of resolvase to site I (Yang & Steitz, 1995). The +3 and +4 phosphate positions are close to where the 'arm' region of resolvase binds in the minor groove (Yang & Steitz, 1995), and these interactions probably contribute significantly to the stability of the dimer complex (Section 1.6; Figure 1.11). The effects on WT-resolvase binding of substitutions at these positions (Figure 5.2) might be due to neutralisation of polar contacts made by resolvase to these phosphate groups, or changes to the DNA conformation such as bending and distortion of the minor groove geometry.

The reduced amount of the synapse formed by NM-resolvase by methylphosphonate substitutions at the -2, +3, and +4 phosphate positions is correlated with reduced dimer complex of WT-resolvase (Figure 5.2). This suggests that the effect of the substitutions on NM-resolvase synapsis could be due to destabilisation of a pre-synaptic interaction of monomers or dimer with site I. However, the reduction in the amount of synapse due to methylphosphonate substitutions at -1 and 0 phosphate positions suggests a synapsis-specific effect, since binding by WT-resolvase was not affected by these substitutions. The crystal structures of the dimer complex (Yang & Steitz, 1995) and the synaptic

complex (Li *et al.*, 2005) provide some clues on the residues that might interact with the phosphate positions identified from this study to be important for synapsis. Figure 5.6 shows some polar residues that are close to the phosphates that are implicated in synaptic interactions in this study. R125 is close to the scissile phosphate in the dimer complex (Figure 5.6, Panel A) and forms a hydrogen bond with the 3' OH group in the post-cleavage synaptic complex (Figure 5.6, Panel B). Interestingly, the R125K mutation led to a reduction in the amount of the synapse formed by NM-resolvase with 70LR site I (Figure 4.4). It was speculated that R125 and R121 might interact with D94 and D95 on the essentially hydrophobic interface of the post-cleavage site I synapse as a gating mechanism for controlling subunit rotation (Li *et al.*, 2005; Grindley *et al.*, 2006). The putative catalytic residues R8, R68, and R71 that are close to the -1, 0, and +1 positions in the resolvase-site I structures (Figure 5.7) do not seem to contribute significantly to the stabilisation of the synapse (Section 4.2.5; Figure 4.11). In both dimer complex and synaptic complex structures, K143 is very close to the -4 position, at which methylphosphonate substitution led to a reduction in the amount of monomer complex of NM-resolvase (Figure 5.2). Contacts at the -4 position might be important for the stabilisation of the monomer complex. K136 is another polar residue that is found on the E-helix close to the centre of site I. However, it does not appear to make any specific contact with the phosphates in the crystal structures.

Falvey & Grindley (1987) reported that ethylation of phosphodiester oxygens at the -2 and -4 positions inhibited site I binding by γδ resolvase, but ethylation at the -3 and +4 positions enhanced binding (Figure 5.8, Panel B). The methylphosphonate substitution experiments carried out in this study agree with their finding on the inhibitory effect at the -2 position, but no enhanced binding was found with substitutions at the -3 and +4 positions (Figure 5.8, Panel A). The specific absence of the monomer complex in the reaction of NM-resolvase with 50LRMeP(-4) (Figure 5.2) might be consistent with the reported inhibition of γδ resolvase binding by phosphate ethylation at the -4 position (Figure 5.8, Panel B). As illustrated in Figure 5.8 (Panel D), ethylation of phosphate oxygens at positions -2, -1, 0, and +1 inhibited the resolution activity of γδ resolvase (Falvey & Grindley, 1987). However, methylphosphonate substitutions at positions -2

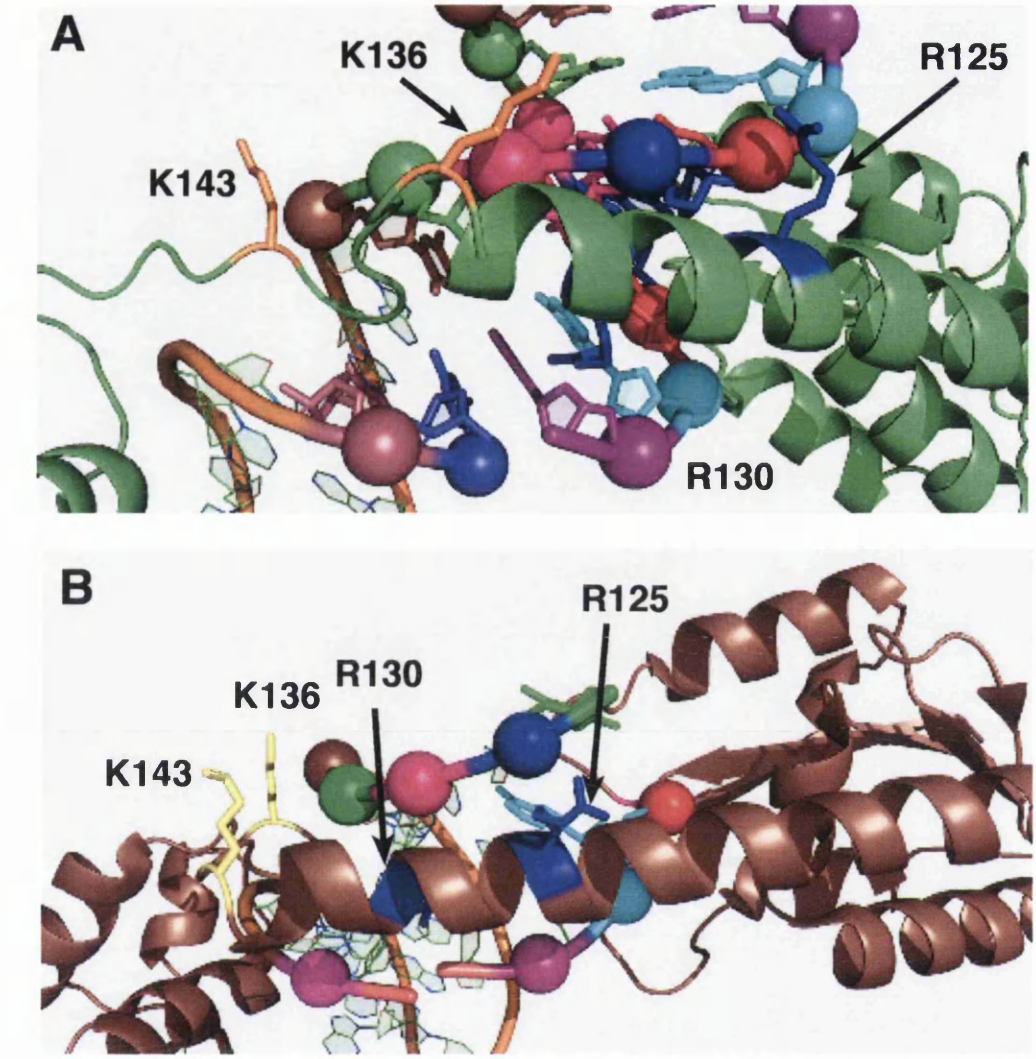

Figure 5.6 Contacts made by γδ resolvase with the modified phosphates in 1GDT and 1ZR4.

Panel A: 1GDT. **Panel B:** 1ZR4. The phosphate positions where methylphosphonate substitution affected synapsis are shown as spheres: -4 (brown), -2 (pink), -1 (blue), and 0 (red). The highlighted phosphates whose modifications did not affect synapsis are coloured as shown in Figure 5.1. The polypeptide backbone of the protein is represented as green (Panel A) and brown (Panel B) cartoons, while the side chain of the charged residues that could potentially make contact with the phosphate positions are shown as sticks: R125 and R130 (blue), and K136 and K143 (yellow). The pictures were generated from PDB coordinates of 1GDT and 1ZR4 (Section 2.35), and monomer B of each structure is shown.

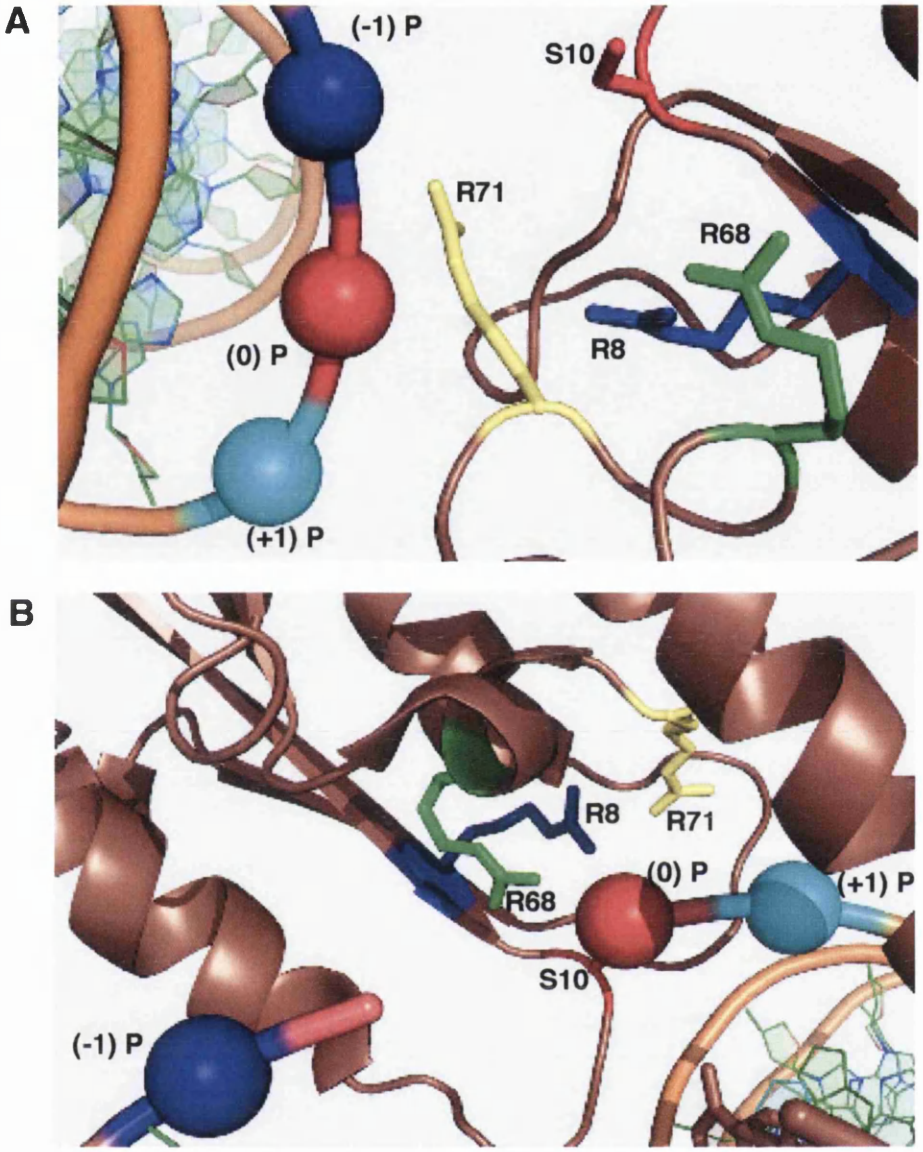

Figure 5.7 Interactions of R8, S10, R68, and R71 with the DNA in 1GDT and 1ZR4. **Panel A:** 1GDT. **Panel B:** 1ZR4. Pictures showing the orientation of R71 towards the scissile phosphate (0) and the one 5' proximal to it (-1) in 1GDT (Panel A). The orientation of the residue has moved toward the 3' proximal phosphate in 1ZR4 (Panel B). The pictures were generated from PDB coordinates of 1GDT and 1ZR4 (Section 2.35), and monomer B of each structure is shown. The polypeptide backbone of resolvase is represented as brown cartoon, while the side chains of the residues are shown as sticks: R8 (blue), S10 (red), R68 (green), and R71 (yellow). The phosphates are shown as coloured spheres: blue (-1), red (0), and cyan (+1).

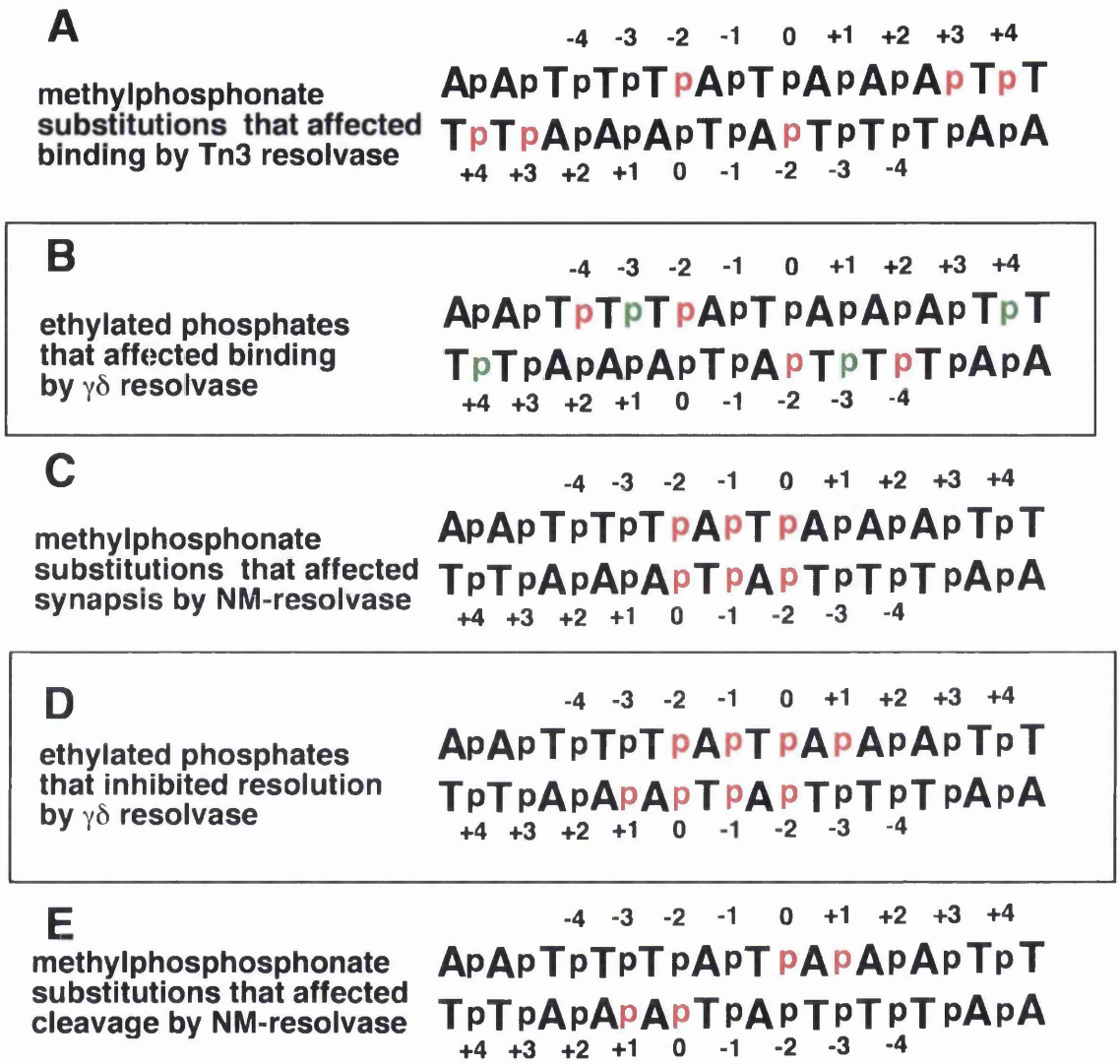

Figure 5.8 Comparison of the phosphate ethylation interference data from Falvey & Grindley (1987) to the methylphosphonate substitution data from this study.
The phosphate positions whose substitution affected the indicated activity (binding, synapsis, cleavage, and resolution) are coloured red. The set of data summarised in Panels A, C, and E are from this study, while those in Panels B and D are from Falvey & Grindley (1987). In Panel B, the phosphates coloured green enhanced site I binding in the phosphate ethylation experiment (Falvey & Grindley, 1987).

and -1 were the ones found to have significant effects on the cleavage activity of NM-resolvase. These differences might be ascribed to the nature and the context of the assays in both sets of experiments. The resolution assays reported by Falvey & Grindley (1987) were carried out with wild-type γδ resolvase on a *res* x *res* substrate, in contrast to the activated mutant used here in site I cleavage assays.

The effects of methylphosphonate substitutions on NM-resolvase synapsis (Figure 5.2) suggest that resolvase-site I interactions in the synapse could involve more DNA contacts than are seen in current crystal structures (Li *et al.*, 2005; Kamtekar *et al.*, 2006). Site I synapsis involves interactions between the catalytic domains of resolvase (Section 1.10), and the effect of methylphosphonate substitution on synapsis (Figure 5.2) is in agreement with the finding that stable tetramerisation of NM-resolvase depends on synapsis to site I (Section 3.3.4). Assembly of the site I synapse might involve specific interaction of resolvase residues in the N-terminal domain with the -1 and 0 phosphate positions. This hypothesis is consistent with the effect of mutations of conserved N-terminal domain residues Y6, Q14, Q19, D36, and R119 on synapsis by NM-resolvase (Section 4.2.2), and of Y6, D67, E118, and E124 on the binding properties of AKSY-resolvase (Section 4.2.3). It could be that these residues, the mutations of which affect the amount of site I synapse formed in bandshift assays, might interact with the DNA around the scissile phosphate in the synapse.

5.3.2 The site I dimer complex of WT-resolvase is functionally different from that of NM-resolvase

The results presented in Figure 5.3 reveal a structural difference between the dimer complex of activated resolvase mutants that formed a stable site I synapse and those that did not. There was no difference in the binding behaviour of WT-resolvase and the activated mutants SY-resolvase and AKSY-resolvase with the 50LRpth site I and the 50LRMeP(0) site I substrates. However, NM-resolvase gave a dimer complex with 50LRpth site I, but not 50LRMeP(0) site I on a TGE polyacrylamide gel. The significant reduction in the amount of NM-resolvase dimer complex with 50LRMeP(0) (Figure 5.3, Panel E) suggests that the methylphosphonate substitution neutralises a specific

phosphate interaction that could be important for the NM-resolvase dimer complex, but not those of WT-resolvase, SY-resolvase, and AKSY-resolvase. Another possibility is that the methylphosphonate substitution might induce some subtle changes in the DNA conformation, which results in instability of NM-resolvase dimer complex on TGE polyacrylamide gel conditions. In either case, the results indicate that protein-DNA interactions are different in the dimer complex of NM-resolvase from those of WT-resolvase, SY-resolvase and AKSY-resolvase. Bandshift assays described in Section 3.2.2 (Figure 3.2) show that the dimer complex of NM-resolvase has an altered mobility compared to the dimer complex of WT-resolvase. In addition, it was not possible to detect the dimer complex in a time course analysis of the assembly of NM-resolvase site I synapse, though monomer complexes were detected at all time points (Figure 3.4). These findings point to the conclusion that the dimer complex formed by NM-resolvase has an altered conformation that might be in a synapsis-competent state, while the dimer complex of WT resolvase, SY-resolvase and AKSY-resolvase are not.

5.3.3 The role of the phosphate 3' to the scissile group in catalysis

Cleavage assays with methylphosphonate-modified substrates show that the phosphodiester bonds at the 0 and +1 positions are important in catalysis (Figures 5.4 and 5.5). The abolition of catalytic activity by the scissile phosphate methylphosphonate substitution (Section 5.2.3) is consistent with the catalytic requirements for phosphoryl transfer reactions (Mizuuchi & Baker, 2002). Neutralisation of the non-bridging phosphodiester oxygens might remove interactions that are important for catalytic activation (see Sections 1.11 and 4.3.3). The effect of the MeP(+1) modification on site I cleavage was rather surprising since the change did not have a negative effect in synapsis assays (Figure 5.2). This suggests that the reduced rate of cleavage caused by the MeP(+1) modification is due to interference with a specific catalytic step. It has been proposed that a non-bridging phosphodiester oxygen immediately 3' to the scissile phosphodiester bond could be involved as a base in the generation of the nucleophile in several enzymatic phosphoryl transfer reactions (Pingoud & Jeltsch, 2001). It is unlikely that phosphate oxygen alone can perform this role in resolvase since the pKa of phosphate (around 1.5) is too low (Kurpiewski *et al.*, 2004) to abstract a proton from the S10 whose

pKa is around 10. Horton *et al.* (1998) proposed that the phosphate 3' to the scissile group may help recruit residues to assemble the functional active site structure in Type II restriction endonucleases. Evidence from methylphosphonate substitutions was used to show that phosphate groups around the scissile phosphate are involved in the assembly of the active site of topoisomerase IB (Tian *et al.*, 2004). The role of the 3' phosphate in resolvase catalysis might involve a similar process of active site assembly by coordinating a positively charged catalytic residue. For instance, in the γδ resolvase dimer-site I complex (Yang & Steitz, 1995), active site R71 coordinates the scissile phosphate and the phosphate group immediately 5' to it (-1 position), whereas it appears to be closer to the 3' proximal phosphate (+1 position) in the post-cleavage synaptic complex (Li *et al.*, 2006; Grindley *et al.*, 2006; Figure 5.7). Further studies are required to ascertain the exact role of the +1 phosphate in catalytic mechanism of resolvase. Experiments with chirally pure methylphosphonate-modified DNA are likely to provide more definite information on the interaction of resolvase with site I in binding, synapsis, and catalysis.

Chapter Six

Conclusions

6.1 Deregulation of resolvase by activating mutations

In this study, the binding and catalytic properties of WT-resolvase were compared with those of a set of activated resolvase mutants in an attempt to understand how activating mutations affect site I synapsis and catalysis. In this section, a model for the effect of the activating mutations on Tn3 resolvase is presented.

The results suggest that the mutations facilitate the engagement of some residues in the active site region with the substrate DNA, an interaction that is necessary for site I synapsis and is dependent on the formation of the *acc* synapse in wild-type resolvase (see Section 1.4.3). The activated mutants are able to assemble the site I synapse in the absence of the *acc* synapse since their active site residues are in a synapsis-competent state. Two lines of evidence suggest that the active site geometry of activated resolvase mutants might be different from that of WT-resolvase.

1. The catalysis of recombination by activated resolvase mutants showed different pH dependence from WT-resolvase (Section 3.3.2). In addition, subtle differences in pH dependence among the mutants were noticeable. One possible explanation is that these differences are due to structural changes in the N-terminal domain of resolvase that result in subtle changes in the geometry of the active site (Section 3.3.2). Different sets of mutations might produce different changes to the active site geometry.
2. Results presented in Section 4.2.6 showed that the mutations V9A, R45K, D67N, E118Q, and R125K had less inhibitory effects on site I cleavage in the context of NM-resolvase than in the less activated resolvase variant AKSY-resolvase (Sections 3.2.1 and 3.2.5). Mutation of some of these residues in wild-type γδ resolvase and Hin recombinase led to loss of catalytic activities (Table 4.1). This suggests that the active site of NM-resolvase has less specific requirements for the mutated residues than that of AKSY-resolvase. Activated mutants likely have more flexible active sites that are able to engage in catalysis in the absence of these conserved residues.

The proposal that activated resolvase mutants might have active sites with subtle structural and functional differences from the WT-resolvase is plausible since resolvase active site residues are not actively engaging the substrate in crystal structures of the pre-cleavage dimer and post-cleavage synaptic complexes (Section 1.12). The proposed facilitation of interactions between active site residues and the DNA by activating mutations is consistent with the negative effects of active site mutations Y6F, Q14E, Q19E, and D36N on site I synapsis by NM-resolvase (see Section 4.2.2). Likewise, another set of mutations in the putative active site and on the 1-2 dimer interface (D67N, E118Q, and E124Q) of AKSY-resolvase restructures the dimer complex and stabilises the site I synapse (Section 4.2.3).

6.2 The 1-2 dimer interface and site I synapsis

The fact that the acid to amide mutations (D67N, E118Q, and E124Q), which stabilise site I synapsis in AKSY-resolvase are in residues found on the dimer interface invites another speculation on the role of the resolvase-site I dimer complex in recombination. WT-resolvase forms mainly the dimer complex in bandshift assays (Section 3.2.1) and fails to catalyse site I x site I reactions (Section 3.2.5; Bednarz *et al.*, 1990). Activated resolvase mutants SY-resolvase and AKSY-resolvase that form mainly dimer complex in bandshift assays did not give significant amounts of the synapse. Changing carboxylate residues (D67, E118, and E124) to amides in AKSY-resolvase led to the disappearance of the dimer complex and stabilises the site I synapse in bandshift assays. This suggests that the WT resolvase-site I dimer complex is unable to synapse because the residues required for synapsis remain locked in the dimer interface. Evidence that the dimer complex of NM-resolvase is structurally different from those of WT-resolvase, SY-resolvase, and AKSY-resolvase is presented in Section 5.3.2. Disulphide crosslinking of M106C residues along the 1-2 interface in γδ resolvase blocks site-specific cleavage and resolution of supercoiled substrates, but allowed some topoisomerase activities (Hughes *et al.*, 1993). In addition, the crosslinked dimer had a reduced affinity for site I, but not the accessory sites II and III. This suggests that distortion of the 1-2 dimer interface is a requirement for the assembly of the site I synapse, and activation of recombination-specific catalysis. Hence, the stable WT-resolvase dimer complex could be a regulatory

mechanism for controlling the engagement of active site residues with the DNA in synapsis. Mutation of REG residues on the dimer interface (Section 1.8) and in other parts of the N-terminal domain might release the residues from their locked state and promote side chain-DNA contacts in the dimer complex that are required for synapsis.

The above considerations on the mechanism by which activating mutations stabilise the site I synapse and activate the complex for catalysis suggest a role for sites II and III of *res* in promoting synapsis and catalysis at site I. In the wild-type enzyme, formation of the *acc* synapse likely forces the site I dimer complex from a locked state into an open conformation that rapidly synapses with its partner dimer complex at the other *res* site. Catalysis is initiated when the side chains of active site residues are brought into contact with the scissile phosphodiester bonds and neighbouring phosphate positions involved in catalysis (Sections 5.3.3). The nature of the signal that triggers catalysis after the assembly of the *res* synapse is unknown. However, evidence exists that *res* synapsis is significantly faster than recombination in wild-type Tn21 resolvase (Parker & Halford, 1991). Likewise, activation of catalysis lags behind site I synapsis by NM-resolvase (Section 3.3.3).

6.3 Activated mutants as tools for studying resolvase catalysis

Activated resolvase mutants were used in this project to study the mechanism of resolvase catalysis based on the premise that they offer the advantage of being simpler to study than the wild-type enzyme. Activated resolvase mutants catalyse site I x site I reactions in the absence of the regulatory sites II and III, do not require substrate supercoiling and directly repeated crossover sites, and form stable site I synapse in polyacrylamide bandshift assays (Section 1.13). Bandshift assays of the mutants of NM-resolvase have identified mutants that are specifically defective in synapsis (e.g. Y6F, D6N, Q19E, R119K, and R125K). These are potential subjects of further investigations (see Figure 4.1). The combination of mutational analysis and chemical modification of the DNA substrate can help elucidate how these residues contribute to synaptic interactions. Characterisation of the catalytic properties of the mutants also revealed a variety of specific and interesting effects (Section 4.2.4). These mutants might provide further insights into the regulation of

catalysis, if they were subjected to a wider range of investigations. For example, the mutant NM-S39A catalyses site I x site I reactions at a slower rate than NM-resolvase but retains the synaptic and catalytic properties of the parent NM-resolvase. Hence, NM-S39A could be useful in analysing aspects of NM-resolvase catalysis that are too fast for certain analytical procedures. The relatively simpler catalytic system of activated resolvase mutants should make them more amenable than WT-resolvase to conventional biochemical analyses such as stopped flow kinetic studies.

6.4 Active site residues and the chemical steps of catalysis

One of the aspects of the mechanism of recombination catalysed by Tn3 resolvase investigated in this project is the role of active site residues in the chemical steps of catalysis (Chapter 4). Conservative mutations of candidate residues and biochemical studies of some of their binding, synaptic, and catalytic properties have revealed which residues are most important for the first phosphoryl transfer reaction, the cleavage step. In addition to the well-characterised role of S10 as the nucleophile, R8, R68, R71, Y6, Q14, Q19, and D36 play important roles in the catalytic process. Of these, S10, Y6, and R8 appear to be essential for catalysis (Sections 42.4 and 4.2.5). However, no definite roles can be ascribed to these residues based on the findings from the mutational studies reported here.

While the residues that mediate the chemical steps of resolvase catalysis have been identified, key questions remain in elucidating the reaction mechanism. Some of these are the identities of the residue or residues that serve as the general base that activates S10 for nucleophilic attack on the scissile phosphate, and the general acid that protonates the 3' O^- of the leaving group (Section 1.11). Evidence presented in Section 4.2.4 shows that it is unlikely that D67 plays the role of general base, as has been proposed (Pan *et al.*, 2001; Grindley *et al.*, 2006). However, its interaction with R68 (Li *et al.*, 2005) might enhance the basicity of the arginine residue such that the pair could serve as the base catalyst. It was proposed that adjacent carboxylate residues (glutamate or aspartate) could polarise the guanidinium functional group of arginine residues sufficiently to enable the arginine to abstract a proton from a potential nucleophile (Guillen-Schlippe & Hedstrom, 2005).

There is also the possibility that the serine recombinases might employ a catalytic mechanism that does not necessarily involve general acid and general base catalysis as do the tyrosine recombinases (Mizuuchi & Baker, 2002). For example, a recent mutational and biochemical analysis of candidate residues in the telomere resolvase ResT fails to identify any residue that matches the criteria for a general acid catalyst (Deneke *et al.*, 2004). Furthermore, a mechanistic description of the chemical steps of resolvase catalysis will need to incorporate the role of the phosphodiester group immediately 3' of the scissile bond which clearly has a catalytic function (Section 5.3.3).

Bibliography

Abdel-Meguid, S.S., Grindley, N.D.F., Templeton, N.S., and Steitz, T.A. (1984) Cleavage of the site-specific recombination protein γδ resolvase: the smaller of the two fragments binds DNA specifically. Proc. Natl. Acad. Sci. USA, 81, 2001-2005.

Adams, C.W., Nanassy, O., Johnson, R.C., and Hughes, K.T. (1997) Role of arginine-43 and arginine-69 of the Hin recombinase catalytic domain in the binding of Hin to the *hix* DNA recombination sites. Mol. Microbiol. 24, 1235-1247.

Akopian, A., and Stark, W.M. (2005) Site-specific DNA recombinase as instrument for genomic surgery. Adv. Genet. 55, 1-23.

Allawi, H.T., Kaiser, M.W., Onufriev, A.V., Ma, W-P., Brogaard, A.E., Case, D.A., Neri, B.P., and Lyamichev, V.I. (2003) Modeling of flap endonuclease interactions with DNA substrate. J. Mol. Biol. 328, 537-554.

Argos, P., Landy, A., Abremski, K., Egan, J.B., Haggard-Ljungquist, E., Hoess, R.H., Kahn, M.L., Kalonis, B., Narayana, S.V.L., Pierson, L.S., Sternberg, N., and Leong, J.M. (1986) The integrase family of site-specific recombinases: regional similarities and global diversity. EMBO J. 5, 433-440.

Arnold, P. (1997) Mutants of Tn3 resolvase. Ph.D. Thesis, University of Glasgow.

Arnold, P.H., Blake, D.G., Grindley, N.D.F., Boocock, M.R., and Stark, W.M. (1999) Mutants of Tn3 resolvase which do not require accessory binding sites for recombination activity. EMBO J. 18, 1407–1414.

Bednarz, A.L., Boocock, M.R., and Sherratt, D.J. (1990) Determinants of correct *res* site alignment in site-specific recombination by Tn3 resolvase. Genes Dev. 4, 2366-2375.

Benjamin, H.W., and Cozzarelli, N.R. (1988) Isolation and characterisation of the Tn3 resolvase synaptic intermediate. EMBO J. 7, 1897-1905.

Benjamin, H.W., and Cozzarelli, N.R. (1990) Geometric arrangements of Tn3 resolvase sites. J. Biol. Chem. 265, 6441-6447.

Benjamin, H.W., Matzuk, M.M., Krasnow, M.A., and Cozzarelli, N.R. (1985) Recombination site selection by the Tn*3* resolvase: topological tests of a tracking mechanism. Cell 40, 147-158.

Benjamin, K.R., Abola, A.P., Kanaar, R., and Cozzarelli, N.R. (1996) Contribution of supercoiling to Tn3 resolvase and phage Mu Gin site-specific recombination. J. Mol. Biol. 256, 50-65.

Birnboim, H.C., and Doly, J. (1979) A rapid alkaline extraction procedure for screening recombinant plasmid DNA. Nucleic Acids Res. 7, 1513-1523.

Blake, D. (1993) Binding of Tn3 resolvase to its recombination site. Ph.D. Thesis, University of Glasgow.

Blake, D.G., Boocock, M.R., Sherratt, D.J., and Stark, W.M. (1995) Cooperative binding of Tn3 resolvase monomers to a functionally asymmetric binding site. Curr. Biol., 5, 1036-1046.

Boocock, M.R., Brown, J.L., and Sherratt, D.J. (1987) Topological specificity in Tn3 resolvase catalysis. *In* DNA Replication and Recombination, T.J. Kelly and R. M^{c}Macken, eds. (Alan R. Liss, New York), pp. 703-718.

Boocock, M.R., Zhu, X., and Grindley, N.D. (1995) Catalytic residues of γδ resolvase act in cis. EMBO J. 14, 5129-5140.

Botfield, M.C., and Weiss, M.A. (1994) Bipartite DNA recognition by the human Oct-2 POU domain: POUs-specific phosphate contacts are analogous to those of bacteriophage lambda repressor. Biochemistry 33, 2349–2355.

Burke, M.E., Arnold, P.H., He, J., Wenwieser S.V., Rowland, S.J, Boocock, M.R., and Stark, W.M. (2004) Activating mutations of Tn3 resolvase marking interfaces important in recombination catalysis and its regulation. Mol. Microbiol. 51, 937-948.

Canosa, I., Ayora, S., Rojo, F., and Alonso, J.C. (1997) Mutational analysis of a site-specifc recombinase: characterization of the catalytic and dimerization domains of the β recombinase of pSM19035. Mol. Gen. Genet. 255, 467-476.

Chen, J., Lee, J., and Jayaram, M. (1992) DNA cleavage in *trans* by the active site tyrosine during Flp recombination: switching protein partners before exchanging strands. Cell 69, 647-658.

Cox, M.M. (1989) DNA inversion in the 2 μm plasmid of *Saccharomyces cerevisiae*. *In* Mobile DNA, D.E. Berg and M.M. Howe, eds. (American Society for Microbiology, Washington, D.C.), pp. 661-670.

Cozzarelli, N.R., Krasnow, M.A., Gerrard, S.P., and White, J.H. (1984) A topological treatment of recombination and topoisomerase. Cold Spring Harbor Symp. Quant. Biol., 49, 383-400.

Craig, N.L. and Nash, H.A. (1983) The mechanism of phage lambda site-specific recombination: site-specific breakage of DNA by Int topoisomerase. Cell 35, 795-803.

Crisona, N.J., Kanaar, R., Gonzalez, T.N., Zechiedrich, E.L., Klippel, A., and Cozzarelli, N.R. (1994) Processive recombination by wild-type Gin and an enhancer-independent mutant. Insight into the mechanisms of recombination selectivity and strand exchange. J. Mol. Biol. 243, 437–457.

Deneke, J., Burgin, A.B, Wilson, S.L., and Chaconas, G. (2004) Catalytic residues of the telomere resolvase ResT: A pattern similar to, but distinct from, tyrosine recombinases and Type IB topoisomerases. J. Biol. Chem. 279, 53699-53706.

Dertinger, D., and Uhlenbeck, O.C. (2001) Evaluation of methylphosphonates as analogs for detecting phosphate contacts in RNA–protein complexes. RNA 7, 622–631.
Dhar, G., Sanders, E.R., and Johnson, R.C. (2004) Architecture of the Hin synaptic complex during recombination: The recombinase subunits translocate with the DNA strands. Cell 119, 33-45.

Falvey, E., and Grindley, N.D.F. (1987) Contacts between γδ resolvase and the γδ *res* site. EMBO J. 6, 815-821.

Falvey, E., Hatfull, G.F., and Grindley, N.D.F. (1988) Uncoupling of the recombination and topoisomerase activities of the γδ resolvase by a mutation at the crossover point. Nature 332, 861-863.

Fersht, A. (1999) Structure and mechanism in protein science: A guide to enzyme catalysis and protein folding; W. H. Freeman and Co.: New York.

Goodsell, D.S., Kopka, M.L., Cascio, D., and Dickerson, R.E. (1993) Crystal structure of CATGGCCATG and its implications for A-tract bending models. Proc. Natl. Acad. Sci. USA 90, 2930–2934.

Gowers, D.M., and Halford, S.E. (2003) Protein motion from non-specific to specific DNA by three-dimensional routes aided by supercoiling. EMBO J., 22, 1410–1418.

Grindley, N.D. (1993) Analysis of a nucleoprotein complex: the synaptosome of γδ resolvase. Science 262, 738-740.

Grindley, N.D.F. (1994) Resolvase-mediated site-specific recombination. *In* Nucleic Acids and Molecular Biology, vol. 8. Eckstein, F., and Liley, D.M.J. (eds). Berlin, Germany: Springer-Verlag, p.236-267.

Grindley, N.D.F. (2002) The movement of Tn3-like elements: transposition and cointegrate resolution. In *Mobile DNA II.* Craig, N., Craigie, R., Gellert, M., and Lambowitz, A., (eds). Washington, DC: American Society for Microbiology Press, pp. 272–302.

Grindley, N.D.F., Lauth, M.R., Wells, R.G., Wityk, R.J., Salvo, J.J., and Reed, R.R. (1982) Transposon-mediated site-specific recombination: identification of three binding sites for resolvase at the *res* sites of γδ and Tn3. Cell 30, 19-27.

Grindley, N.D.F., Whiteson, K.L., and Rice, P.A. (2006) Mechanism of site-specific recombination. Ann. Rev. Biochem. 75, 567-605.

Guillen Schlippe, Y.V., and Hedstrom, L. (2005) A twisted base? The role of arginine in enzyme-catalysed proton abstractions. Arch. Biochem. Biophys. 433, 266-278.

Haffter, P. and Bickle, T.A. (1988) Enhancer-independent mutants of the Cin recombinase have a relaxed topological specificity. EMBO J. 7: 3991-3996.

Hallet, B., and Sherratt, D.J. (1997) Transposition and site-specific recombination: adapting DNA cut-and-paste mechanisms to a variety of genetic rearrangements. FEMS Microbiol. Rev. 21, 157-178.

Hatfull, G.F., and Grindley, N. (1986) Analysis of γδ resolvase mutants *in vitro*: evidence for an interaction between serine-10 of resolvase and site-I of *res*. Proc. Natl. Acad. Sci. USA 83, 5429-5433.

Hatfull, G.F., and Grindley, N.D.F. (1988) Resolvases and DNA-invertases: a family of enzymes active in site-specific recombination. *In* Genetic Recombination, R. Kucherlapati and G.R. Smith, eds. (American Society for Microbiology, Washington, D.C.), pp. 357-396.

Hatfull, G.F., Sanderson, M.R., Freemont, P.S., Raccuia, P.R., Grindley, N.D.F., and Steitz, T.A. (1989) Preparation of heavy atom derivatives using site-directed mutagenesis: Introduction of cysteine residues into γδ resolvase. J. Mol. Biol. 208, 661-667.

Hatfull, G.F., Noble, S.M., and Grindley, N.D.F. (1987) The γδ resolvase induces an unusual DNA structure at the recombinational crossover point. Cell 49, 103-110.

Heichman, K.A., Moskowitz, I.P.G., and Johnson, R.C. (1991) Configuration of DNA strands and mechanism of strand exchange in the Hin invertasome as revealed by analysis of recombinant knots. Genes Dev. 5, 1622-1634.

Hoess, R.H., and Abremski, K. (1985) Mechanism of strand cleavage and exchange in the Cre-lox site-specific recombination system. J. Mol. Biol. 181, 351-362.

Horton, N.C., Newberry, K.J., and Perona, J.J. (1998) Metal ion-mediated substrate-assisted catalysis in type II restriction endonucleases. Proc. Natl. Acad. Sci. USA 95, 13489-13494.

Hughes, R.E., Hatfull, G.F., Rice, P., Steitz, T.A., and Grindley, N.D.F. (1990) Cooperativity mutants of γδ resolvase identify an essential interdimer interaction. Cell 63, 1331-1338.

Hughes, R.E., Rice, P.A., Steitz, T.A., and Grindley, N.D.F. (1993) Protein-protein interactions directing resolvase site-specific recombination: a structure-function analysis. EMBO J. 12, 1447-1458.

Jiang, Y.L., Ichikawa, Y., Song, F., and Stivers, J.T. (2003) Powering DNA repair through substrate electrostatic interactions. Biochemistry 42, 1922-1929.

Johnson, R.C., and Bruist, M.F. (1989) Intermediates in Hin-mediated DNA inversion: a role for Fis and the recombinational enhancer in the strand exchange reaction. EMBO J. 8, 1581-1590.

Kamtekar, S., Ho, R.S., Cocco, M.J., Li, W., Wenwieser, S.V.C.T., Boocock, M.R., Grindley, N.D.F., and Steitz, T.A. (2006) Implications of structures of synaptic tetramers of γδ resolvase for the mechanism of recombination. Proc. Natl. Acad. Sci. USA 103, 10642-10647.

Kanaar, R., van de Putte, P., and Cozzarelli, N.R. (1988) Gin-mediated DNA inversion: product structure and the mechanism of strand exchange. Proc. Natl. Acad. Sci. U S A. 85, 752-756.

Kanaar, R.A., Klippel, E., Shekhtman, J.M., Dungan, J.M., Kahmann, N.R. and Cozzarelli, N.R. (1990) Processive recombination by the phage Mu Gin system: Implications for the mechanisms of DNA strand exchange, DNA site alignment, and enhancer action. Cell 62, 353-366.

Klippel, A., Cloppenborg, K., and Kahmann, R. (1988) Isolation and characterisation of unusual *gin* mutants. EMBO J. 7, 3983-3989.

Klippel, A., Kanaar, R., Kahmann, R., and Cozzarelli, N. R. (1993) Analysis of strand exchange and DNA-binding of enhancer-independent Gin recombinase mutants. EMBO J. 12, 1047-1057.

Krasnow, M.A., and Cozzarelli, N.R. (1983) Site-specific relaxation and recombination by the Tn3 resolvase: recognition of the DNA path between oriented *res* sites. Cell 32, 1313-1324.

Krogh, B.O., and Shuman, S. (2000) Catalytic mechanism of DNA topoisomerase IB. Mol. Cell 5, 1035-1041.

Kurpiewski, M.R., Engler, L.E., Wozniak, L.A., Kobylanska, A., Koziolkiewicz, M., Stec, W.J., and Jen-Jacobson, L. (2004) Mechanisms of coupling between DNA recognition specificity and catalysis in EcoRI endonuclease. Structure 12, 1775-1788.

Laemmli, U. K. (1970) Cleavage of structural proteins during the assembly of the head of bacteriophage T4. Nature 227, 680-685.

Lane, D., Prentki, P., and Chandler, M. (1992) Use of gel retardation to analyse protein-nucleic acid interactions. Microbiol. Rev. 56, 509-528.

Lee, J., Whang, I., Lee, J., and Jayaram, M. (1994) Directed protein replacement in recombination full sites reveals *trans*-horizontal DNA cleavage by FLP recombinase. EMBO J. 13, 101-109.

Lee, J.Y., Chang, J., Joseph, N., Ghirlando, R., Rao, D.N., and Yang W. (2005) MutH complexed with hemi- and unmethylated DNAs: coupling base recognition and DNA cleavage. Mol. Cell 20, 155-166.

Leschziner, A.E., and Grindley, N.D.F. (2003) The architecture of the γδ resolvase crossover site synaptic complex revealed by using constrained DNA substrates. Mol. Cell 12, 775–781.

Leschziner, A.E., Boocock, M.R., and Grindley, N.D. (1995) The tyrosine-6 hydroxyl of γδ resolvase is not required for the DNA cleavage and rejoining reactions. Mol. Microbiol. 15, 865-870.

Li, W., Kamtekar, S., Xiong, Y., Sarkis, G.J., Grindley, N.D.F., and Steitz, T.A. (2005) Structure of a synaptic γδ resolvase tetramer covalently linked to two cleaved DNAs. Science 309, 1210-125.

Liu T., Liu D., DeRose E.F., and Mullen G.P. (1993) Studies of the dimerization and domain structure of γδ resolvase. J Biol Chem. 268, 16309-16315.

MacDonald, A. (1999) New methods for the structural analysis of intermediates in Tn3 site-specific recombination. Ph.D. Thesis, University of Glasgow.

Mizuuchi, K. and Baker, T.A. (2002) Chemical mechanisms for mobilising DNA. In *Mobile DNA II.* Craig, N., Craigie, R., Gellert, M. and Lambowitz, A., (eds).Washington, DC: American Society for Microbiology Press, pp. 12–23.

Mizuuchi, K., Nobbs, T.J., Halford, S.E., Adzuma, K., and Qin, J. (1999) A new method for determining the stereochemistry of DNA cleavage reactions: application to the SfiI and HpaII restriction endonucleases and to the MuA transposase. Biochemistry 38, 4640–4648.

Murley, L.L., and Grindley, N.D. (1998) Architecture of the γδ resolvase synaptosome: oriented heterodimers identify interactions essential for synapsis and recombination. Cell 95, 553-562.

Nanassy, O.Z., and Hughes, K.T. (1998) *In vivo* identification of intermediate stages of the DNA inversion reaction catalyzed by the *Salmonella* Hin recombinase. Genetics 149, 1649–1663.

Nanassy, O.Z., and Hughes, K.T. (2001) Hin recombinase mutants functionally disrupted in interactions with Fis. J. Bacteriol. 183, 28–35.

Newman, B.J., and Grindley, N.D.F. (1984) Mutants of γδ resolvase: a genetic analysis of the recombination function. Cell 38, 463-469.

Nobles, S.A., Fisher, E.F., and Caruthers, M.H. (1984) Methylphosphonates as probes of protein–nucleic acid interactions. Nucleic Acids Res. 12, 3387–3404.

Nollmann, M., Byron, O., and Stark, W.M. (2005) Behavior of Tn3 resolvase in solution and its interaction with *res*. Biophys. J. 89, 1920-1931.

Nollmann, M., He, J., Byron, O., and Stark, W.M. (2004) Solution structure of the Tn3 resolvase-crossover site synaptic complex. Mol. Cell 16, 127-137.

Nunes-Duby, S.E., Azaro, M.A., and Landy, A. (1995) Swapping DNA strands and sensing homology without branch migration in lambda site-specific recombination. Curr. Biol. 5, 139–148.

Pan, B., Maciejewski, M.W., Marintchev, A., and Mullen, G.P. (2001) Solution structure of the catalytic domain of γδ resolvase. Implications for the mechanism of catalysis. J. Mol. Biol. 310, 1089–1107.

Parker, C.N., and Halford, S.E. (1991) Dynamics of long-range interactions on DNA: the speed of synapsis during site-specific recombination by resolvase. Cell 66, 781-791.

Pingoud A., and Jeltsch, A. (2001) Structure and function of type II restriction endonucleases. Nucleic Acids Res. 29, 3705–3727.

Reed, R.R. (1981) Transposon-mediated site-specific recombination: a defined *in vitro* system. Cell 25, 713-719.

Reed, R.R., and Grindley, N.D.F. (1981) Transposon-mediated site-specific recombination in vitro: DNA cleavage and protein-DNA linkage at the recombination site. Cell 25, 721-728.

Reed, R.R., and Moser, C.D. (1984) Resolvase-mediated recombination intermediates contain a serine residue covalently linked to DNA. Cold Spring Harbor Symp. Quant. Biol. 49, 245-249.

Rice, P.A., and Steitz, T.A. (1994a) Model for a DNA-mediated synaptic complex suggested by crystal packing of γδ resolvase subunits. EMBO J. 13, 1514-1524.

Rice, P.A., and Steitz, T.A. (1994b) Refinement of γδ resolvase reveals a strikingly flexible molecule. Structure 2, 371-384.

Rimphanitchayakit, V., and Grindley, N.D.F. (1990) Saturation mutagenesis of the DNA site bound by the small carboxy-terminal domain of γδ resolvase. EMBO J. 9, 719-725.

Salvo, J.J., and Grindley, N.D.F. (1988) The γδ resolvase bends the *res* site into a recombinogenic complex. EMBO J. 7, 3609-3616.

Sanderson, M.R., Freemont, P.S., Rice, P.A., Goldman, A., Hatfull, G. F., Grindley, N. D. F., and Steitz, T. A. (1990) The crystal-structure of the catalytic domain of the site-specific recombination enzyme γδ resolvase at 2.7-Å resolution. Cell 63, 1323-1329.

Sarkis, G.J., Murley, L.L., Leschziner, A.E., Boocock, M.R., Stark, W.M., and Grindley, N.D.F. (2001) A model for the γδ resolvase synaptic complex. Mol. Cell 8, 623–631.

Sessions, R.B., Oram, M., Szczelkun, M.D., and Halford, S.E. (1997) Random walk models for DNA synapsis by resolvase. J. Mol. Biol. 270, 413-425.

Sherratt, D.J. (1989) Tn3 and related transposable elements: site-specific recombination and transposition. *In* Mobile DNA, D.E. Berg and M. Howe, eds. (American Society for microbiology, Washington, D.C.), pp. 163-184.

Smith, M.C.M., and Thorpe, H.M. (2002) Diversity in the serine recombinases. Mol. Microbiol. 44, 299–307.

Stark, W.M., and Boocock, M.R. (1994) The linkage change of a knotting reaction catalysed by Tn3 resolvase. J. Mol. Biol. 239, 25-36.

Stark, W.M., Boocock, M.R., and Sherratt, D.J. (1992) Catalysis by site-specific recombinases. Trends Genet. 8, 432-439.

Stark, W.M., Grindley, N.D.F., Hatfull, G.F., and Boocock, M.R. (1991) Resolvase-catalysed reactions between *res* sites differing in the central dinucleotide of subsite I. EMBO J. 10, 3541-3548.

Stark, W.M., Parker, C.N., Halford, S.E., and Boocock, M.R. (1994) Stereoselectivity of DNA catenane fusion by resolvase. Nature 368, 76-78.

Stark, W.M., Sherratt, D.J., and Boocock, M.R. (1989) Site-specific recombination by Tn3 resolvase: topological changes in the forward and reverse reactions. Cell 58, 779-790.

Stivers, J.T., and Nagarajan, R. (2006) Probing enzyme phosphoester interactions by combining mutagenesis and chemical modification of phosphate ester oxygens. Chem. Rev. 106, 3443-3467.

Studier, F.W., Rosenberg, A.H., Dunn, J.J., and Dubendorff, J.W. (1990) Use of T7 RNA polymerase to direct expression of cloned genes. Methods Enzymol., 185, 60–89.

Symington, L.S. (1982) Transposon-encoded site-specific recombination. Ph.D. thesis, University of Glasgow.

Tian, L., Claeboe, C.D., Hecht, S.M., and Shuman, S. (2003) Guarding the genome: electrostatic repulsion of water by DNA suppresses a potent nuclease activity of topoisomerase IB. Mol. Cell 12, 199–208.

Tian, L., Claeboe, C.D., Hecht, S.M., and Shuman, S. (2004) Remote phosphate contacts trigger assembly of the active site of DNA topoisomerase IB. Structure 12, 31–40.

Tian, L., Claeboe, C.D., Hecht, S.M., and Shuman, S. (2005) Mechanistic plasticity of DNA topoisomerase IB: Phosphate electrostatics dictate the need for a catalytic arginine. Structure 13, 513-520.

Tomky, L.A., Strauss-Soukup, J.K., and Maher, L.J. (1998) Effects of phosphate neutralization on the shape of the AP-1 transcription factor binding site in duplex DNA. Nucleic Acids Res. 26, 2298–29305.

Tousignant, A., and Pelletier, J.N. (2004) Protein motions promote catalysis. Chem Biol. 11, 1037-1042.

Wasserman, S.A., Dungan, J.M., and Cozzarelli, N.R. (1985) Discovery of a predicted DNA knot substantiates a model for site-specific recombination. Science 229, 171-174.

Watson, M.A., Boocock, M.R., and Stark, W.M. (1996) Rate and selectivity of synapsis of *res* recombination sites by Tn*3* resolvase. J. Mol. Biol. 257, 317-329.

Wenwieser, S.V.C.T. (2001) Subunit interactions in regulation and catalysis of site specific recombination. PhD Thesis, University of Glasgow.

West, K.L., and Austin, C.A. (1999) Human DNA topoisomerase IIβ binds and cleaves four-way junction DNA *in vitro*. Nucleic Acids Res. 27, 984–992.

Xu, Y., Potapova, O., Leschziner, A.E., Grindley, N.D., and Joyce C.M. (2001) Contacts between the 5' nuclease of DNA polymerase I and its DNA substrate. J. Biol. Chem. 276, 30167-30177.

Yang, W., and Steitz, T.A. (1995) Crystal structure of the site-specific recombinase γδ resolvase complexed with a 34 bp cleavage site. Cell 82, 193-207.

Yang, W., Lee, J. Y., and Nowotny, M. (2006) Making and breaking nucleic acids: Two-Mg^{2+}-ion catalysis and substrate specificity. Mol. Cell 22, 5-13.

GLASGOW
UNIVERSITY
LIBRARY